Subcellular beta-adrenergic signaling in hippocampus: implications for memory consolidation and stress response

By

JOSEPH M. MARTINEZ
DISSERTATION

Submitted in partial satisfaction of the requirements for the degree of

DOCTOR OF PHILOSOPHY

in

Neuroscience

in the

OFFICE OF GRADUATE STUDIES

of the

UNIVERSITY OF CALIFORNIA

DAVIS

Approved:

Yang Kevin Xiang, Chair

Gene Gurkoff

Tim Hanks

Johannes Hell

Manuel Navedo

Jennifer Whistler

Committee in Charge

2022

Table of Contents

For JS, my world. I could not have done it without you.

Acknowledgements

First, I would like to thank my advisor and mentor Dr. Kevin Xiang. Dr. Xiang taught me how to be a better scientist. He was always available for any questions I had and always answered them patiently and thoroughly. He encouraged me to seek out new challenges and to try for funding and fellowships even if I was discouraged by the unlikelihood of successfully receiving them. He advised me on how to navigate laboratory settings and how to approach scientific inquiries with rigor and an open mind. He asked for hard work but never more than he asked of himself. Most importantly he taught me to follow data wherever it leads, to be unafraid to propose and try new experiments, and to approach the opportunity to learn with joy. I am eternally grateful he took a chance on me and let me join his lab. Any future success in my career can be directly traced to the skills and knowledge he provided me with.

Additionally, I would like to thank Dr. Ao Shen for teaching me the techniques I would need to complete this research and for allowing me to continue the project he started. He provided the overexpression data in this dissertation and continued to teach me even after moving on to a faculty position. I would also like to thank the Xiang Lab and Rita Xu, Dr. Ying Wang, Dr. Chaoqun Zhu, Dr. Patricia Zhang, and Dr. Aleksandra Jovanovic. Your advice and guidance were invaluable during my research. Rita, our lab would not be able to run without you.

To Dr. Manuel Navedo and Dr. Johannes Hell, thank you for all the mentoring and advice during our time together on the Pharmacology Training Grant as well as during journal clubs and our labs' many collaborations. Our random discussions in the hallway and the sharing of ideas and perspectives were a highlight of my time at UC Davis. I know I am a better scientist for it. To Dr. Hell, thank you for being my co-mentor on the DSPAN award and advising me on postdoctoral positions and science and general. I am going to miss our science discussions. I would also like to thank my dissertation committee (Dr. Kevin Xiang, Dr. Johannes Hell, Dr. Manuel Navedo, Dr. Jennifer Whistler, Dr. Tim Hanks, and Dr. Gene Gurkoff) for all the advice and encouragement as I completed my dissertation research and for all the feedback on this document. Advice and suggestions from our meetings substantively improved the quality of this work and forced me to consider new perspectives and interpretations of my hypotheses. The arrestin work in the project can be directly attributed to our meeting

I would also like to thank Dr. Paula Grammas and Dr. Susan Bergeson. My previous mentors always saw the best in me and provided me with endless encouragement and were always ready to provide sage advice even years after we parted ways. Their joy for science and endless encouragement have been amazing and inspiring. I would like to thank Dr. Marty Usrey of UC Davis's neuroscience graduate group for looking out for me my first year and ensuring that I was able to successfully complete all requirements despite months of rehabilitation from emergency surgery my first year. I would also like to thank Dr. Gene Gurkoff and Dr. Arne Ekstrom for going above and beyond to encourage me when I panicked and struggled during preliminary exams. A few words when someone is struggling can make all the difference in the world and small acts can change a life. Their acts of kindness and encouraging words certainly changed mine. I only hope I can also have such a positive impact on someone starting out their careers.

To my family, thank you for all the encouragement and help as I completed this work. Your support served as the foundation for all that have accomplished during this doctorate and in life.

Finally, I would like to thank and acknowledge all the training grants I have been so fortunate to be trained on including the UC Davis IMSD Fellowship R25GM056765, the Training Program in Basic Neuroscience T32MH082174, the Predoctoral Training in Pharmacological Sciences T32GM099608, and the NIH Blueprint D-SPAN Award F99NS120523. That funding and training made all my work and future career possibilities a reality.

Funding for this research was provided by NIH T32GM099608, GM GM129376, and NIH F99NS120523.

Abstract

Learning and memory-related behaviors in mammals depend on prototypical GPCR signaling and subsequent changes in gene expression. Immediate early gene (IEG) expression is necessary for memory and is induced by increased nuclear cyclic adenosine monophosphate (cAMP) signaling. However, the downstream mechanisms mediating this process have remained unclear. Here, we demonstrate in detail a surprising mechanism by which the G-protein coupled receptor (GPCR) β_2 Adrenergic Receptor (β_2AR) under stimulation indirectly facilitates nuclear cAMP signaling via sequestration of a phosphodiesterase (PDE)4D5/β-arrestin complex. By combining compartment localized cAMP biosensors, Förster resonance energy transfer (FRET)-based live cell imaging, immunofluorescent imaging, and transgenic mice, we found the following:

- Deletion of G-protein receptor kinase (GRK) phosphorylation sites on β_2AR (GRKΔ) blocked agonist-induced receptor internalization to the endosomal compartment.
- This loss of GRK/arrestin mediated internalization also reduced nuclear cAMP in hippocampal neurons.
- Loss of nuclear cAMP signaling impaired nuclear PKA-mediated immediate early genes (IEGs) expression in neurons.
- In animals, loss of GRK phosphorylation resulted impairment of long-term memory in a Morris water maze, a deficit in learning induced IEG expression, but intact working memory.
- In wildtype neurons, β_2AR stimulation promoted internalization of the receptor to the endosome, and β-arrestin-dependent recruitment of cAMP-degrading PDE4D5 to the internalized receptor.
- Intriguingly, inhibition of β-arrestin-PDE4D recruitment alone prevented β_2AR-dependent increases in nuclear cAMP signaling in neurons and PDE4D5 recruitment.
- Furthermore, direct PDE4 inhibition was sufficient to rescue the β_2AR-dependent nuclear cAMP signal *in vitro,* and *in vivo* ameliorated the long-term memory deficits of GRKΔ mice.
- PDE4D5 but not other PDE isoforms were found enriched in the nucleus of neurons and stimulation of β_2AR causes the movement of PDE4D5 out of the nucleus into the cytosol.
- Additionally, Stimulation with other GPCR agonists also caused ligand dependent trafficking of PDE4D5, suggesting the proposed mechanism may have implications for other Gs-coupled

- Receptors. Additionally, we found removal of GRK phosphorylation sites on β_2AR at serines 355/356 or knockout of β_2AR resulted in aberrant anxiety response in the elevated plus Maze (EPM).
- Furthermore, we show that knockout of β_1AR results in a loss of both anxiety response in the EPM and acute stress response in a force swim test (FST).

This work therefore indicates learning and memory relies critically upon the endosomal, GRK-phosphorylated β_2AR sequestration of a β-arrestin/PDE4D complex, which indirectly facilitates nuclear cAMP signaling by effectively removing a PDE4D blockade of cAMP signaling from the nucleus. Therefore, these data constitute a novel and major mechanism by which learning and memory-related behaviors in mammals are regulated by GPCR signaling, at the endosome as well as suggest regulation of stress or memory controlled by different β-adrenergic subtype. These data also suggest differential βAR subtype regulation of stress response.

Graphical Abstract

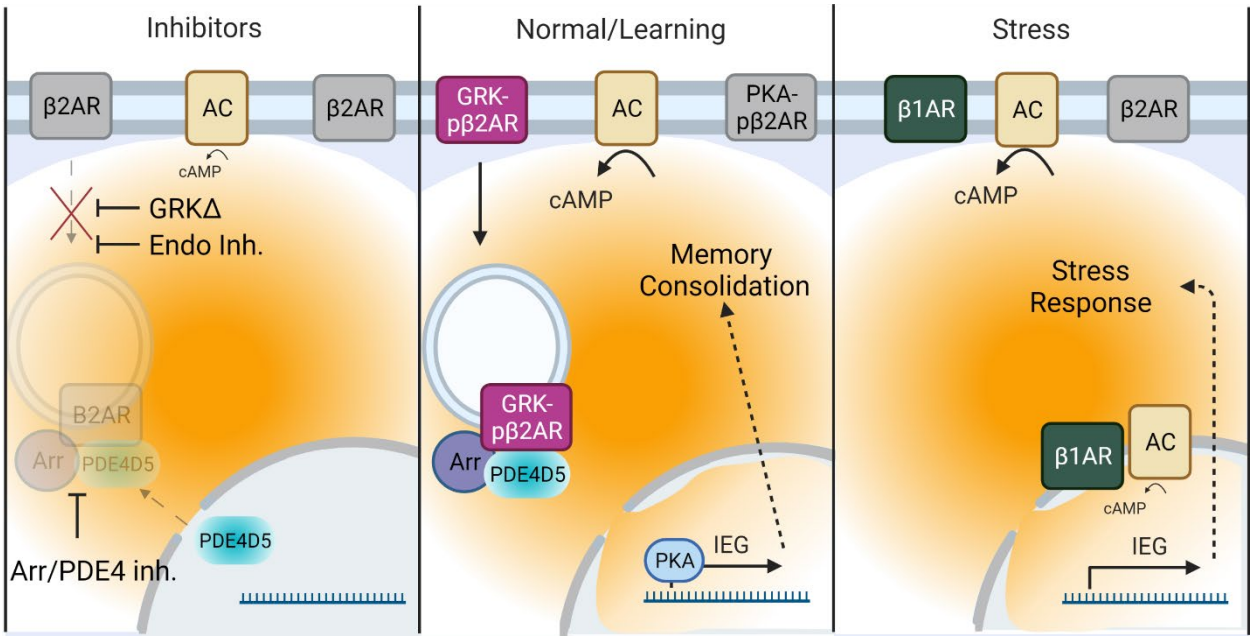

Abbreviations

Barb – Barbadin

cAMP – cyclic adenosine monophosphate

CFP – cyan fluorescent protein

CGP – CGP20712a

CGRP – calcitonin gene-related peptide

CIPL – cumulative integrated path length

CNS – central nervous system

ConA – concanavalin A

CREB – cAMP response element-binding protein

CytoD – cytochalasin D

D22 – decennium22

DKO – $\beta_1\beta_2$AR double knock out

Dyngo – dyngo4a

Epac – exchange factor directly activated by cAMP

EPM – Elevated plus maze

FRET – Förster resonance energy transfer

FST – forced swim test

GEF – guanine-nucleotide exchange factor

GPCR – G-protein coupled receptor

GRK – G-protein receptor kinase

GRK-pβ_2AR – GRK-phosphobeta-2 adrenergic receptor

GRKΔ - β_2AR with serine to alanine mutations (S355/356A) at the GRK phosphorylation sites on the receptor

ICI – ICI 188,551

IEG – immediate early gene

ISO – isoproterenol

LC – locus coeruleus

LTCC – L-type calcium channel

LTD – long term depression

LTP – long term potentiation

MAP kinase – mitogen-activated protein kinase

MWM – Morris water maze

NE – norepinephrine

NFAT – nuclear factor of activated T-cells

NLS-ICUE3 – nuclear location sequence-ICUE3

OCT3 – organic cation transporter 3

pCREB – phosphoCREB

PDE - phosphodiesterase

PKA – protein kinase A

PKA-pβ_2AR – PKA-phosphobeta-2 adrenergic receptor

PKAΔ - β_2AR with serine to alanine mutations (S262/262A) at the PKA phosphorylation sites on the receptor

PMAT – plasma membrane amine transporter

PM-ICUE3 – plasma membrane-ICUE3

Thig – Thigmotaxis

WM-MWM – working memory Morris water maze

YFP – yellow fluorescent protein

αAR – alpha adrenergic receptor

β_1AR – beta-1 adrenergic receptor

β_2AR – beta-2 adrenergic receptor

β_3AR – beta-3 adrenergic receptor

βAR – beta-

Chapter 1: Introduction

The central noradrenergic system modulates neural activity in a broad range of cognitive functions, including arousal, stress, and learning and memory [1, 2]. Norepinephrine (NE) in the central nervous systems (CNS) originates from a small midbrain region known as the locus coeruleus (LC) with projections innervating numerous brain regions. LC firing can be both tonic or, during behavior, switch to burst firing and can be thought of as volumetric signaling [3]. However, NE signaling also participates in more precise signaling activity. This is achieved in part through heterogenous expression of multiple types of α- and β-adrenergic receptors (ARs) throughout the various cell types in the CNS similarly to the diverse expression and function of ARs in the periphery. NE signaling plays an essential role in attentional allocation and learning and memory [4-8]. Despite the importance of NE signaling in the brain in both normal and perturbed function, very little mechanistic information as to how the diverse set of ARs of the brain perform these numerous functions exists creating a large knowledge gap. This dissertation aims to fill a small portion of this gap in our fundamental understanding of NE signaling in learning and memory by focusing on elucidating the mechanistic underpinnings of how noradrenergic signaling in the brain affects learning-mediated immediate early gene (IEG) expression and subsequent memory consolidation. We will begin dissecting β_2AR subcellular cAMP signaling by examining the role GRK phosphorylation of β_2AR and subsequent internalization of the receptor plays in nuclear cAMP signaling. We follow those studies examining how internalization of β_2AR facilitates subcellular cAMP signaling by examining IEG expression and the role β_2AR-mediated IEG expression plays in memory as well as interesting findings regarding beta-adrenergic signaling in stress response. Lastly, we will discuss future directions for research into βAR signaling in learning and memory, stress and fear, and neurodegenerative disorders.

Molecular mechanisms and immediate early gene expression in learning and memory

One of the ways information is stored in the brain is through activity dependent changes in synaptic signaling [9]. Learning leads to persistent changes in synaptic activities in networks of neurons by modulation of the strength of connections within those networks. This modulation of the synaptic connection strength is known as synaptic efficacy [10] and mainly depends on the presynaptic probability of

neurotransmitter release and the amount of neurotransmitter per vesicle, and, postsynaptically, on the number of activated receptors [11]. Information is stored by the changes in synaptic efficacy within the neuronal network. Within the network, changes that increase synaptic efficacy are known as long term potentiation (LTP) and those that decrease synaptic efficacy are known as long term depression (LTD). Both LTP and LTD are non-physiological in nature. Data exits in support of a role for potentiation in learning and memory. For example, knockout of NMDRs in hippocampal region CA3 are impaired in acquiring new memory of a novel platform location in a water maze but retained previously learned platform locations suggesting NMDRs are necessary hippocampal encoding of novel information [12]. Other evidence suggests models of LTP and LTD *in vitro* are similar to what would occur *in vivo* under physiological control [9, 13]. However, these data are only suggestive that plasticity is involved in learning and memory but do not support experimentally induced LTP and LTD as the mechanism for learning and memory. Indeed, Robert Morris suggested criteria necessary to support the hypothesis that synaptic plasticity is the mechanism by which memories are encoded. In his view there is a preponderance of data supporting the necessity of synaptic plasticity for learning and memory but minimal data supporting sufficiency[14]. While it is clear modulating synaptic efficacy as the mechanistic underpinnings of memory has merit, the reality is much more nuanced and complicated and is eloquently reviewed here [15, 16].

Synaptic plasticity modulation depends on numerous receptor activities responding to the gamut of available neurotransmitters (reviewed in [17]) with much of the early work occurring in rabbit hippocampus [18] and later work elaborating on the role glutamate receptors [19-21] and calcium channels [22-26] play. Numerous events including unblocking of silent synapses and increased receptor numbers at the synapse lead to synaptic potentiation. The long-term stabilization of synaptic potentiation beyond these transient changes requires de novo mRNA expression of immediate early genes and neurotrophic factors such as BDNF [27]. One way in which this gene expression occurs is through cyclic adenosine monophosphate (cAMP) dependent protein kinase A (PKA) activation [28]. PKA consists of two regulatory subunits bound to two catalytic subunits where the regulatory subunits act as inhibitors of the catalytic subunits. Upon binding of four cAMP molecules (two for each regulatory subunit), the catalytic subunits are released and free to phosphorylate multiple downstream targets including ion channels, other proteins, and kinases such as ERK and MAPK [29]. Activated nuclear located PKA, either residing in the nucleus already or through

diffusion of catalytic subunits to the nucleus, can phosphorylated cAMP response element binding protein (CREB) [30]. Along with ERK and MAPK mediated processes, CREB can regulate gene expression including IEGs and neurotropic factors such as BDNF [31]. IEG mRNAs are transcribed within minutes after stimulation, either through growth factors, synaptic activity, or other cellular process (reviewed in [32]). In addition to IEG transcription being relatively quick, it is generally transient and does not require *de novo* protein synthesis [33]. IEG protein products are generally unstable and can be designated for degradation without ubiquitination [34]. FOS genes, for example, reach peak expression roughly 30 minutes to an hour after stimulation and begin to decline roughly 90 minutes to two hours post stimulation although there is a fair amount of variability depending on cell population or stimulus type [35-40]. IEG expression is a key step in the stabilization of LTP and formation of memories [41, 42]. Importantly, stimulation of GPCRs such as β_2AR is known to control IEG and other gene expression through cAMP/PKA signaling which targets ERK, MAPKs, and CREB [43-49].

Norepinephrine signaling in the brain

The central noradrenergic system modulates neural activity in a broad range of cognitive functions, including arousal, stress, and learning and memory [1, 2]. Activation of noradrenergic receptors by norepinephrine enhances memory while receptor antagonists block the effects of many memory-enhancing treatments. For example, norepinephrine regulation of memory is disrupted when inhibitors are administered to many areas of the rodent brain, particularly the hippocampus and amygdala [50-53]. At the systems and cognitive levels, functional behavior requires the dynamic processes of retrieval of past information and formation of new memories. Both retrieval and encoding of new memories require and are modulated by the allocation of attentional resources [54]. Norepinephrine (NE), a catecholamine neurotransmitter and neurohormone, plays a modulatory role in attentional allocation [4]. Through specific innervation and heterogenous expression of adrenergic receptors in the CNS across multiple cell types, NE participates in modulation of vigilance, wakefulness and attention in information processing, working and long-term memory and related long-term potentiation (LTP), memory retrieval, and cognitive flexibility (Reviewed in [54-58]).

In the CNS, noradrenergic innervation consists of two primary ascending projections from the brain stem: the dorsal and ventral noradrenergic bundles. The dorsal noradrenergic bundle originates from the

locus coeruleus (LC) and comprises the majority of NE signaling and projections in the CNS. The ventral noradrenergic bundle arises from several pons and medulla nuclei including subcoeruleus areas, the ventrolateral reticular formation of the pons and medulla, and the medial subnucleus of the nucleus tractus solitarius. These areas send NE projections to the hypothalamus, preoptic area, and lateral horn of the spinal column, and the extended amygdala as well as to other brain stem nuclei [59-62]. Non-LC nuclei contribute to autonomic regulation (reviewed in [63-65]). The LC is one of the smallest (~45,000 to 60,000 cells in humans [66]) but most extensively projecting nuclei in the brain, from neocortex to spinal cord [67, 68]. Efferents from the caudal LC project primarily cortically and in an ipsilateral manner while sub-cortical projects exhibit a more bilateral distribution [69, 70]. Individual LC projections can branch to innervate different brain regions or collateralize with other individual projections innervating functionally related circuits. LC neurons also demonstrate segregation based on projection to the primary motor cortex or regions of the prefrontal cortex. These segregated projections also show differences in excitability and expression of proteins suggesting subsets of LC neurons may release NE asynchronously in some contexts [71, 72].

The LC regulates NE signaling through innervation of multiple brain regions (**Figure 1.1** and [55]) acting through adrenergic receptors in those regions creating functional NE signaling domains throughout the brain. For example, The LC extensively innervates the cerebral cortex and is the sole source of cortical NE signaling with close correlation of LC activity and NE release within the cortex [2, 73, 74]. Cortical LC projections are believed to play a role in wakefulness [58]. LC activity correlates with arousal level with inactivation of the LC reducing cortical activity [75-78]. The LC is also the sole source of NE signaling in the hippocampus contributing to NE signaling involvement in memory formation and retrieval [79-84]. These data highlight how NE signaling can affect specific brain processes as specific innervation, along with heterogenous receptor expression, allow NE from a single brain nucleus to precisely, dynamically, and differentially affect specific brain regions.

The LC, whose name means “blue spot” in Latin, is identified by the blue pigmentation of NE containing neurons. Early work in rodents and primates demonstrated nearly all the cells of the LC contain dopamine beta hydroxylase (DBH) [85]. DBH, an enzyme which converts dopamine into norepinephrine, is the penultimate step in the catecholamine biosynthetic pathway (**Figure 1.2, [85, 86]**). Notably,

phenylethanolamine N-methyltransferase (PNMT), the enzyme that catalyzes the last step in catecholamine synthesis methylating NE into epinephrine, shows limited expression in the brain. PMNT is found in the olfactory bulb, the medulla and pons, and the hypothalamus and small amounts of epinephrine have been found in the brain [87-89]. PMNT is, however, highly expressed in the adrenal medulla, and in lower levels in the spinal cord, brain stem, and cardiomyocytes [89-92]. Therefore, NE is the primary adrenergic ligand in the brain whereas its methylated counterpart, epinephrine acts mostly in the periphery and as a neurohormone. Upon release, reuptake of NE occurs primarily via the norepinephrine transporter (NET) which is located on the plasma membranes of noradrenergic neurons. However, the dopamine transporter (DAT) can also transport NE back into presynaptic neurons [93, 94]. The monoamine oxidase (MAO) family of flavoproteins catalyze oxidation reactions of primary and secondary amines, polyamines, amino acids, and methylated lysine side chains in proteins [95]. Degradation of catecholamines occurs via oxidation catalyzed by MAO-A and -B. MAO-A and MAO-B are isoenzymes with differing substrate affinities. MAO-A oxidizes dopamine, serotonin, tryptamine, tyramine, NE, and epinephrine and MAO-B oxidizes dopamine, phenylethylamine, tryptamine, tyramine, and benzylamine [96-98]. MAO-A and MAO-B share roughly 60% sequence identity and in their catalytic regions two cysteines in MAO-A and three cysteines in MAO-B are important for catalytic activity as replacement of the three-cysteine region of MAO-B with that of MAO-A alters its catalytic activity to resemble the latter [99]. MOA-B also metabolizes xenobiotic amines including the dopaminergic neurotoxin 1-methyl-4-phenyl-1,2,3,6-tetrahydropyridine (MPTP). Metabolism of MPTP by MAO-B induces a Parkinsonian syndrome similar to Parkinson's disease. Additionally, MAO-B, generally thought to be the primary driver of CNS dopamine metabolism, is implicated in the generation of free radicals in dopaminergic neurons and inhibition of MAO-B increases dopamine half-life in the synaptic cleft and reduces oxidative stress [100]. Therefore, MAO-B inhibitors are being investigated for use in Parkinson's disease. However, recent work has shown MAO-A, in striatal neurons, primarily degrades dopamine while MAO-B is involved in control of GABA levels [101] suggesting MAO isotype function varies by neuron field. MAO-A, due to its metabolic action against several neurotransmitters, has multiple, less well-defined actions in the CNS. MAO-A activity is increased in depressed patients while smokers have reduced MAO-A levels. The high rate of smoking in depressed patients may be related [102-104]. Low MAO-A brain levels are also associated with aggressive and antisocial behavior [105-107]. In

heart failure where adrenergic receptor desensitization and depressed cardiac output are hallmarks, increased MAO-A levels desensitizes beta adrenergic receptors [108]. These data demonstrate crucial roles for MAOs in NE signaling. While the importance of information processing, memory, and allocation of attentional resources is well appreciated and studied in the CNS, the mechanisms by which adrenergic metabolism and signaling participates in and contributes to these processes are much less well understood.

Norepinephrine and beta-adrenergic receptors in the brain and periphery

G-coupled protein receptors (GPCRs), consisting of seven transmembrane domains, are the largest and most diverse group of membrane receptors in eukaryotic cells and are responsible for mediating many of the physiological responses to hormones, neurotransmitters, and environmental inputs [109-111]. As such, GPCRs and their signaling cascades are highly druggable targets with 108 GPCRs accounting for ~34% of FDA approved drugs [112, 113]. Adrenergic receptors are a class of GPCRs that are involved in global neural modulation as well as learning and memory [114]. Adrenergic receptors can be classified as alpha and beta receptors. Adrenergic receptors have a myriad of functions both centrally, as discussed above, and in the periphery, ranging from right or flight response and heart function to metabolism and immune system function. The focus of this work is beta adrenergic receptors, specifically β_1- and β_2AR. However, it is important to recognize that alpha-adrenergic receptors and β_3ARs are known to participate in a wide variety of cognitive processes. More information about each can be found here (Reviewed in [115-119]).

β_2AR is the prototypical GPCR and consists of 7 transmembrane alpha-helices with 3 extracellular and intracellular loops [111]. The intracellular loops & C-terminus are involved with intracellular signaling after receptor activation [120]. These regions contain several serine sites that are preferentially phosphorylated by PKA (S261/262) or GRK2 (S355/356) after agonist binding that induce functionally distinct signaling pathways (**Figure 1.2**). β_2AR preferentially binds to the stimulatory Gs protein but can also couple with inhibitory Gi. Classically, two major signaling pathways result from activation of β_2AR. First, ligand binds in its binding pocket on the receptor resulting in a conformational change favorable for coupling to the heterotrimeric Gs protein. Once coupled the Gs protein a bound GDP on the Gαs subunit is exchanged for GTP with the receptor acting as a guanine-nucleotide exchange factor (GEF) [121]. This exchange results in dissociation of the Gαs subunit from the βγ-subunits. The Gαs subunit then diffuses

and activates adenylyl cyclase (AC). AC, in turn, converts ATP into the ubiquitous secondary messenger cAMP. cAMP then diffuses and activates PKA. PKA, in turn can phosphorylate β_2AR itself or one of its many other downstream targets such as the L-type calcium channel (LTCC) Cav1.2 [122]. Cav1.2 accounts for over 80% of the brains LTCC signaling. $Ca_V1.2$ forms a unique signaling complex with the β_2AR containing all necessary effector proteins, i.e., Gs, AC, and PKA, to foster localized and potent upregulation of channel activity [123-127]. β_2AR promotes PKA phosphorylation of LTCC $Ca_V1.2$ at Ser 1928 and phosphorylation of S1928 is absolutely required for increasing channel opening probability and Ca^{2+} influx. [128]. Calcium influx pays a major role in LTP. These data highlight one way in which β_2AR-mediated PKA signaling can modulate learning.

The second major pathway involves β-arrestin mediated internalization of the receptor. After ligand binding, β_2AR adopts a conformation that allows GRK to phosphorylate the receptor. These phosphorylation events within the intracellular regions of β_2AR promote recruitment and subsequent high-affinity binding of β-arrestin to the receptor [129, 130]. Once β-arrestin is bound to the receptor, it interacts with adapter protein-2 (AP2) and then interacts with dynamin and clathrin to induce clustering β_2AR into clathrin-coated pits leading to clathrin-mediated internalization [131]. This internalization of the receptor relocates it to the endosome where, classically, it was thought that the receptor was either recycled or marked for degradation. In this way, β-arrestin “arrests” the G-protein signal and desensitizes the cell to NE signaling. As more research was done, it become apparent that internalization of β_2AR was not simply meant for desensitization, receptor recycling, or degradation. Through work with Gs mimetic nanobody 80 (Nb80), it was shown β_2AR is found in an active confirmation on the endosome. Further it was shown that all the machinery necessary for receptor stimulation mediated G-protein release was also present at the endosome but not downfield effectors suggesting direct, subcellular endosomal signaling from internalized β_2AR [132-134]. Indeed, evidence suggests internalization of β_2AR can regulate gene expression [135, 136], however these data are not definitive. In support, blockade of β_2AR-mediated internalization attenuates overall cellular cAMP production as well attenuates stimulation-mediated transcriptional response. [49]. Functionally, β-arrestin-mediated signaling has been shown to be involved in memory consolidation [137], extinction learning [138], and fear learning [139].

β_1ARs are also widely expressed in the CNS [140]. β_1ARs are also Gs coupled GPCRs and share a similar amino acid sequence with 57% sequence identity and 70% at the pocket residues [141]. Notwithstanding this sequence homology, β_1AR has a roughly 10-fold higher selectivity for NE than β_2AR. Epinephrine, meanwhile, with only a methyl group difference from NE has no selectivity bias for β_1AR or β_2AR [141]. Like β_2ARs, β_1ARs undergo internalization as part of receptor trafficking [142]. However, while β_1- and β_2ARs have highly conserved pocket residues, intracellularly they are not conserved with β_1AR lacking GRK phosphorylation sites and the docking sites for β-arrestin binding found on β_2AR [143]. Instead β_1AR traffics via its PDZ domain and interactions with AKAP79 and SAP97 [142, 144]. Interestingly, while *in vitro* data show β_1ARs weakly interact with β-arrestins and have minimal if any clathrin mediated internalization[145-148], β_1ARs still signal through mitogen-activated protein (MAP) kinases. Activation of MAP kinase had been thought to require internalization of GPCR-β-arrestin complexes[149-152]. However, rather than internalizing, β_1ARs catalyze clathrin-coated structures upon stimulation. These structures accumulate β-arrestin then dissociate from the receptor and transduce MAP kinase signal. These data provide a mechanism by which GPCR stimulation can signal through β-arrestin at a distance affecting subcellular signaling without receptor internalization providing an alternative subcellular signaling mechanism that does not require GPCR internalization [153]. Internalization of β_1AR via association of its carboxy terminus with membrane-associated guanylate kinase inverted domain-2 (MAGI-2) following stimulation also occurs [154]. However, studies have shown β_1AR can still interact weakly with β-arrestins under certain conditions and undergo moderate levels of arrestin mediated internalization [155, 156]. It has been shown β_1AR can signal subcellularly from the Golgi, ER/SR, and work from Dr. Paul Gasser has shown singling from β_1AR from the nuclear envelope in astrocytes [157-161]. These studies suggest β_1AR signaling at both the PM and subcellularly likely play a role in mediate the effects of NE signaling in the CNS. However, as with β_2AR, there are limited mechanistic studies examining β_1AR signaling the brain with the vast majority of studies dealing with peripheral tissue such as the heart.

In the periphery βAR signaling participates in numerous physiological processes including cardiac function, lung function, inflammatory responses, and metabolism [162-166]. In the healthy heart, β_2ARs are present in low levels in cardiomyocytes whereas non-cardiomyocyte cells in the heart (endothelial cells and fibroblasts) have rich β_2AR expression [167]. In cardiac fibroblasts, β_2AR inhibits collagen production and

subsequent fibrosis [168, 169]. However, chronic βAR stimulation can lead to cardiac hypertrophy and fibrosis. Interestingly, deletion of β_2AR in cardiomyocytes can enhance fibrosis in aging and diabetic cardiomyopathy [169]. Increased sympathetic drive during heart failure increases GRK2 levels with levels in failing myocardium correlating with cardiac dysfunction and improved cardiac function during heart failure associated with lower GRK2 levels [170-173]. Metabolic disorders such as diabetes mellitus can cause cardiomyopathy via depression of Akt signaling and increases in Foxo1-mediated gene expression [174]. In diabetes mellitus, hyperinsulinemia stimulates recruitment of GRK2 to the insulin receptor[175] which is in complex with β_2AR, promoting Gi-based signaling via GRK phosphorylation of the receptor. This Gi-biased signaling inhibits cardiac contractility [176]. We have shown pretreatment of HEK293 cells expressing β_2AR with pertussis toxin has no effect on isoproterenol induced phosphorylation of β_2AR by PKA or GRK suggesting phosphorylation of β_2AR by PKA and GRK is not dependent on Gi coupling [177]. Gs to Gi switching can also be facilited via phosphorylation of β_2AR sties by PKA on the third intracellular loop and C-terminal tail of the receptor [178]. In primary cell lines, cardiomyocytes and atrial membrane preparations have shown β_2AR coupling to Gi [179-182]. Additionally, over expression of β_2AR in rat superior cervical ganglion neurons results in β_2AR coupling to Gi [183]. In the CNS, Gs to Gi switching by GRK phosphorylation of β_2AR by PKA phosphorylation has not been examined in detail but is highly unlikely to be limited to only peripheral systems. β_2ARs are found in numerous cell types within the lungs including airway smooth muscle, epithelial cells, vascular endothelial cells, and inflammatory cells [184, 185]. In alveolar epithelium β_2AR signaling regulates protein production needed for ion and fluid transport. β_2AR stimulation leads to airway smooth muscle contraction, vasodilation, and bronchorelaxation via the Gs/PKA pathway and agonists are used to treat asthma and chronic obstructive pulmonary disease (COPD) [185, 186]. Conversely, knockout of β-arrestin2 prevented allergic inflammation in an asthma model [187]. βAR signaling is also involved in inflammatory responses. Stimulation of βAR signaling via exercise has been shown to protect amyloid beta induced microglia activation and neuroinflammation and knockout of βARs prevents exercise invoked protection [188]. Additionally, pro-inflammatory monocytes responses to LPS challenge require β_1AR stimulation [189] while anti-inflammatory macrophage responses require β_2AR activity [190].

Subpopulations of β2AR delineated by kinase phosphorylation of the receptor exist in signal hippocampal neurons and are spatially segregated.

Work from our lab has shown that functionally distinct and selectively phosphorylated subpopulations of β_2ARs exist in hippocampal neurons [191]. These subpopulations of β_2ARs are preferentially phosphorylated at either a PKA (S261/262) or GRK (S355/356) site on the c-terminus of the receptor and undergo distinct membrane trafficking depending on phosphorylation status of β_2AR after stimulation. PKA-phospho(p)β2AR remains at the PM while GRK-pβ_2AR internalize after receptor stimulation (**Figure 1.3**). Interestingly, these βAR subpopulations are also spatially segregated in mature hippocampal neurons with PKA-pβ_2AR enriched in dendrites and GRK-pβ_2AR primarily on the soma. The distinct kinase preference combined with distinct spatial localization correlate with the classical signaling pathways of β_2AR with the PKA-pβ_2AR subpopulation facilitating membrane Gs-PKA signaling and calcium influx via the L-type calcium channel (LTCC) (among other signaling) in dendrites and contributions to e-LTP while the GRK-pβ_2AR subpopulation, residing on the soma, internalizes to contribute to gene expression and l-LTP. It is important to note that this study did not examine the presence of either β_2AR subtype at synapses and it is likely that both are present to facilitate calcium signaling as well as desensitization. LTCC subunit $\alpha_1$1.2 and β_2AR have been shown to form a membrane complex in the brain. Additionally, isoproterenol stimulation induces β_2AR-dependent neuronal LTCC activation [192]. Further, PKA phosphorylation of serine 1928 of $\alpha_1$1.2 displaces β_2AR from $\alpha_1$1.2 and promotes channel activation [125, 128]. B_1AR/β_2AR double knockout (DKO) hippocampal neurons expressing mutant PKA-β_2AR with PKA phosphorylation sites inactivated but not WT-β_2AR or mutant GRK-β_2AR with GRK phosphorylation sites inactivated promote phosphorylation of LTCC at serine 1928 on the $\alpha_1$1.2 subunit under stimulation. Reintroduction of WT or mutant GRK-β_2AR but not mutant PKA-β_2AR to DKO hippocampal neurons promotes stimulation induced receptor dissociation from $\alpha_1$1.2 and increases nPo of LTCC. These data suggest stimulation-induced PKA-pβ_2AR is necessary to promote PKA-phosphorylation and activation of the LTCC in hippocampal neurons[127]. These β_2AR subpopulations display distinct structural properties as well with the GRK-pβ_2AR subpopulation preferentially existing as receptor monomers while the PKA-pβ_2AR subpopulation existing predominantly as dimers. Based on distribution and ability to activate L-type calcium channels it is reasonable to suggest

the PKA-pβ_2AR subpopulation are more relevant to activities in dendrites such as synaptic transmission than the GRK-pβ_2AR subpopulation. However, as LTCC is found at both synapses and the soma the lower relative number of PKA-pβ_2AR in the soma still likely contributes to calcium dependent CaMKII/nuclear shuttling of pCREB and NFAT. In contrast, the internalization of GRK-pβ_2AR suggests a more likely role for this subpopulation in endosomal based nuclear signaling. Indeed, internalization of β_2AR has been suggested as necessary for receptor-mediated gene expression [49] although alternative hypotheses exit. Further, stereotyped gene responses to βAR stimulation occurs by increased receptor containing endosomes in a ligand dose-dependent manner [193]. Together, these data suggest the GRK-pβ_2AR may provide mechanistic insight into internalization mediated signaling.

The role of phosphodiesterases in regulating microdomains of cAMP signaling

cAMP and other cyclic nucleotide secondary messengers have many downstream effectors in addition to PKA such as multiple isoforms of EPAC, various cyclic nucleotide gated ion channels, and Popeye domain-containing proteins (POPDCs) [194-196]. Additionally, cells can contain multiple Gs coupled GPCRs that each respond to different hormones. As such, cells must tightly regulate the activity of these secondary messengers. Phosphodiesterases (PDEs) are a metallohydrolase superfamily of enzymes that degrade 3',5'-cyclic nucleotides such as cAMP and cGMP by breaking the phosphodiester bond of these secondary messenger molecules and therefore are important regulators of cyclic nucleotide signaling [197]. PDEs consist of 11 different families all of which have multiple different isoforms. Canonically PDEs hydrolyze cAMP (PDE1, 2, 3, 4, 7, 8, 10, 11) or cGMP (PDE1, 2, 3, 5, 6, 9, 10, 11) although PDEs will also hydrolyze other non-canonical 3', 5'- cyclic nucleotides (**Figure 1.4 and** [198-220]). PDEs are also localized both to different cell types and to different cellular locations. For example, PDE4D5 is known be localized in the nucleus in complex with PKA and AKAP95 [221] and PDE10A is enriched in striatal medium spiny neurons but not found in each class of striatal interneuron [222]. Additionally, no two PDEs share the same substrate affinity, localization, and cell type expression (Reviewed in [220]). There also appears to be unique regional distribution for every PDE isoform in the CNS [223]. One way PDEs regulate subcellular signaling is through localization to specific subcellular targets. In the case of β_2AR, PDE4D isoforms have been shown to be functionally and physically

associated with the receptor in multiple cell types including fibroblasts and myocytes [224-228]. Additionally, following β_2AR stimulation, β-arrestins can recruit PDE4D isoforms to the receptor at the plasma membrane [228]. Further, PDE4D8 associates with β_2AR at the plasma membrane while PDE4D5 is located in the nucleus [221, 227, 229]. GRK phosphorylation of β_2AR also promotes β-arrestin mediated recruitment of PDE4D isoforms [230]. Serine to alanine mutations on β_2AR at serine 355/356 ablates arrestin recruitment to the receptor and inhibition of GRK2 prevents PDE4D interaction with β_2AR [231, 232]. β_1AR has also been shown to associated with PDE4D8 rather than PDE4D5 [224]. Interestingly, β_1AR efficiently interacted with PDE4D while β_2AR has negligible interaction with PDE4D in pull down experiments suggesting direct interaction of PDE4D- β_1AR and arrestin dependent PDE4D-β_2AR interaction [224]. Notably this experiment was conducted purified proteins and my not reflect biological reality as other studies show PDE4D9 and PDE4D8 binding to β_2AR at resting conditions in cardiomyocytes [227]. Additionally, β_1AR/PDE4D complex is formed at basal conditions and agonist binding dissociates the β_1AR complex [224] These data suggest β-arrestin is needed for PDE4D5/β_2AR interaction while β_1AR/PDE4D complexes directly although other data show other PDE4D isoforms interacting with β_2AR [227].. In cardiomyocytes, stimulation of prostaglandin E_2 induced cAMP at the plasma membrane activates plasma membrane associated PKA. This PKA then phosphorylates β_2AR-associated PDE4D. Phosphorylation at Ser126 is known to increase PDE4D activity [233] without affecting the PDE4D/β_2AR complex. The increased PDE4D activity prevents cAMP diffusion from the plasma membrane to the sarcoplasmic reticulum [234]. These data highlight some of the ways in which PDEs can regulate GPCR-mediated cAMP production dynamically in response to receptor stimulation.

Because of the relative promiscuity of cyclic nucleotides, having myriad downstream effectors and inducers, it is necessary to tightly regulate both their functional lifetime and localization within cells. This is achieved through the action of PDEs. Through differing subcellular localization and differential expression in various tissues, tightly regulated and compartmentalization of cyclic nucleotide signaling is achieved. As such PDEs act as barriers to the free diffusion of cyclic nucleotides. In addition, movement of PDEs by diffusion or through interaction with other partners within cells can help achieve dynamic control of cyclic nucleotide signaling within the cell. For example, PDEs are known to associate with various GPCRs as well as arrestin proteins, both of which can affect movement within the cell. While

PDEs are considered one of the primary drivers of cyclic nucleotide compartmentalization, more recent work suggests that condensates of PKA-regulatory subunits within the cell may also contribute to compartmentalization of cAMP [235]. These condensates are proposed to act as a sink for cAMP and compensate for the relatively slow kinetics of PDE enzymes by keeping cAMP from diffusing long enough for PDE to hydrolyze it. However, the studies currently done on PKA regulatory condensates are not in physiological conditions and it remains to be seen if or how they contribute to normal cellular activity. Regardless of the contributary role these condensates play in cAMP signaling, PDEs are necessary to break down cyclic nucleotides and remain the primary driver of compartmentalization of cyclic nucleotides within cells.

Clinically, there are numerous diseases and conditions where aberrant, compartment specific cyclic nucleotide signaling is implicated. There are also numerous other conditions were altering cyclic nucleotide signaling could be therapeutic. As such, PDEs are oft therapeutic targets for numerous diseases and conditions in both the periphery and the CNS. These include but are not limited to cancer, erectile dysfunction, hypertension, and cardiac hypertrophy in the periphery [236-240] and in Alzheimer's disease, Parkinson's disease, Huntington's disease, depression, and motor function in the CNS [223, 241-247]. However, because of the ubiquitous nature of PDEs in both the CNS and the periphery, inhibitors targeting only one family of PDEs often have myriad side effects limiting their clinical efficacy. An example of this is PDE4 inhibitors have failed clinical trials in part due to intolerable, systemic effects of PDE4 inhibition separate from therapeutic targets [248-251] while new PDE4D inhibitors appear to have fewer side effects in early animal experiments [252].

Subcellular beta-adrenergic signaling in hippocampus: implications for memory consolidation and stress response

Utilizing a combination of overexpression of point mutant β_2ARs, primary neuron culture, transgenic mice, FRET based live cell imaging and camp biosensors, gene expression, and behavioral assays we investigated the mechanism by which internalization of β_2AR regulates nuclear cAMP signaling and subsequent gene expression *in vitro* via a novel sequestration mechanism of a cAMP degrading phosphodiesterase. Additionally, we examined the functional implications a loss of GRK-pβ_2AR-mediated

internalizations on hippocampal mediated spatial memory *in vivo*. Finally, we pursued interesting findings about the role of adrenergic signaling in stress response. This work provides insight into an alternative mechanism by which internalization of β_2AR facilitates nuclear cAMP signaling rather than directly signaling to the nucleus from the endosome. Further, this work shows that a loss of properly timed IEG expression mediated by β_2AR internalization is necessary for memory consolidation but not working memory. Lastly, we suggest a differential role for β_1AR and β_2AR in stress and anxiety response.

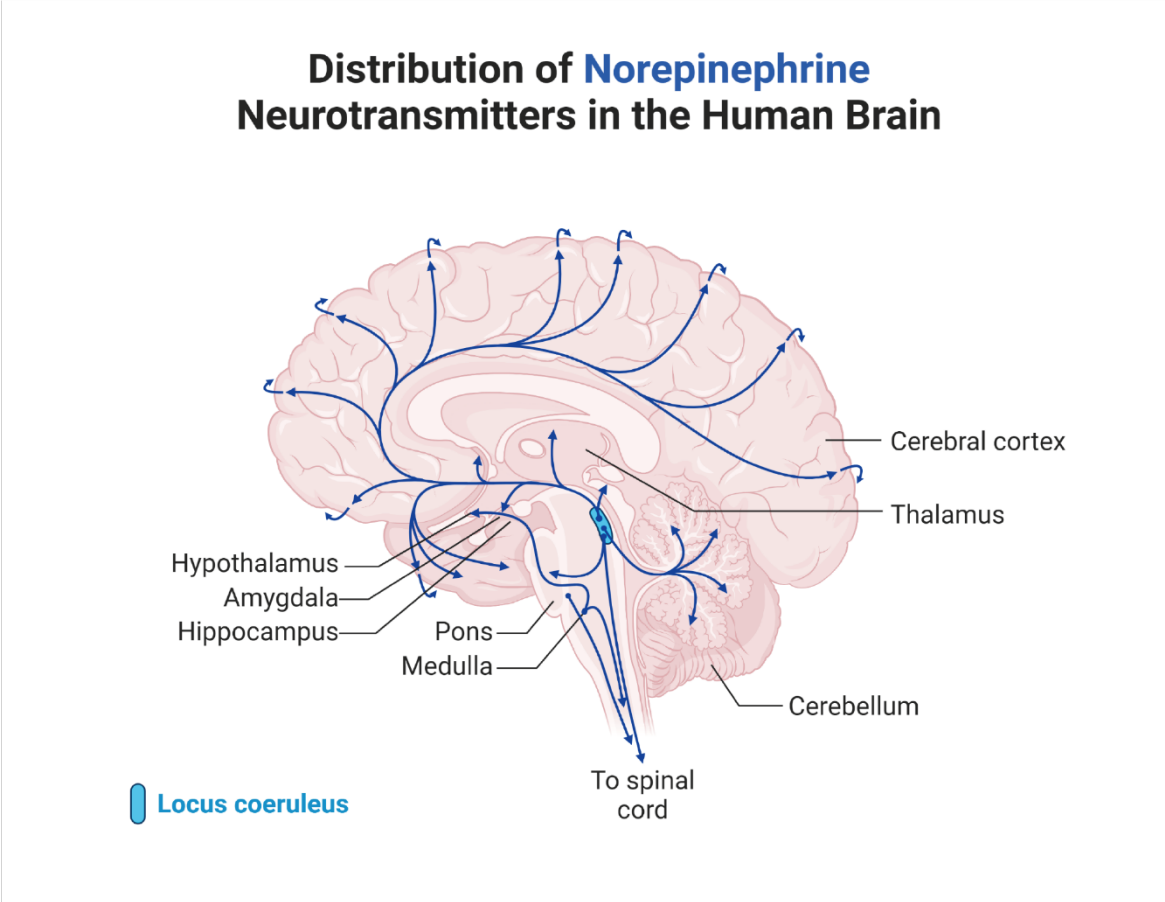

Figure 1.1 – Distribution of norepinephrine signaling in the human brain

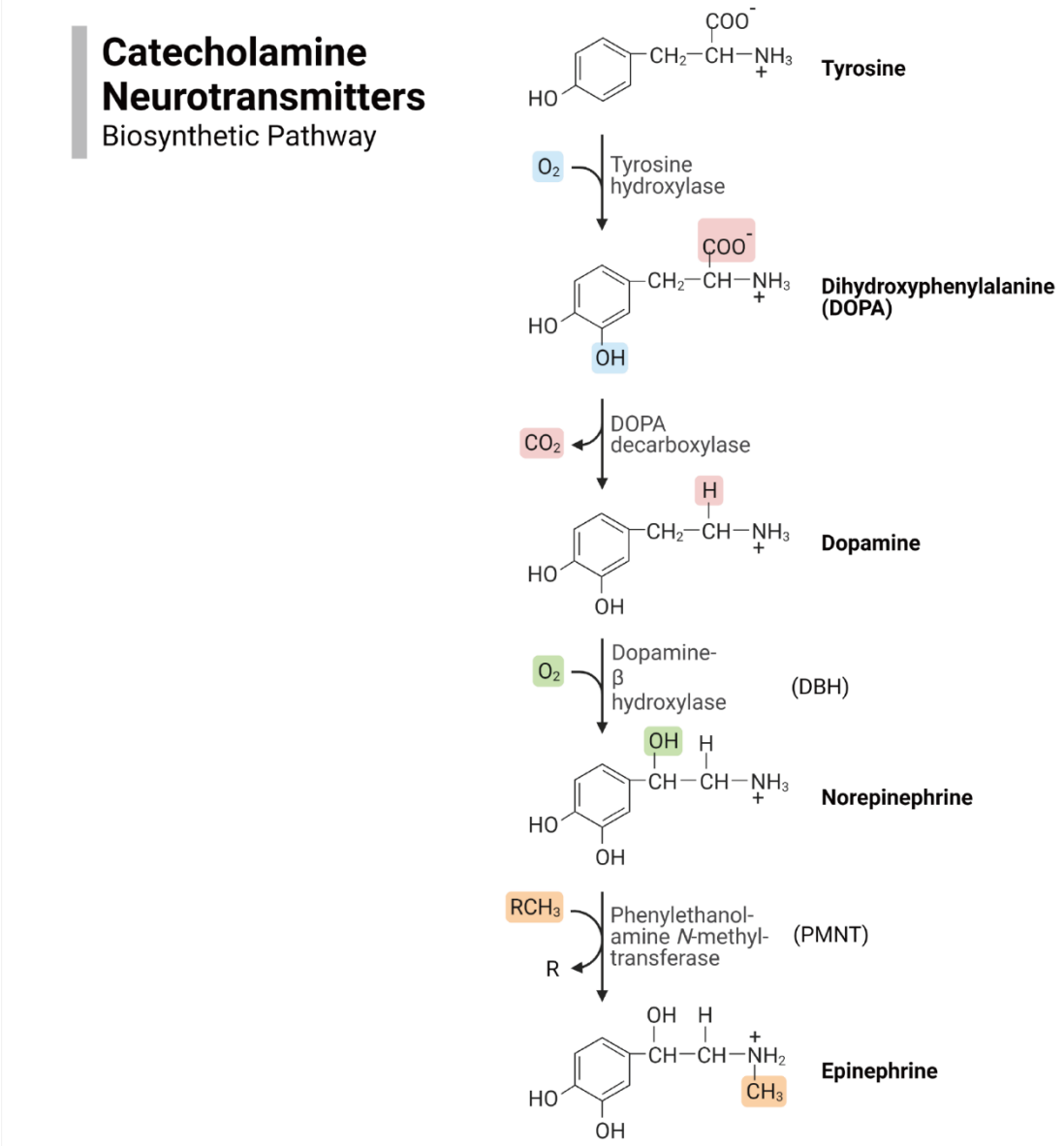

Figure 1.2 – Catecholamine synthesis

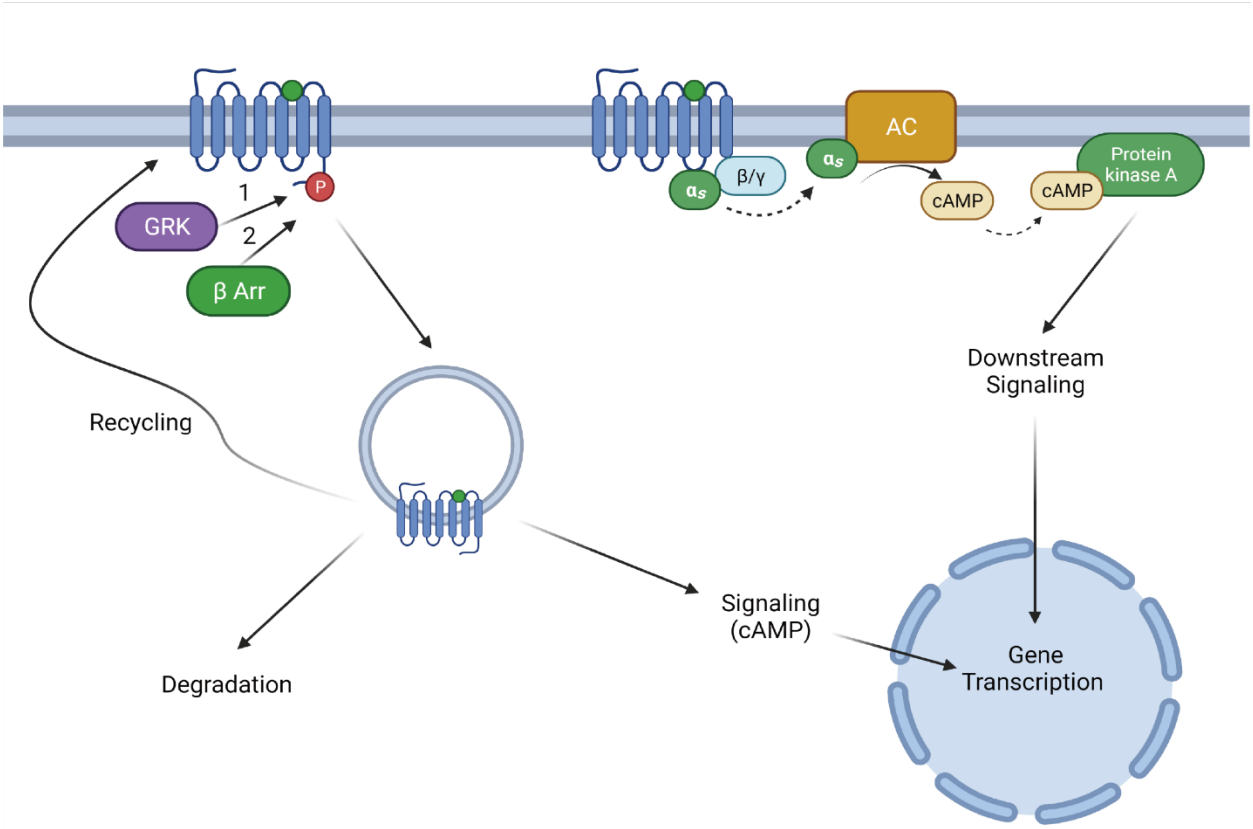

Figure 1.3 – Canonical β2AR signaling pathways.

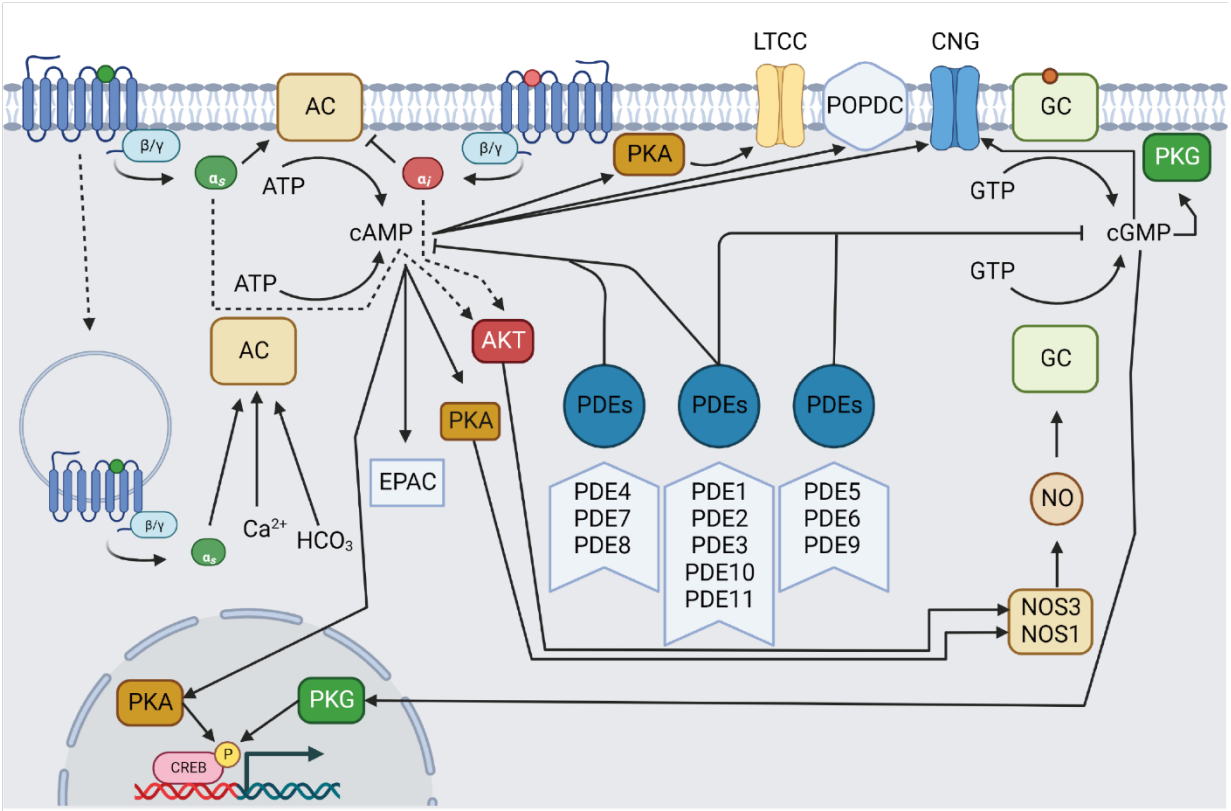

Figure 1.4 – Cyclic nucleotide signaling is regulated by PDEs

Chapter 2: GRK phosphorylation and subsequent internalization of β_2AR controls IEG expression via nuclear cAMP signal.

Introduction

The molecular basis of hippocampal learning and memory consolidation is thought to lie in long term potentiation via increases in immediate early gene (IEG) expression [47, 48]. IEG expression is regulated by activation of cAMP response element binding protein (CREB) in neuron nuclei following neurohormone stimulation. G-protein coupled receptors (GPCRs) are the largest and most diverse group of membrane receptors extant responsible for physiological responses to hormones, neurotransmitters, and environmental inputs [253]. Activation of GPCRs promotes nuclear cAMP signaling to enhance IEG expression [46]. The β_2-adrenergic receptor (β_2AR) is a prototypical GPCR that can mediate nuclear cAMP signal and is known to be crucial to hippocampal learning and memory [140, 254-257]. Internalization of β_2AR is also known to regulate gene expression [49]. However, the exact mechanism by which β_2AR regulates nuclear signaling and gene expression remains unclear.

Agonist stimulation promotes not only G-protein signaling but also phosphorylation of β_2AR by G-protein receptor kinase (GRK)- and protein kinase A (PKA) at distinct sites on the receptor itself [258]. These phosphorylation events are implicated in the two well-defined, classical β_2AR receptor trafficking and signaling pathways ([128, 149, 178] and **Figure 1.3**). Recent work from our lab has shown GRK and PKA selectively phosphorylate functionally distinct, spatially segregated subpopulations of β_2ARs in individual neurons [127]. PKA-phosphorylated β_2ARs reside on the cell surface and terminal processes in hippocampal neurons, mediating the phosphorylation and activation of L-type calcium channels (LTCC) [127]. In comparison, GRK-phosphorylated β_2ARs are enriched in endosomes in but not limited to the soma. Emerging evidence show GPCRs can be activated after internalization, and agonist-induced β_2AR internalization alters the expression of many genes [5, 45, 49, 136, 259, 260]. However, direct cAMP signaling from these endosomal receptors to the nucleus has not been observed raising questions about the mechanistic underpinnings of endosomal β_2AR-mediated nuclear cAMP signaling.

Additionally, studies have established a critical role for the phosphodiesterase 4D (PDE4D) family in regulating subcellular cAMP signaling by preventing free diffusion of cAMP and non-specific, unregulated activation numerous of downstream signaling partners. This, in turn, sets up cAMP microdomains and/or

gradients of cAMP [224, 261-265]. PDE4D isoforms are functionally and physically associated with β_2AR in fibroblasts and myocytes [224-228]. Moreover, β-arrestins coordinate PDE4D recruitment to β_2AR upon agonist stimulation [228]. While β-arrestin recruitment to β_2AR is ablated when the GRK phosphorylation sites of the receptor are mutated [231], inhibition of GRK2 also prevents PDE4D interaction with β_2AR [232]. This includes PDE4D8 at the PM [227, 229] and PDE4D5 distributed in the nucleus in the resting state [221]. Further, when GRK phosphorylation sites are inactivated, arrestin recruitment to β_2AR is ablated [231]. Additionally, inhibition of GRK2 prevents PDE4D interaction with β_2AR [232]. We postulate that endosomal GRK-phosphorylated β_2ARs may indirectly shape the subcellular (including nuclear) cAMP signal by relocating PDE4D isoforms via transient arrestin-mediated receptor internalization.

We have developed β_2AR constructs as well as a knock-in mouse strain via CRISPR Cas9 technology expressing endogenous β_2AR harboring a mutant GRK (S355/356A, GRKΔ) site. We examined the role of GRK phosphorylation of β_2AR on receptor-induced nuclear cAMP signaling in neurons utilizing fluorescence resonance energy transfer (FRET)-based subcellular localized cAMP biosensors in live cell imaging. In this chapter, our data identify a loss of GRK phosphorylation of β_2AR and subsequent internalization leads to a loss of nuclear cAMP signaling. This nuclear cAMP signaling loss is associated with impaired immediate early genes (IEGs) expression in both an overexpression system and in primary neurons expressing endogenous receptors levels. These data provide evidence supporting the necessity of the GRK-pβ_2AR subpopulation and its ability to endocytose to the endosome in generating β_2AR-mediated nuclear cAMP and subsequent gene expression.

Results

Inactivation of the GRK phosphorylation (S355/356) site attenuates β_2AR-induced nuclear cAMP signaling and immediate early genes expression.

We aimed to explore the cellular effects of selective phosphorylation of the β_2-adrenergic receptor (β_2AR) in the CNS. We applied FRET-based ICUE3 sensors localized to the PM (PM-ICUE3) and nucleus (NLS-ICUE3) to detect subcellular cAMP signals induced by β_2AR subpopulations in primary hippocampal neurons (**Figure 2.1A**). Neurons from β_1/β_2AR double knockout (DKO) mice were co-transfected with cAMP ICUE3 biosensors and either wild type (WT)-, GRKΔ(S355/356A), or PKAΔ(S262/262A)-β_2AR

(**Supplementary Figure 2.1A**) to isolate the receptor action (**Figure 2.1B**). Consistent with our previous report [127], β-agonist isoproterenol (ISO) stimulation promoted GRK phosphorylation of S355/356 on a subpopulation of β_2AR (**Figure 2.1C**), which underwent internalization and displayed an intracellular distribution in primary hippocampal neurons. A subpopulation of β_2AR phosphorylated by PKA at S261/262 remained at the plasma membrane (PM). Utilizing β_2AR active conformation specific and Gs mimetic nanobody 80 (Nb80) [266], we showed that Nb80 displayed similar increases in binding to WT and mutant β_2ARs after stimulation with ISO (1μM) (**Figure 2.1D and 2.1E**). Thus, these point mutations do not affect β_2AR from achieving an active conformational state and engaging G protein binding to promote cAMP generation although PKA site phosphorylation does desensitize β_2AR for adenylyl cyclase signaling. Stimulation with ISO (1μM) generated equivalent cAMP signals at the PM in WT-, GRKΔ-, and PKAΔ-β_2AR expressing neurons (**Figure 2.1F and 2.1G**). Deletion of the GRK but not the PKA phosphorylation site attenuated the nuclear cAMP signal (**Figure 2.1H and 2.1I**). Deletion of the GRK but not PKA phosphorylation sites on β_2AR significantly reduced expression of IEGs such as cFOS, FOSB, RHOB, and OLIG2 following stimulation vs untreated control neurons (Δ/ΔCT) suggesting phosphorylation of β_2AR by GRK is necessary for promoting nuclear cAMP signaling and subsequent gene expression (**Figure 2.1J-2.1M**).

We next sought to determine if pharmacological inhibition of GRK phosphorylation of β_2AR prevents nuclear cAMP signaling (**Figure 2A**). Inhibition of GRK with paroxetine but not PKA with H89 attenuated nuclear cAMP signaling while leaving cAMP signal at the PM intact (**Figure 2.2B-2.2E**). Inhibition of GRK also attenuated IEGs expression (**Figure 2.2F-2.2I**). Paroxetine is also a selective serotonin reuptake inhibitor (SSRI). Fluoxetine, an SSRI without any action against GRK, was included as a control. Fluoxetine had no effect on the ISO-induced cAMP signal nor IEGs expression (**Figures 2.2B-2.2I**). Additionally, treatment of neurons expressing WT β_2AR an pretreated with Dyngo4A reduced nuclear but not PM cAMP signal (**Supplementary Figure 2.2A and 2.2B**). Moreover, we expressed either cytosolic or nuclear localized PKI (cyto-PKI or NLS-PKI), a protein inhibitor of PKA, in hippocampal neurons. We found that nuclear but not cytosolic PKI inhibited IEGs expression (**Figure 2.2J and 2.2K**). These data indicate β_2AR-mediated nuclear cAMP signal requires phosphorylation at S355/356 of β_2AR by GRK and subsequent

internalization of the receptor, and that nuclear cAMP signal affects IEGs expression via activation of nuclear PKA.

Endogenous β2AR-induced cAMP signaling in the nucleus requires GRK mediated receptor phosphorylation and internalization.

We next generated whole body knockin GRKΔ mice (**Supplementary Figure 2.3A**) to study the *in vivo* consequences of endogenous β_2AR phosphorylation site inactivation. We next examined endogenous β_2AR-mediated nuclear cAMP signal in primary hippocampal neurons isolated from GRKΔ mice. The hippocampi from GRKΔ and WT mice had similar morphology, protein expression of β_2AR and phosphodiesterase 4 (PDE4), and cAMP levels (**Supplemental Figure 2.3B-2.3E**). Utilizing FRET biosensors (**Figure 2.3A**) we found GRKΔ and WT hippocampal neurons showed similar nuclear cAMP signaling in response to ISO stimulation (**Figure 2.3E and 2.3G**). After preincubation with CGP20712a (CGP), a selective β_1AR inhibitor, we observed a loss of nuclear cAMP signal in response to ISO stimulation in GRKΔ neurons (**Figure 2.3F and 2.3G**). CGP had no effect on ISO induced cAMP signal on the PM in WT and GRKΔ neurons (**Figures 2.3B-2.3D**). In contrast, selective activation of β_1AR (in the presence of β_2AR inhibitor ICI118551) induced similar cAMP levels between WT and GRKΔ neurons (**Supplementary Figure 2.3F-2.3I**). We next examined the role of internalization by utilizing multiple endocytosis inhibitors which attenuated nuclear cAMP in WT neurons (**Figure 2.3H-2.3J, Supplementary Figure 2.3J and 2.3K**). We also utilized barbadin, a β-arrestin-AP2 interaction inhibitor which allows for formation of the β-arrestin-GRK-β_2AR complex but prevents β-arrestin from binding clathrin via adaptor protein 2 [267]. Barbadin inhibited β_2AR internalization and nuclear cAMP (**Figure 2.3K and 2.3L, Figure 2.4I**), supporting that both GRK phosphorylation and receptor internalization are necessary for β_2AR-mediated nuclear signaling.

Interaction of phosphodiesterase 4 and arrestin are necessary for nuclear cAMP signaling; Inhibition of PDE4 rescues nuclear cAMP signal in GRKΔ neurons.

cAMP is highly compartmentalized within the cell to prevent activation of secondary partners unnecessarily. These cAMP microdomains are established in part by various isoforms of phosphodiesterase (PDE), including PDE4D isoforms associated with β_2AR [224, 227, 228, 263]. It is also established that β-arrestin binds to GRK phosphorylated β_2AR [129] and can recruit and scaffold PDE4D

to activated receptor to regulate cAMP signal [268]. Here, we utilized a myristoylated peptide derived from β-arrestin-2, Pep-arr2[269], which inhibits arrestin/PDE4 binding. The Pep-arr2 peptide but not a mutant control peptide with multiple charged amino acids replaced by alanines attenuated β_2AR-mediated nuclear cAMP signaling in WT neurons (**Figure 2.4A-2.4C**). Additionally, neither Pep-arr2 nor mutant peptide affected β_2AR internalization upon ISO stimulation (**Figure 2.4I**). Moreover, inhibition of PDE4 but not PDE3 rescued the nuclear cAMP signaling in GRKΔ hippocampal neurons while modestly increasing nuclear cAMP signaling in WT neurons (**Figure 4D-4H)**. These data highlight the essential role of PDE4 in regulating nuclear cAMP signaling and suggest GRK phosphorylation of β_2AR sequesters β-arrestin and PDE4 on endosome via receptor internalization, allowing the cAMP signal to reach the nucleus.

Sequestration of PDE4 plays a critical role in β_2AR internalization-dependent nuclear cAMP signaling in primary hippocampal neurons.

We next examined distribution of various PDE4 isoforms in WT primary hippocampal neurons. Neurons were isolated and immunofluorescence was used to determine cellular distributions (nuclear vs non-nuclear (**Supplementary Figure 2.4A**) of PDE4D5, PDE4D8, PDE4D9, and PDE4B. PDE4B has been shown to be distributed near the PM [225] and was included as a control. We found that PDE4D5, but not other isoforms had a primarily nuclear distribution (**Figure 2.5A and 2.5B**). PDE4D5 antibody shows minimal signal in PDE4D-KO MEF cells suggesting PDE4D specificity (**Supplementary Figure 2.4B**) We also examined the relative expression of various PDE isoforms in hippocampi isolated from WT and GRKΔ mice. GRKΔ mice show slightly reduced expression of PDE2A and 5A and an increased expression of PDE4D relative to WT (**Figure 2.5C and 2.5D**). Additionally, Pep-arr2 reduced agonist-induced PDE4D5 association with β_2AR (**Figure 2.5E**). Together, these data provide evidence that PDE4D5 has a nuclear distribution and could affect β_2AR-mediated nuclear cAMP signal via association with β_2AR after receptor stimulation.

We next examined how β_2AR stimulation affected PDE localization. PDE4D5 displayed a strong reduction of nuclear localization in wild type hippocampal neurons after ISO stimulation while GRKΔ neurons showed nuclear PDE4D5 before and after ISO stimulation. Additionally, pretreatment with Arr-Pep but not mutant peptide prevented stimulation induced movement of PDE4D5 to the cytosol. Lastly, barbadin

pretreatment also prevented PDE4D5 movement out of the nuclear upon receptor stimulation (**Figure 2.5A and 2.5B**). Together these data suggest stimulation of β_2AR facilitates nuclear cAMP signal via arrestin mediated sequestration of PDE4D5 from the nucleus to the cytosol.

We further assessed the PDE4D5 trafficking induced by other GPCR stimulation in WT neurons. While stimulation with ISO promoted robust nuclear export of PDE4D5, other Gs-PCR agonists such as dopamine, CGRP, and urocortin didn't elicit complete movement of PDE4D out of the nucleus but caused a change in PDE4D5 distribution around the nuclear envelope (**Figures 2.7A and 2.7B**). In comparison, some Gq-PCR agonists elicited no trafficking of PDE4D5 (**Figure 2.7A and 2.7B**). Moreover, we found stimulation of ISO caused robust increases in immediate early gene (IEG) expression, whereas dopamine but not CGRP and PGE1 elicited only small increases (**Figure 2.7C**).

Discussion

Endosomal GPCRs are postulated to deliver cAMP to the nucleus promoting gene expression in physiology and disease [270]. However, the molecular mechanisms on how endosomal GPCRs deliver nuclear cAMP signal are not clear. We have recently shown agonist-driven subpopulations of GRK-phosphorylated β_2AR distributed to endosomes in hippocampal neurons [127]. The present study provides insights into the GRK phosphorylated β_2AR subpopulation and how it contributes to cAMP signals reaching the nucleus via nuclear export of PDE4D5 in living neurons. Our data reveal that deletion of GRK phosphorylation sites on β_2AR prevent nuclear cAMP signaling and nuclear PKA-mediated IEGs expression. Further studies show inhibition of β-arrestin-dependent recruitment of PDE4D5 to β_2AR prevents receptor-induced nuclear cAMP signaling *in vitro*. Inhibition of PDE4 rescues nuclear signaling *in vitro* in hippocampal neurons with deficiency in GRK phosphorylation of β_2AR as well. Moreover, there is differential PDE4D5 export and subsequent IEG expression in cortical neurons depending on the types of GPCR stimulation; only some Gs-coupled GPCRs cause nuclear export of PDE4D5. Together this work highlights the critical role of GRK-phosphorylated β_2AR in agonist-induced nuclear export of PDE4D5, facilitating cAMP signal propagation into the nucleus to promote IEGs expression and long-term memory. Together this work indicates that endosomal GRK-phosphorylated β_2AR recruits a β-arrestin/PDE4D5 complex, indirectly promoting cAMP signal propagation into the nucleus to promote nuclear PKA-mediated IEGs expression.

After agonist stimulation, GRK phosphorylation of β_2AR results in β-arrestin mediated recruitment of different PDE4D isoforms [230, 268], including PDE4D8, normally associated with the receptor at the PM, and PDE4D5 [227, 229], normally distributed in the nucleus [221]. β-arrestin recruitment to β_2AR is ablated when the GRK phosphorylation sites of the receptor are mutated [231]. Additionally, inhibition of GRK2 prevents PDE4D interaction with β_2AR [232]. Here, while GRKΔ receptors fail to undergo agonist-induced internalization and promote cAMP signal in the nucleus, inhibition of PDE4 rescues nuclear cAMP signaling. Internalization of β_2AR promotes β-arrestin mediated recruitment of PDE4D isoforms from the nucleus to the cytoplasm, altering cAMP microdomains, including permitting cAMP signal to reach the nucleus. Indeed, interfering with β-arrestin/PDE4D interaction using a myristoylated peptide [269] causes reduced PDE4D5/β_2AR association and prevents agonist-mediated movement of PDE4D5 from the nucleus to the cytoplasm, and a loss of nuclear cAMP signal without affecting internalization. These data suggest that internalization of GRK-phosphorylated β_2AR alone is insufficient for the receptor to deliver cAMP signal to the nucleus, and additional recruitment and sequestration of PDE4D5 to endosomal GRK-phosphorylated β_2AR is also required.

It is important to note that, while our data suggests endosomal cAMP signaling would be suppressed/restricted by β-arrestin recruiting PDEs to the endosome, local cAMP signaling may still facilitate Epac-based activation of ERK and CaMKII pathways [271, 272]. Our data also do not preclude the possibility that endosomal β_2AR can be further divided into subpopulations. For example, a subset of endosomal β_2ARs may not recruit arrestin/PDE complexes. These receptors could initiate cAMP signaling. It is also possible diffusion of Gαs subunits from active, arrestin/PDE4D5 recruiting endosomal β_2ARs may activate β_2AR internalization independent endosomal adenylyl cyclase 9-produced cAMP signaling [273] to the nucleus. We also show differential PDE4D5 export and subsequent IEG expression in cortical neurons depending on the types of GPCR stimulation; only some Gs-coupled GPCRs cause nuclear export of PDE4D5. Work in MEF cells demonstrated stimulation with dopamine, urocortin, and relaxin, all Gs-PCRs, do not induce nuclear cAMP [234]. Further, pretreatment with dopamine prevented ISO induced nuclear cAMP signal. Urocortin only partially inhibited ISO induced nuclear cAMP and relaxin had no effect [234]. These data may help explain the differential trafficking of PDE4D5 in cortical neurons when stimulating with other GPCR agonists as it demonstrates differential effects on β_2AR-mediated nuclear cAMP signal and

likely alters the dynamics of PDE4D5 export. Indeed, dopamine and urocortin stimulation appears to enrich PDE4D5 around the nuclear envelope (**Figure 2.7B**) which may explain the ablation of β_2AR-mediated nuclear cAMP [234] by preventing exogenous cAMP from reaching the nucleus. Further, this strongly suggests the source of cAMP is exogenous rather than nuclear in origin. Despite these caveats, our data argue against the current notion of endosomal signaling. Rather, these data suggest nuclear cAMP signaling is unlikely to originate from endosomal GRK-phosphorylated β_2AR due to an increased association of PDE4D isoforms. We therefore propose recruitment of β-arrestin/PDE4D5 to GRK-phosphorylated β_2AR on the endosome functionally sequester PDE4D5 and act in synergy with other cAMP sources, facilitating membrane bound β_2AR subpopulation-produced cAMP signal reaching the nucleus and drive receptor-mediated IEG expression (**Figure 2.6A**).

Taken together, our data show a subpopulation of GRK phosphorylated β_2AR in mice is critical for nuclear cAMP signaling and IEG expression. Our data support that the GRK-phosphorylated β_2AR subpopulation is necessary to recruit PDE4D5, which are critical in facilitating receptor-cAMP signal propagation into the nucleus. These data reveal an indirect role for endosomal receptors to regulate nuclear cAMP signals in physiological settings, an alternative to postulated direct endosomal receptor signaling to the nucleus (**Figure 2.8A**).

Limitations of study and alternative interpretations

It is important to note limitations and alternative interpretations of the data presented herein. We posit GRK phosphorylation of β_2AR causes arrestin-mediated internalization of the receptor and recruits PDE4D5 from the nucleus to the cytosol allowing for cAMP to propagate to the nucleus. This nuclear cAMP signal induced IEG expression. However, several limitations exit. While the FRET and immunofluorescence data combine to assert arrestin is necessary for movement of PDE4D5 out of the nucleus, this study does not explain the how β-arrestin facilitates the movement of PDE4D5 out of the nucleus. Both β-arrestin1 and β-arrestin2 could be involved in our proposed PDE4D5 export form the nucleus. However, we hypothesize β-arrestin2 mediated this export. β-arrestin2 preferentially facilitates internalization of the β_2AR from the PM to the endosome. β-arrestin2 has both nuclear export sequences (NES, $L^{395}XL^{397}$) [274] and nuclear location sequence (NLS, K^{157}) [275] whereas β-arrestin1 only has an

NLS motif (K^{157})[275]. β-arrestin2 but not β-arrestin1 has been shown to redistribute the prooncogenic ubiquitin ligase Mdm2 [274] and JNK3 kinase [276]from the nucleus to the the cytoplasm. This redistribution depends on the presence of the NES ($L^{395}XL^{397}$) in the C terminus of β-arrestin2, which mediates the nuclear export of β-arrestin2 by leptomycin B-sensitive exportins [277]. Indeed, an initial isolation of primary hippocampal neurons from β-arrestin2 knockout mice transfected with NLS-ICUE3 revealed ablation of nuclear cAMP signal similar to GRKΔ hippocampal neurons (data not shown). However, these data need to be repeated several more times. Conversely, β_2AR is a prototypical class A GPCR [278]. As such, β-arrestin2 is at most only transiently complexed with the receptor and may not be present at all at the endosome. While it could be the case that transient presence of β-arrestin2 with the receptor is enough to facilitate PDE4D5 export from the nucleus, it remains unclear if β-arrestin2 is present at the nucleus and/or the endosome to facilitate said export or how this export of PDE4D5 occurs. Further, the present of only an NLS motif (K^{157}) suggests β-arrestin1 is located in the nucleus. It could be the case that β-arrestin1 facilitates PDE4D5 localization to the nucleus. However, if or how β-arrestin1 is involved with PDE4D5 nuclear enrichment remains unclear. Further detailed studies are necessary to dissect the mechanism of PDE4D5 export proposed in this study.

This study focuses on β_2AR signaling. However, α-adrenergic receptors also respond to NE signaling and can couple to both Gs and Gi. Indeed, α-adrenergic receptors are known to be involved in learning and memory[116-119]. While beyond the scope of this study, future studies are needed to determine the contributions of these α-receptors in the context of the observations presented in this study.

The data presented herein also offer alternative interpretations. While the data presented suggest nuclear cAMP is not being produced at the endosome due to recruitment of PD4D5. Rather, internalization of the receptor facilitates cAMP signaling reaching the nucleus. However, these data do not explain the source of the nuclear cAMP signaling. One possible source is cAMP produced at the plasma membrane by the PKA-p β_2AR subpopulation is reaching the nucleus from the plasma membrane. However, another interpretation of these data does not require internalization of the receptor. Phosphorylation of β_2AR by PKA may facilitate switching of Gs to Gi or simply decoupling Gs from β_2AR thereby desensitizing adenylyl cyclase and reducing cAMP production at the plasma membrane. In PKAΔ

expressing neurons, we show intact nuclear cAMP signaling but in GRKΔ expressing neurons, we see ablated nuclear cAMP signal (**Figure 2.1H and 2.1I**). It could be the case that PKAΔ expressing neurons, which no longer can desensitize adenylyl cyclase signaling via phosphorylation of β_2AR, is producing more cAMP at the PM and this overabundance of cAMP is overwhelming PDE blockades in various cellular domains to reach the nucleus (**Figure 2.8B**). Data showing cytoplasmic expression of PKI does not reduce IEG expression (**Figure 2.2J and 2.2K**) also supports this hypothesis as cytoplasmic PKI would affect plasma membrane bound PKA, prevent desensitization of adenylyl cyclase signaling, and allow cAMP to propagate to the nucleus. Further support for this interpretation is the rescue data in GRKΔ neurons (**Figure 2.4E and 2.4F**). Rather than relieve the PDE4D5 blockade in the nucleus, PDE4 inhibition results in fewer plasma membrane located receptors to be active in order for the nuclear signal to propagate. While this interpretation of the data does not fit with the endocytosis inhibitor data presented (**Figure 2.3I-2.3L**), the relative preponderance of off target effects associated with endocytosis inhibitors does not rule out this hypothesis. Additionally, this hypothesis provides no explanation for the observed PDE4D5 (**Figure 2.6A and 2.6B**) movement out of the nucleus under β_2AR stimulation. One possible explanation for this is that endocytosis does allow PDE4D5 to leave the nucleus helping to facilitate propagation of the increased cAMP signal at the plasma membrane. This mechanism would still result in β_2AR subpopulations working in concert to facilitate nuclear cAMP signaling. Regardless of the caveats outlined above, this hypothesis is worth investigating further. Indeed, experimentally this hypothesis could be easily tested using FRET and the NLS-ICUE3 sensor along with overexpression of mutant β_2AR with both GRK and PKA phosphorylation sites removed in DKO neurons. If this hypothesis is correct, these GRKΔ/PKAΔ expressing neurons would have normal nuclear cAMP signal.

Methods

Experimental model and subject details

Animals

Animals were housed in a UC Davis AAALAC certified vivarium on a 12-hour day/night cycle (7am to 7pm), grouped 3-5 mice per cage, and provided free access to food and water. β_1AR/β_2AR double knockout (DKO) mice were obtained from Jackson Laboratories (Bar Harbor, MW; #003810) to

produce P0-P1 postnatal DKO pups. GRKΔ mice were developed by Cyagen (Santa Clara, CA) and backcrossed 9 times to obtain a clean C57Bl6/J background. These mice were used to produce P0-P1 pups or aged to 70-130 days for biochemical studies. Wild type C57Bl6/J mice were obtained from Jackson Laboratories (Bar Harbor, ME; #000664) to produce P0-P1 postnatal WT pups and aged to 70-130 days for biochemical studies. All animals were handled according to approved institutional animal care and use committee (IACUC) protocols (#21993) of the University of California at Davis and in accordance with NIH guidelines for the use of animals.

Method Details

Cell culture

Human Embryonic Kidney Cells

Human embryonic kidney 293 (HEK293) cells were obtained from American Type Culture Collection (ATCC, Manassas, VA) and maintained in Dulbecco's modified Eagle's medium (Corning, MA) supplemented with 10% fetal bovine serum (Sigma-Aldrich, St. Louis MO). HEK293 cells were transfected with plasmids using polyethylenimine (PEI) according to manufacturer's instructions (Sigma-Aldrich, St. Louis, MO).

Primary Neuron Culture

Primary mouse hippocampal or cortical neurons were isolated and cultured from early postnatal (P0-P1) wild type C57Bl6/J (Jackson Laboratories), β_1AR/β_2AR double knockout (DKO) mouse pups, and GRKΔ-KI (developed by Cyagen; Santa Clara, CA) as previously described [127]. Briefly, pups were decapitated, brains were removed and placed in ice cold HBSS, and hippocampi or cortices dissected out under a dissection scope. Hippocampi were then dissociated by 0.25% trypsin treatment in HBSS at 37^{o}C for 16 minutes. After digestion, hippocampi were moved to cold HBSS containing 25% FBS gently mixed, then moved HBSS containing 10% FBS and gently mixed, and finally into HBSS prewarmed in an incubator containing 5% CO2 at 37^{o}C. Hippocampi were then triturated at room temperature using a Pipet-aid (Drummond) set to slow using a 10 mL serological pipet until no more pieces of tissue were visible. Solution was spun down for 4 minutes at 1100 RPM, HBSS aspirated, and pellet resuspended in

Neurobasal medium supplemented with GlutaMax (Thermo Fisher Scientific, Waltham, MA), gentamicin (Promega), B-27 (Thermo Fisher Scientific, Waltham, MA) and 10% FBS and counted. Neurons were plated on poly-D-lysine-coated (Sigma-Aldrich, St. Louis MO: #P6407) #0 12 mm glass coverslips (Glaswarenfabrik Karl Hecht GmbH & Co. KG, Sondheim, Germany; REF 92100100030) for imaging and FRET at a density of 7500 cells/cm^2 and 10,000 cells/cm^2, respectively.

Neurons were transfected using the Ca^{2+}-phosphate method as previously describe[127]. Briefly, cultured neurons at either 3-5 days *in vitro* (DIV), 6–8 days DIV, or 10–12 DIV were switched to pre-warmed Eagle's minimum essential medium (EMEM, Thermo Scientific, MA) supplemented with GlutaMax 1 hour before transfection, conditioned media were saved. DNA precipitates were prepared by 2×HBS (pH 6.96 DKO neurons, pH 7.02 WT and GRKΔ neurons) and 2 M $CaCl_2$. After incubation with DNA precipitates for 1 h, neurons were incubated in 10% CO_2 pre-equilibrium EMEM for 20 min, then replaced with conditioned medium. WT and GRKΔ neurons were transfected with PM-ICUE3 using Lipofectamine3000 (Thermo Fisher Scientific, Waltham, MA) following manufacturer's protocol. FRET biosensor PM-ICUE3, and NLS-ICUE3 have been previously described [279].

Western Blot

Hippocampi excised from the brains from handled control animals were used for this study. Hippocampi were excised, flash frozen in liquid nitrogen, and stored at -80 C until use. Tissue was homogenized in lysis buffer (25 mmol/L HEPES, ph 7.4; 5 mmol/L EDTA; 150 mmol/L NaCl; 0.5% Triton X-100; and protease and phosphatase inhibitors containing 2 mmol/L Na_3VO_4, 1 mmol/L PMSF, 10 mmol/L NaF, 10 µg/mL Aprotinin, 5 mmol/L Bestatin, 10 µg/mL Leupeptin, and 2 µg/mL Pepstain A). Protein was quantified using a Pierce BSA assay (ThermoFisher, #23225) and read on a CLARIOStar plate reader (BMG Labtech, Cary, NC). Equal amounts of protein (50 µg) were resolved on an 8% acrylamide SDS-PAGE gel. Bands were detected using anti-β_2AR (Santa Cruz #sc-570 lot# L0809), anti-PDE4 (Abcam # ab14628), and anti-γ-tubulin (Sigma-Aldrich #T7451). Primary antibodies were revealed with IRDye 800 CW Goat anti-Mouse IgG secondary antibody (1:5000 #926-32210, Licor, NE) or IRDye 800 CW Goat anti-Rabbit IgG secondary antibody (1:5000 #926-32211, Licor, NE) using a Bio-Rad

ChemiDoc MP Imager (Bior-Rad Laboratories, Hercules, CA). Optical density of bands was analyzed using Image J software (NIH; https://imagej.nih.gov/ij/). The arbitrary unit (A.U.) for western blots was defined as the ratio of intensity of the protein of interest relative to the intensity of a reference protein as indicated.

Co-Immunoprecipitation

Co-immunoprecipitation was carried out on 293 cells homogenized in 0.4 mL of lysis buffer (composition) then centrifuged for 30 minutes at 4C and 13,200 rpm. Supernatant was transferred to a fresh centrifuge tube and 10 µL Protein A-Sepharose beads (GE17-0780-01, Millipore, MA) and 1.0 µg of control IgG antibody (sc-66931, SCBT, CA) was added. Tubes were then incubated for 1 hour at 4C to preclear samples. Precleared samples (1 mL) were then incubated with 30 µL Protein A-Sepharose beads and 2 µg of Anti-flag M1 (Sigma-Aldrich, # F3040) or anti-IgG antibody (sc-66931, SCBT, CA) at 4C overnight. After incubation, beads were rinsed with lysis buffer 3 times. The washed beads were then mixed with 30 µL 2x SDS loading buffer (#161-0747, Bio-Rad Laboratories, CA) and subject to electrophoresis for probing FLAG-β_2AR, Nb80, PDE4D5. Gel images were taken and quantified using a Bio-Rad ChemiDoc MP Imager.

Förster Resonance Energy Transfer (FRET)

FRET measurements were performed as previously described [227]. Briefly, DKO primary hippocampal neurons were co-transfected with FLAG-β_2AR (WT, GRKΔ, or PKAΔ) and either PM-ICUE3 or NLS-ICUE3 via the calcium phosphate method. WT or GRKΔ primary hippocampal neurons were transfected with NLS-ICUE3 via the calcium phosphate method. Cells were imaged on a Zeiss Axiovert 200M microscope with a 40×/1.3 numerical aperture oil-immersion lens and a cooled CCD camera using MetaFluor software. Dual emission ratio imaging was acquired with a 420DF20 excitation filter, a 450DRLP diachronic mirror, and two emission filters (475DF40 for cyan and 535DF25 for yellow). The acquisition was set with 0.2 s exposure in both channels and 20 s elapses. Images in both channels were subjected to background subtraction, and ratios of yellow-to-cyan were calculated at different time points.

For traces, ratios were normalized to baseline. Maximum FRET ratios were calculated as % change from baseline after treatment. Cells were treated as described in figures.

cAMP measurements

Hippocampi extracted from WT C57Bl6/J or GRKΔ mice aged 70-130 days were solubilized according to manufacturer's protocols (Promega cAMP Glo Max, V1681, Madison, WI) and cAMP levels were determined from dilution curve using a microplate reader (CLARIOStarPlus, BMG Labtech).

qRT-PCR

Total RNA was extracted from cells and tissue using Tri-Reagent (Sigma-Aldrich T9424, St. Louis, MO) via manufacturer's protocols. Briefly, cells tissue was homogenized in Tri-Reagent and phase separated using chloroform. The clear, aqueous layer was transferred to a fresh tube and precipitated with isopropyl alcohol. Following precipitation, the RNA pellet was washed twice using 80% ethanol, dried, mixed with RNAse/DNAse free water. Genomic DNA was removed using a DNAse kit (Sigma-Aldrich AMPD1) per manufacturer's protocol. RNA was then quantified using a CLARIOStarPlus microplate reader. Reverse transcription was carried out on extracted RNA using a high-capacity cDNA reverse transcription kit (Applied Biosystems #4368814 and a thermocycler (Veriti 96-well Thermal Cycler, Applied Biosystems). qRT-PCR was carried out on cDNA using PowerUp SYBR Green Master Mix (Applied Biosystems, #A25742) and appropriate primers using a QuantStudio3 Real Time PCR system (Applied Biosystems).

Confocal Microscopy

Wild type hippocampal neurons were isolated as described above. At DIV 9, cells were transfected with mEYFP-FLAG-β_2AR using the calcium phosphate method described above. The next day, cells were then pretreated with Arr2 peptide (1 μM), mutated control peptide (1 μM), and barbadin (50 μM) for 30 minutes and CGP20207a (3 μM) for 5 minutes and then treated with or without isoproterenol (1 μM) for 20 minutes. Cells were then rinsed with ice cold PBS without calcium fixed with 4% paraformaldehyde for 20 minutes and then rinsed with ice cold PBS without calcium again. Cells were then permeabilized using ice cold PBS containing 0.2% Triton-X100 and 2% goat serum for 15 minutes

and then washed with ice cold PBS containing 0.05% Triton-X100, 0.2% BSA, and 0.2% goat serum three times. Coverslips were dried and then mounted on glass slides using anti-fade mounting media containing DAPI (H1500-Vector Laboratories, Burlingame, CA) and left to dry overnight. Confocal imaging was carried out using a Leica Falcon SP8 FLIM microscope using a 63x/1.4 oil objective.

Wild type and GRKΔ hippocampal neurons were isolated as described above. At DIV 14, cells were treated with or without 10 μM isoproterenol for 30 minutes. Cells were then rinsed with ice cold PBS without calcium fixed with 4% paraformaldehyde for 20 minutes and then rinsed with ice cold PBS without calcium again. Cells were then permeabilized using ice cold PBS containing 0.2% Triton-X100 and 2% goat serum for 15 minutes and then washed with ice cold PBS containing 0.05% Triton-X100, 0.2% BSA, and 0.2% goat serum three times. Coverslips were then incubated with PDE4D5 (1:50, Abcam Ab14626, Cambridge, UK) antibody overnight at 4C. Cover slips where then washed 3 more times, incubated with Goat anti-rabbit IgG (H+L) Alexa-488 secondary antibody (1:1000, Invitrogen A-11034, Waltham, MA) in the dark, then washed three more times. Next, coverslips were mounted on glass slides using anti-fade mounting media containing DAPI (H1500-Vector Laboratories, Burlingame, CA). Confocal imaging was carried out using a Leica Falcon SP8 FLIM microscope using a 63x/1.4 oil objective.

Primary hippocampal neurons isolated from β_1/β_2AR double knockout (DKO) mice at 7-14 DIV were transfected with cAMP biosensor PM-ICUE3 or NLS-ICUE3 together with FLAG-tagged human β_2AR as described above. Cells were then rinsed with ice cold PBS without calcium fixed with 4% paraformaldehyde for 20 minutes and then rinsed with ice cold PBS without calcium again. Cells were then permeabilized using ice cold PBS containing 0.2% Triton-X100 and 2% goat serum for 15 minutes and then washed with ice cold PBS containing 0.05% Triton-X100, 0.2% BSA, and 0.2% goat serum three times. Coverslips were dried and then mounted on glass slides using anti-fade mounting media containing DAPI (H1500-Vector Laboratories, Burlingame, CA) and left to dry overnight. Confocal imaging was carried out using a Leica Falcon SP8 FLIM microscope using a 63x/1.4 oil objective.

Primary hippocampal neurons isolated from β_1/β_2AR double knockout (DKO) mice at 7-14 DIV were transfected with FLAG-tagged human β_2AR as described above. Cells were then rinsed with ice cold PBS without calcium fixed with 4% paraformaldehyde for 20 minutes and then rinsed with ice cold PBS

without calcium again. Cells were then permeabilized using ice cold PBS containing 0.2% Triton-X100 and 2% goat serum for 15 minutes and then washed with ice cold PBS containing 0.05% Triton-X100, 0.2% BSA, and 0.2% goat serum three times and incubated with primary antibody (PKA-pβ_2AR or GRK-pβ_2AR) overnight. Cells were then washed 3 more times and incubated with secondary antibody (pPKA261/262 - Clone 2G3 and 2E, pGRK355/356 – clone 10A5 were kindly provided by Dr. Richard Clark, UT Houston) for 1 hour at room temperature, and then washed 3 more times. Coverslips were dried and then mounted on glass slides using anti-fade mounting media containing DAPI (H1500-Vector Laboratories, Burlingame, CA) and left to dry overnight. Confocal imaging was carried out using a Leica SP8 Falcon FLIM microscope using a 63x/1.4 oil objective.

Brain tissue harvested, cryosliced, and mounted as described below. Mounted slices were permeabilized using ice cold PBS containing 0.2% Triton-X100 and 2% goat serum for 15 minutes and then washed with ice cold PBS containing 0.05% Triton-X100, 0.2% BSA, and 0.2% goat serum three times. Slices were dried and then coverslips mounted using anti-fade mounting media containing DAPI (H1200-Vector Laboratories, Burlingame, CA) and left to dry overnight. Confocal imaging was carried out using a Leica Falcon SP8 FLIM microscope using a 63x/1.4 oil objective.

Brain Tissue Harvest

Animals were anesthetized with isoflurane, brains removed, and hippocampi excised as previously described [280]. Briefly, tissue was snap frozen for biochemical analysis, fixed in 10% buffered formalin phosphate (SF100, Thermo Fisher Scientific, Waltham MA) at 4 C for histochemical staining, or placed in TRI reagent (T9424, Sigma-Aldrich, St. Louis, MO) for RNA extraction. After 3 days in formalin, brains were transferred to 30% sucrose and left a minimum of 3 days to dehydrate at 4C. Following dehydration, brains were mounted in Tissue Tek OCT medium (#4853, Sakura Finetek, Torrance, CA), frozen, and cryo-sectioned using a Leica CM1860 cryostat into 40 µM sections which were mounted onto tissue-specific glass slides (Thermo-Fisher #12-550-15, Waltham, MA) for staining.

Diagram development.

Diagrams were created with BioRender.com

Data Analysis

Data were analyzed using GraphPad Prism9 software (GraphPad Inc., San Diego, CA) and expressed as mean ± S.E.M. as indicated in figure legends. Differences between two groups were assessed by appropriate two-tailed unpaired Student's *t*-test. Differences among three or more groups were assessed by one-way ANOVA with Tukey's post hoc test. $P < 0.05$ was considered statistically significant.

Figure 2.1

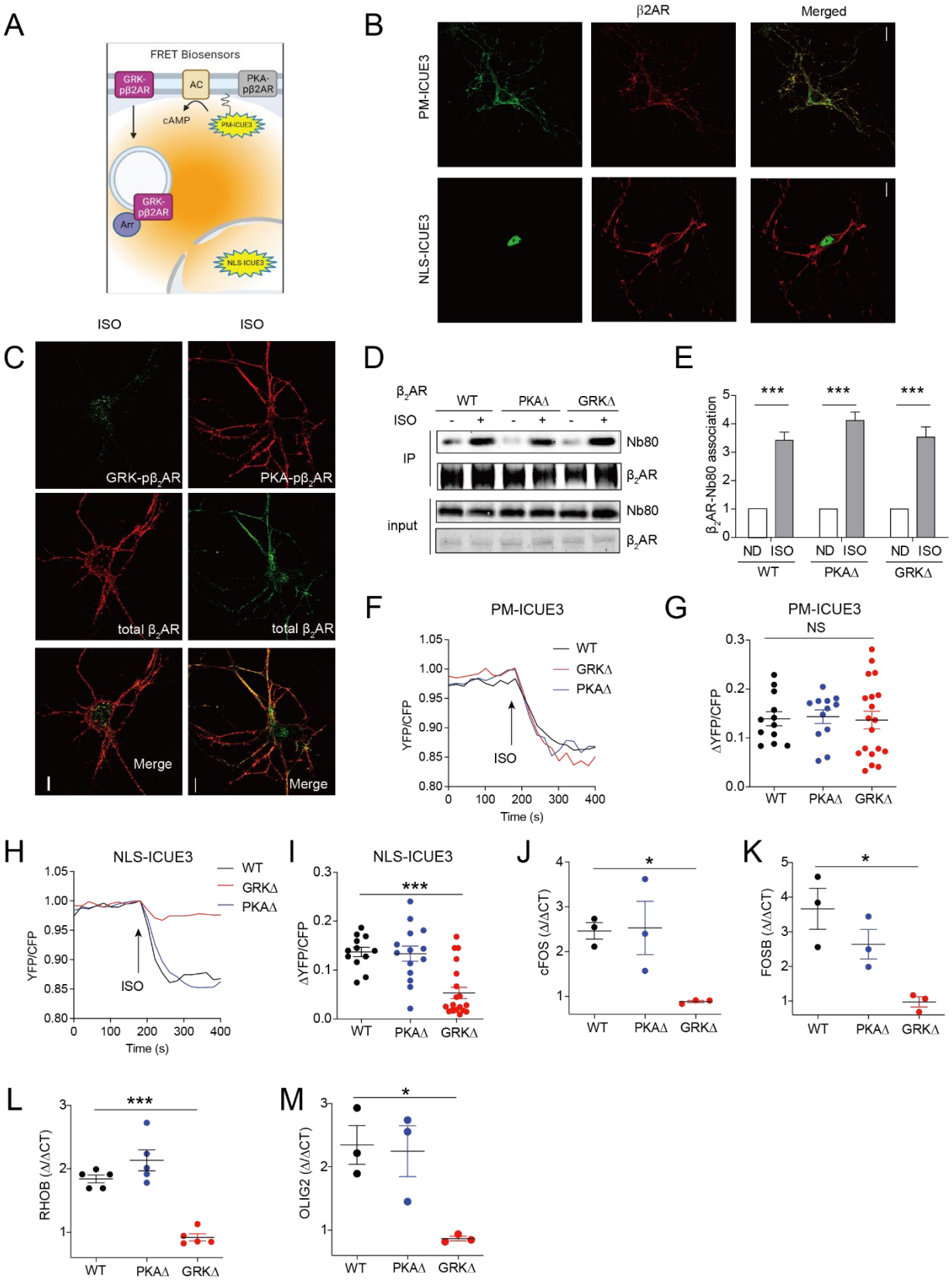
A
FRET Biosensors
GRK-pβ2AR
AC
PKA-pβ2AR
cAMP
PM-ICUE3
GRK-pβ2AR
Arr
NLS-ICUE3
B
β2AR
Merged
PM-ICUE3
NLS-ICUE3
C
ISO
ISO
GRK-pβ2AR
PKA-pβ2AR
total β2AR
total β2AR
Merge
Merge
D
β2AR
WT
PKAΔ
GRKΔ
ISO
IP
Nb80
β2AR
input
Nb80
β2AR
E
β2AR-Nb80 association
ND ISO
WT
PKAΔ
GRKΔ
F
PM-ICUE3
YFP/CFP
ISO
Time (s)
WT
GRKΔ
PKAΔ
G
PM-ICUE3
NS
ΔYFP/CFP
WT
PKAΔ
GRKΔ
H
NLS-ICUE3
YFP/CFP
ISO
Time (s)
WT
GRKΔ
PKAΔ
I
NLS-ICUE3
ΔYFP/CFP
WT
PKAΔ
GRKΔ
J
cFOS (ΔΔCT)
WT
PKAΔ
GRKΔ
K
FOSB (ΔΔCT)
WT
PKAΔ
GRKΔ
L
RHOB (ΔΔCT)
WT
PKAΔ
GRKΔ
M
OLIG2 (ΔΔCT)
WT
PKAΔ
GRKΔ

Figure 2.1. Inactivation of a β_2AR GRK-phosphorylation site reduces nuclear cAMP signal and cAMP-dependent gene transcription in primary hippocampal neurons via loss of endocytosis.

(A) Diagram of subcellular localization of the ICUE3 sensor at the plasma membrane (PM-ICUE3) and nucleus (NLS-ICUE3) in neurons. (B) Representative images of primary hippocampal neurons isolated from β_1/β_2AR double knockout (DKO) mice were transfected with cAMP biosensor PM-ICUE3 or NLS-ICUE3 (green) together with FLAG-tagged human β_2AR (red) as indicated. C) Primary hippocampal neurons isolated from DKO mice were transfected with FLAG-tagged WT β_2AR as indicated. Cells were treated with 1 □M ISO for 5 minutes, fixed, and immunostained with antibodies specific for phosphorylated β_2AR at either S261/262 (PKA-pβ_2AR, Right) or S355/356 (GRK-pβ_2AR, Left). (D and E) Immunoprecipitation of WT- or mutant-β_2AR and β_2AR conformation-specific Gs mimetic nanobody Nb80 after 1 μM ISO treatment for 10 minutes as indicated. The pull down β_2AR and Nb80 were detected via western blot and quantified. (n = 4). ***p<0.001 by 1-way ANOVA followed by Tukey's test. (F and G) Primary hippocampal neurons isolated from DKO mice were transfected with cAMP biosensor PM-ICUE3 or NLS-ICUE3 together with WT or mutant β_2AR (S261/262A, PKAΔ and S355/356A, GRKΔ) as indicated. Cells were treated with 1 μM ISO and changes in ICUE3 FRET(YFP/CFP) ratio were measured. (H and I) The maximum changes in ICUE3 FRET ratio with ISO treatment are plotted. Data represents mean ± SEM of individual neurons from 8 isolations. ***p<0.001 vs WT by 1-way ANOVA followed by Tukey's test. (J-M) DKO neurons were infected with lentiviral vectors for WT or mutant β2AR for 4 days. Transcriptional changes of indicated genes in response to a 2-hour stimulation of 1 μM ISO were measured by qRT-PCR and compared to unstimulated cells. N=3-5 *p<0.05; ***p<0.001 vs WT by one way ANOVA followed by Tukey's test. Data represents mean ± SEM of individual experiments. See also Figure S2.1 and S2.2

Figure 2.2

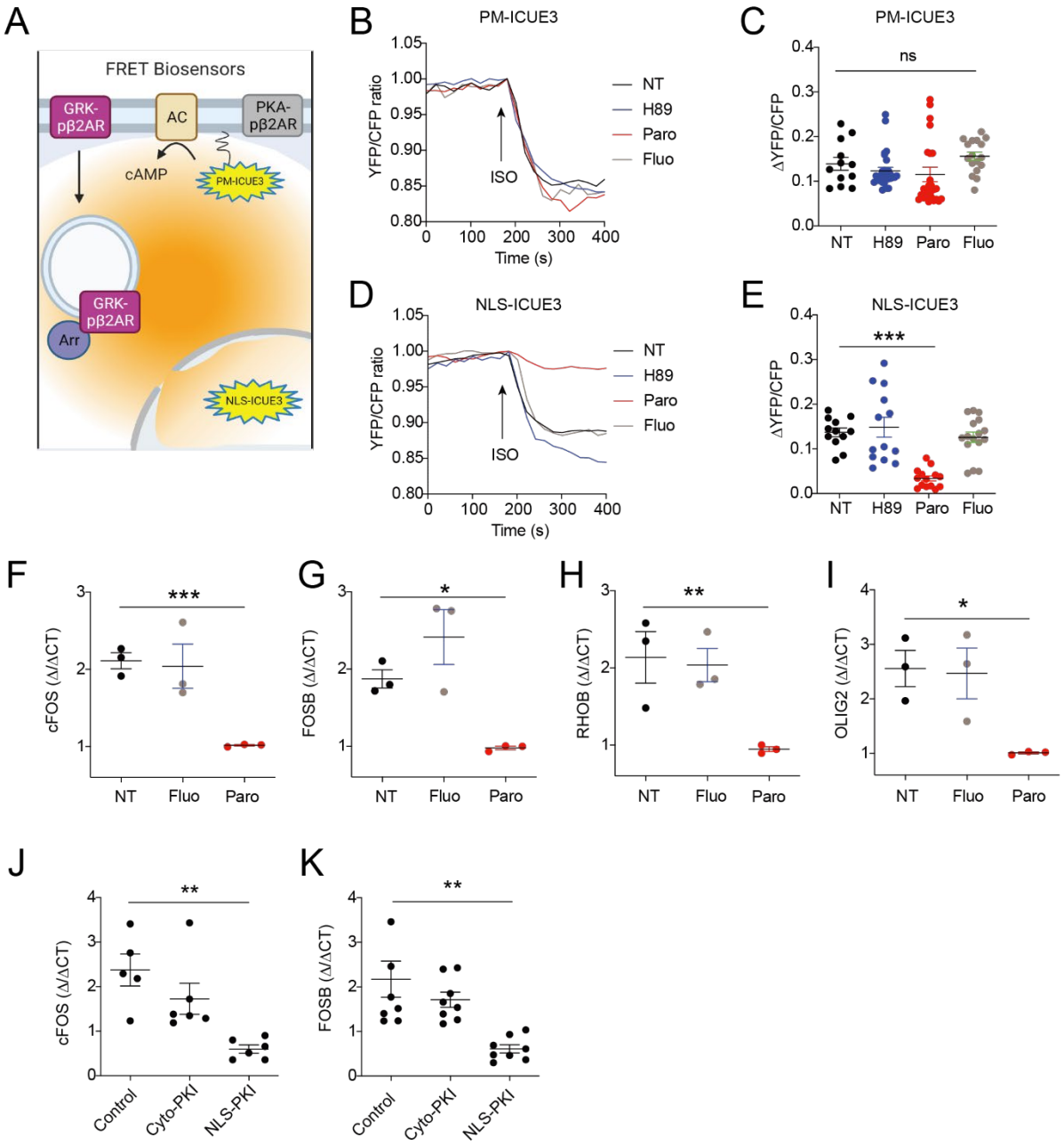
A
FRET Biosensors
GRK-pβ2AR
AC
PKA-pβ2AR
cAMP
PM-ICUE3
GRK-pβ2AR
Arr
NLS-ICUE3
B
PM-ICUE3
YFP/CFP ratio
ISO
Time (s)
NT
H89
Paro
Fluo
C
PM-ICUE3
ns
ΔYFP/CFP
D
NLS-ICUE3
E
NLS-ICUE3
***
F
cFOS (Δ/ΔCT)
G
FOSB (Δ/ΔCT)
H
RHOB (Δ/ΔCT)
I
OLIG2 (Δ/ΔCT)
J
cFOS (Δ/ΔCT)
Control
Cyto-PKI
NLS-PKI
K
FOSB (Δ/ΔCT)

Figure 2.2. Pharmacologic inhibition of GRK reduces nuclear cAMP signal and cAMP-dependent gene transcription in primary hippocampal neurons.

(A) Diagram of subcellular localization of the ICUE3 sensor at the plasma membrane (PM-ICUE3) and nucleus (NLS-ICUE3) in neurons. (B-E) Primary hippocampal neurons isolated from DKO mice were transfected with cAMP biosensor PM-ICUE3 or NLS-ICUE3 together with WT or mutant β_2AR as indicated. Cells were pretreated with H89 (10 μM), Paroxetine (30 μM), or Fluoxetine (30 μM) for 30 minutes prior to stimulation with 1 μM ISO. Changes in cAMP FRET ratio were measured. The maximum changes in ICUE3 FRET (YFP/CFP) ratio relative to baseline after ISO treatment are plotted. Data represent the mean ± SEM of individual neurons from eight isolations. ***p<0.001 vs. no-pretreatment (NT) by 1-way ANOVA followed by Tukey's test. (F-G) Primary hippocampal neurons isolated from β_1/β_2AR double knockout DKO neurons were infected with lentiviral vectors for WT-β_2AR for 4 days. Neurons were pretreated with Paroxetine (30 μM) or Fluoxetine (30 μM) for 30 minutes before 2-hour stimulation with 1 μM ISO. Transcriptional changes of indicated genes in response to ISO stimulation compared to unstimulated cells were measured by qRT-PCR. Data represent mean ± SEM. N = 3 *p<0.05; **p<0.01; ***p<0.001 vs NT by one way ANOVA followed by Tukey's test. (J, K) Primary hippocampal neurons isolated from WT mice were infected with adenoviruses expressing RFP (control), cytosol-PKI, or NLS-PKI for 3 days. Neurons were treated for 2 hours with 1 μM ISO. Transcriptional changes were measured by qRT-PCR and compared to unstimulated cells (ND). Data represent the mean ± SEM. N = 5 **p<0.01 by one-way ANOVA followed by Tukey's test.

Figure 2.3

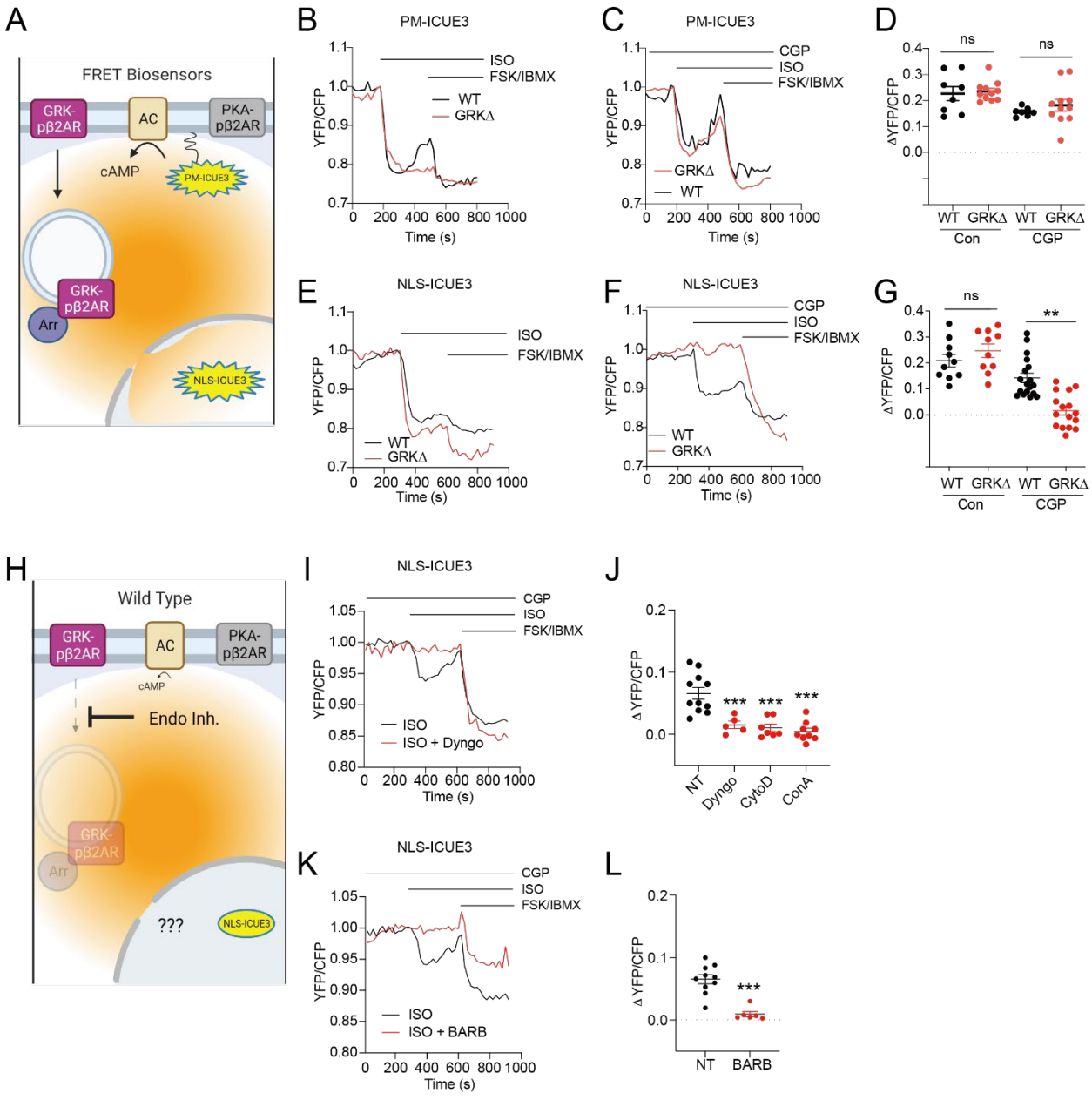
A
FRET Biosensors
GRK-pβ2AR
AC
PKA-pβ2AR
cAMP
PM-ICUE3
GRK-pβ2AR
Arr
NLS-ICUE3
B
PM-ICUE3
ISO
FSK/IBMX
WT
GRKΔ
YFP/CFP
Time (s)
C
PM-ICUE3
CGP
ISO
FSK/IBMX
GRKΔ
WT
YFP/CFP
Time (s)
D
ns
ns
ΔYFP/CFP
WT GRKΔ WT GRKΔ
Con
CGP
E
NLS-ICUE3
ISO
FSK/IBMX
WT
GRKΔ
YFP/CFP
Time (s)
F
NLS-ICUE3
CGP
ISO
FSK/IBMX
WT
GRKΔ
YFP/CFP
Time (s)
G
ns
**
ΔYFP/CFP
WT GRKΔ WT GRKΔ
Con
CGP
H
Wild Type
GRK-pβ2AR
AC
PKA-pβ2AR
cAMP
Endo Inh.
GRK-pβ2AR
Arr
???
NLS-ICUE3
I
NLS-ICUE3
CGP
ISO
FSK/IBMX
ISO
ISO + Dyngo
YFP/CFP
Time (s)
J
ΔYFP/CFP
***
***
***
NT
Dyngo
CytoD
ConA
K
NLS-ICUE3
CGP
ISO
FSK/IBMX
ISO
ISO + BARB
YFP/CFP
Time (s)
L
ΔYFP/CFP
***
NT
BARB

Figure 2.3. Endogenous β2AR-induced cAMP signaling in the nucleus requires GRK mediated receptor phosphorylation and endocytosis.

Primary hippocampal neurons isolated from WT or GRKΔ mice were transfected with cAMP biosensor NLS-ICUE3 or PM-ICUE3 as indicated. (A) Diagram of subcellular localization of the ICUE3 sensor at the plasma membrane (PM-ICUE3) and nucleus (NLS-ICUE3) in neurons. (B-G) Neurons were pretreated with or without 300 nM CGP20712a (CGP, 5 minutes) before stimulation with 100 nM ISO and followed by 10 μM forskolin (FSK) and 1 μM IBMX (as positive control) as indicated. The changes in YFP/CFP FRET ratio were recorded. Dot plots show the maximum FRET response (YFP/CFP) ratio relative to baseline in WT and GRKΔ-KI neurons after ISO treatment. Data represent mean ± SEM of individual mice. ** $p<0.01$ vs WT via student's t-test (H) Diagram of endocytosis inhibitor administration. (I and J) Primary hippocampal neurons isolated from WT or GRKΔ mice were transfected with cAMP biosensor NLS-ICUE3. Neurons were treated with 300 nM CGP20217a (CGP) as indicated during FRET measurement. Neurons were also pretreated with Dyngo4a (1 μM, 30 minutes), concanavalin A (25 ug/ml, 30 minutes), or cytochalasin D (10 μM, 30 minutes) before stimulation with 100 nM ISO followed by 10 μM forskolin (FSK) and 1 μM IBMX as indicated. The changes in ICUE3 YFP/CFP FRET ratio were recorded. Dot plots show the maximum changes in FRET ratio relative to baseline in WT and GRKΔ neurons after ISO treatment. Data represent mean ± SEM of individual neurons from 4 isolations. ***$p<0.001$ vs NT by 1-way ANOVA followed by Tukey's test. (K and L) Neurons were pretreated with barbadin (50 μM, 30 minutes) before stimulation with 100 nM ISO followed by 10 μM forskolin (FSK) and 1 μM IBMX. The changes in NLS-ICUE3 YFP/CFP FRET ratio were recorded. (e) Dot plots show the maximum changes in FRET ratio relative to baseline in WT and GRKΔ neurons after ISO treatment. Data represent mean ± SEM of individual neurons from 4 isolations. ****$p<0.001$ vs NT by student's t-test. See also Figure S2.3.

Figure 2.4

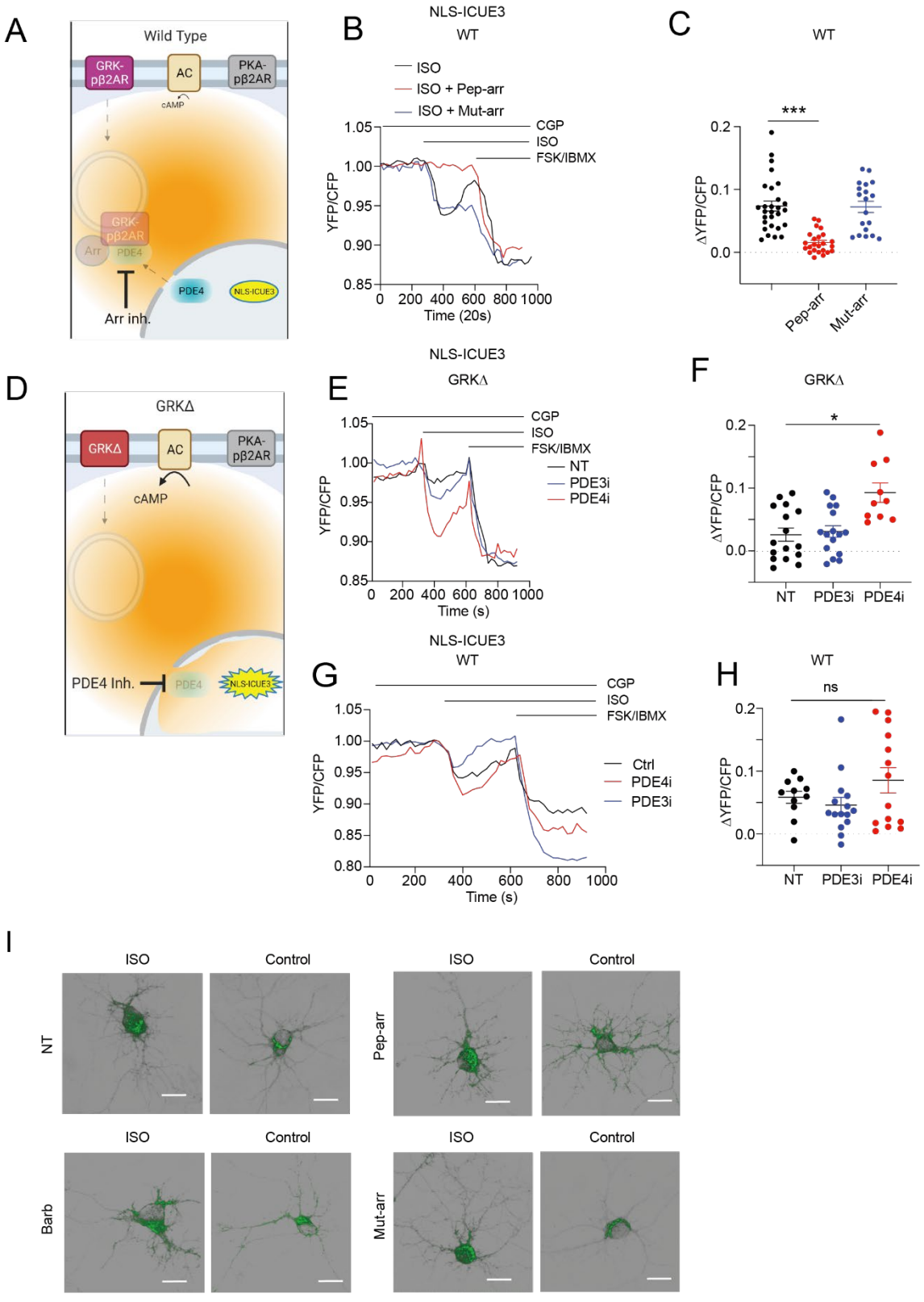
A
Wild Type
GRK-pβ2AR
AC
PKA-pβ2AR
cAMP
GRK-pβ2AR
Arr
PDE4
PDE4
NLS-ICUE3
Arr inh.
B
NLS-ICUE3
WT
ISO
ISO + Pep-arr
ISO + Mut-arr
CGP
ISO
FSK/IBMX
YFP/CFP
Time (20s)
C
WT
***
ΔYFP/CFP
Pep-arr
Mut-arr
D
GRKΔ
GRKΔ
AC
PKA-pβ2AR
cAMP
PDE4 Inh.
PDE4
NLS-ICUE3
E
NLS-ICUE3
GRKΔ
CGP
ISO
FSK/IBMX
NT
PDE3i
PDE4i
YFP/CFP
Time (s)
F
GRKΔ
*
ΔYFP/CFP
NT
PDE3i
PDE4i
G
NLS-ICUE3
WT
CGP
ISO
FSK/IBMX
Ctrl
PDE4i
PDE3i
YFP/CFP
Time (s)
H
WT
ns
ΔYFP/CFP
NT
PDE3i
PDE4i
I
ISO
Control
ISO
Control
NT
Pep-arr
ISO
Control
ISO
Control
Barb
Mut-arr

Figure 2.4. PDE4D controls β2AR-induced cAMP signaling in the nucleus via arrestin.

(A) Diagram of arrestin peptide inhibition in neurons. (B and C) WT primary hippocampal neurons were transfected with cAMP biosensor NLS-ICUE3. Neurons were pretreated Pep-arr or mut-arr peptide (1 μM, 10 minutes) and CGP20712a (300 nM, 5 minutes) before baseline recording and stimulation with ISO (100 nM, 5 minutes) followed by 10 μM forskolin (FSK) and 1 μM IBMX. Representative traces show changes in FRET ratio in neurons. Dot plots show the maximum changes in FRET ratio relative to baseline after ISO treatment. Data represent mean ± SEM of individual neurons from 5 isolations. ***p<0.001 vs NT via 1-way ANOVA followed by Tukey's test. (E-H) WT and GRKΔ Neurons were stimulated with 100 nM ISO together with 100 nM cilostamide (PDE3i) or 100 nM rolipram (PDE4i) and followed by 10 μM forskolin (FSK) and 1 μM IBMX. Representative traces show changes in FRET ratio in WT and GRKΔ neurons. Dot plots show the maximum changes in NLS-ICUE3 FRET ratio relative to baseline in WT and GRKΔ neurons after ISO treatment in the presence of PDE inhibitors. Data represent mean ± SEM of individual neurons from 4 isolations. *p<0.05 vs NT by 1-way ANOVA followed by Tukey's test. (I) Pep-arr peptides do not interfere with normal internalization of β_2AR in response to ISO stimulation. Images of WT primary hippocampal neurons (expressing mYFP-β_2AR. Neurons were pretreated with 1 μM Pep-arr or Mut-arr peptide for 10 minutes or 50 μM barbadin for 30 minutes before 1 μM ISO stimulation for 20 minutes.

Figure 2.5

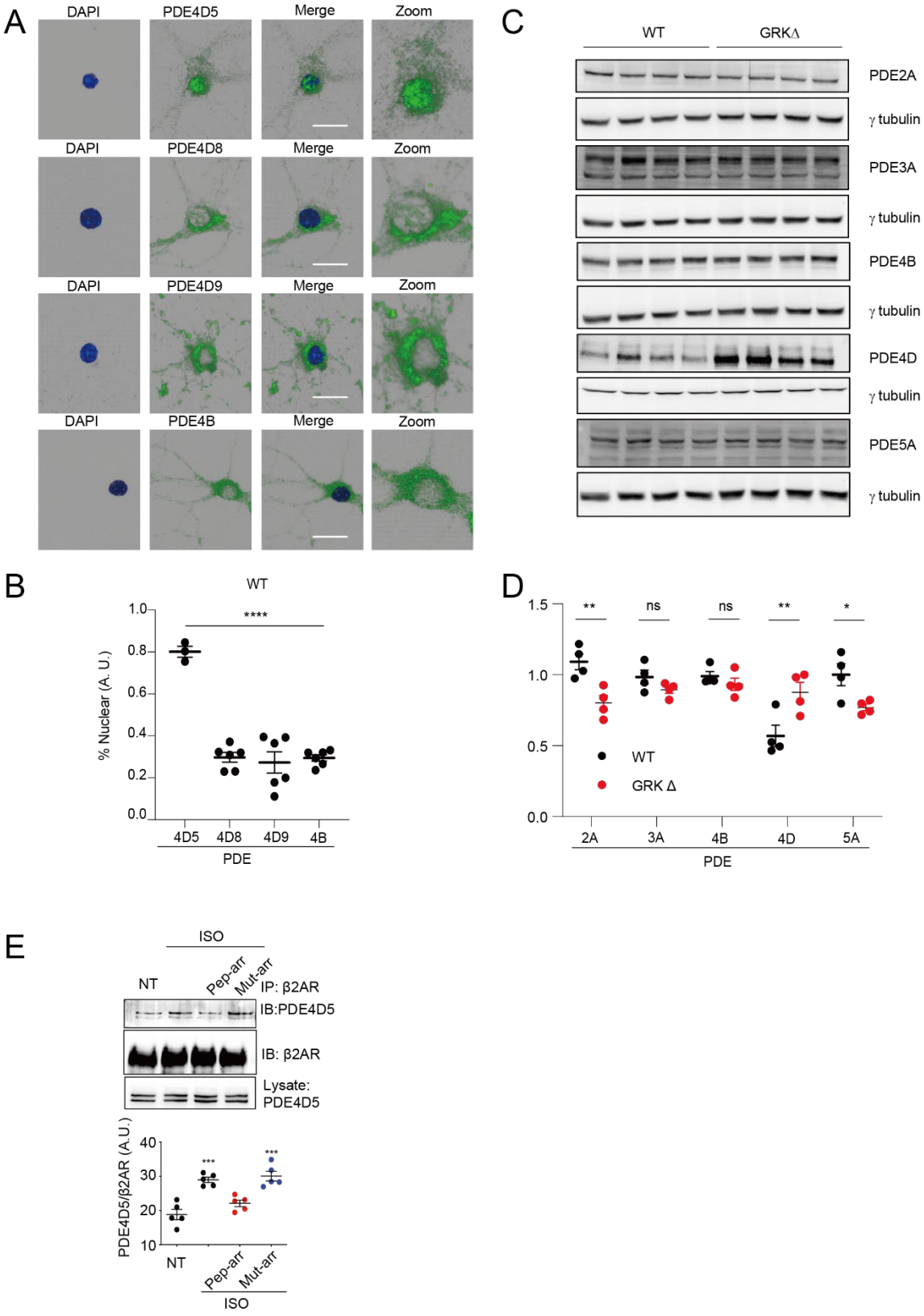
A
DAPI
PDE4D5
Merge
Zoom
DAPI
PDE4D8
Merge
Zoom
DAPI
PDE4D9
Merge
Zoom
DAPI
PDE4B
Merge
Zoom
C
WT
GRKΔ
PDE2A
γ tubulin
PDE3A
γ tubulin
PDE4B
γ tubulin
PDE4D
γ tubulin
PDE5A
γ tubulin
B
WT
****
% Nuclear (A. U.)
1.0
0.8
0.6
0.4
0.2
0.0
4D5
4D8
4D9
4B
PDE
D
**
ns
ns
**
*
1.5
1.0
0.5
0.0
WT
GRK Δ
2A
3A
4B
4D
5A
PDE
E
ISO
NT
Pep-arr
Mut-arr
IP: β2AR
IB:PDE4D5
IB: β2AR
Lysate:
PDE4D5
PDE4D5/β2AR (A.U.)
40
30
20
10
***
***
NT
Pep-arr
Mut-arr
ISO

Figure 2.5. PDE4D5 but not other PDE4 isoforms show nuclear localization; Arrestin peptide reduced β2AR/PDE4D5 interaction.

(A and B) Primary hippocampal neurons isolated from WT pups were grown to DIV14 treated with or without 10 μM ISO for 30 mins, fixed, and stained with antibodies for PDE4D5, PDE4D8, PDE4D9, or PDE4B (Green) or DAPI (blue) as indicated. Scale bar = 20 μM. Quantification of % Nuclear PDE expression (Nuclear (defined by DAPI staining)/total PDE intensity for cell across a line through the middle of the image). ****p<0.0001 via 1-way ANOVA followed by Tukey's test. (C and D) Expression of PDE isoform protein from WT and GRKΔ hippocampi as assessed via western blot. Quantification of western blot normalized to housekeeping gene γ-tubulin. *p<0.05, **p<0.01 vs WT via 1-way ANOVA followed by Tukey's test. (E) HEK293 cells transfected with WT-β_2AR were pretreated with Pep-arr peptide (1 μM, 30 minutes) that disrupts β-arrestin-PDE4 binding or mutant-arr peptide as control before stimulation with ISO (10 μM, 30 minutes). The β_2AR and PDE4 complex was immunoprecipitated before western blot. Data represent mean ± SEM of individual experiments. N = 5, ***p<0.001 vs NT via 1-way ANOVA followed by Tukey's test. See also Figure S2.4

Figure 2.6

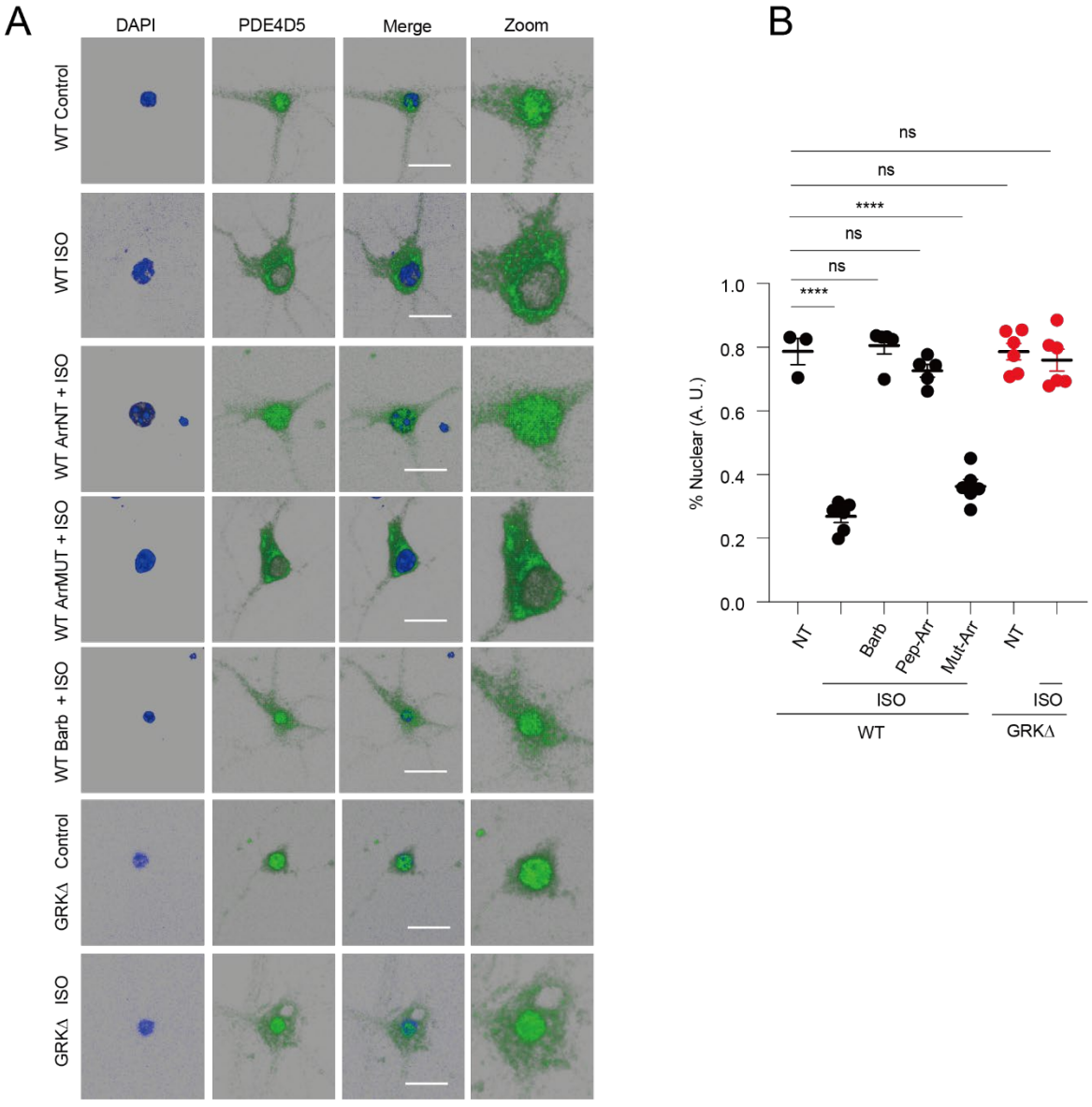
A
DAPI
PDE4D5
Merge
Zoom
WT Control
WT ISO
WT ArrNT + ISO
WT ArrMUT + ISO
WT Barb + ISO
GRKΔ Control
GRKΔ ISO
B
ns
ns
****
ns
ns
****
1.0
0.8
0.6
0.4
0.2
0.0
% Nuclear (A. U.)
NT
Barb
Pep-Arr
Mut-Arr
NT
ISO
ISO
WT
GRKΔ

Figure 2.6. Stimulation of β2AR relocates PDE4D5 to the cytoplasm in wild type hippocampal neurons while GRKΔ neurons show no relocation of PDE4D5 upon agonist stimulation.

(A) Primary hippocampal neurons isolated from WT and GRKΔ pups were grown to DIV14 pretreated with Arr Peptide (1 μM, 10 mins), Mutant Arr Peptide (1 μM, 10 mins), or barbadin (30 μM, 30 mins) as indicated then treated with or without 10 μM ISO for 30 mins, fixed, and stained with antibodies for PDE4D5 (Green) or DAPI (blue). Scale bar = 20 μM (B) Quantification of % Nuclear PDE expression (Nuclear (defined by DAPI staining)/total PDE intensity for cell across a line through the middle of the image). ****$p<0.0001$ via 1-way ANOVA followed by Tukey's test.

Figure 2.7

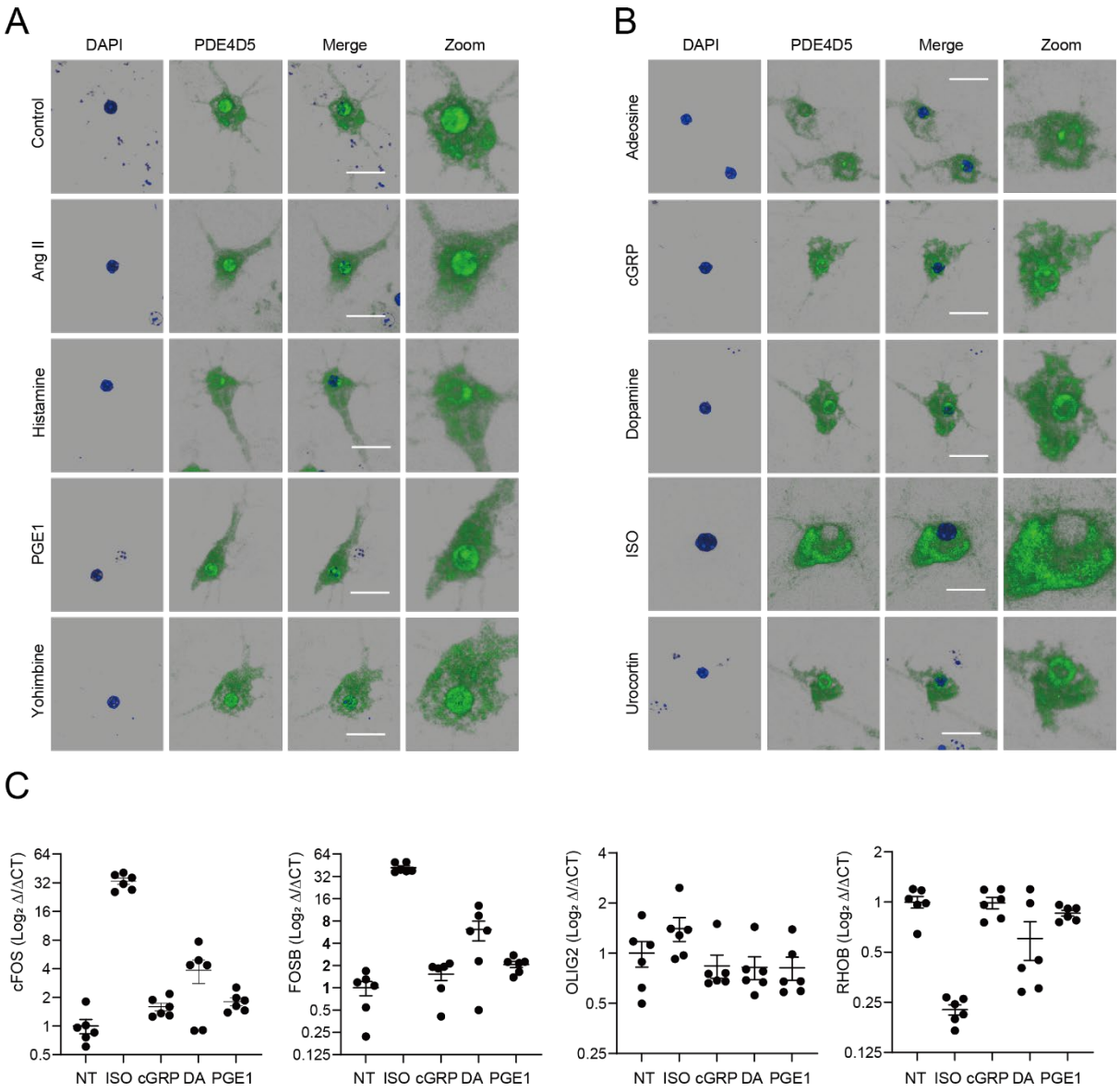
A
DAPI
PDE4D5
Merge
Zoom
Control
Ang II
Histamine
PGE1
Yohimbine
B
DAPI
PDE4D5
Merge
Zoom
Adeosine
cGRP
Dopamine
ISO
Urocortin
C
cFOS (Log2 Δ/ΔCT)
FOSB (Log2 Δ/ΔCT)
OLIG2 (Log2 Δ/ΔCT)
RHOB (Log2 Δ/ΔCT)
NT ISO cGRP DA PGE1

Figure 2.7. Characterization of PDE4D5 relocation upon GPCR stimulation in primary neurons using immunofluorescence.

(A, B) Primary cortical neurons were isolated from WT c57Bl6J mice and grown to DIV 10-14. Following GPCR stimulation for 30 minutes, cells were fixed and stained for PDE4D5 (Green) and DAPI (Blue). (C) GPCR mediated stimulation of IEG expression following 2 hours of stimulation assessed via qRT-PCR. Stimulation of listed agonists was at 1 μM concentration.

Figure 2.8

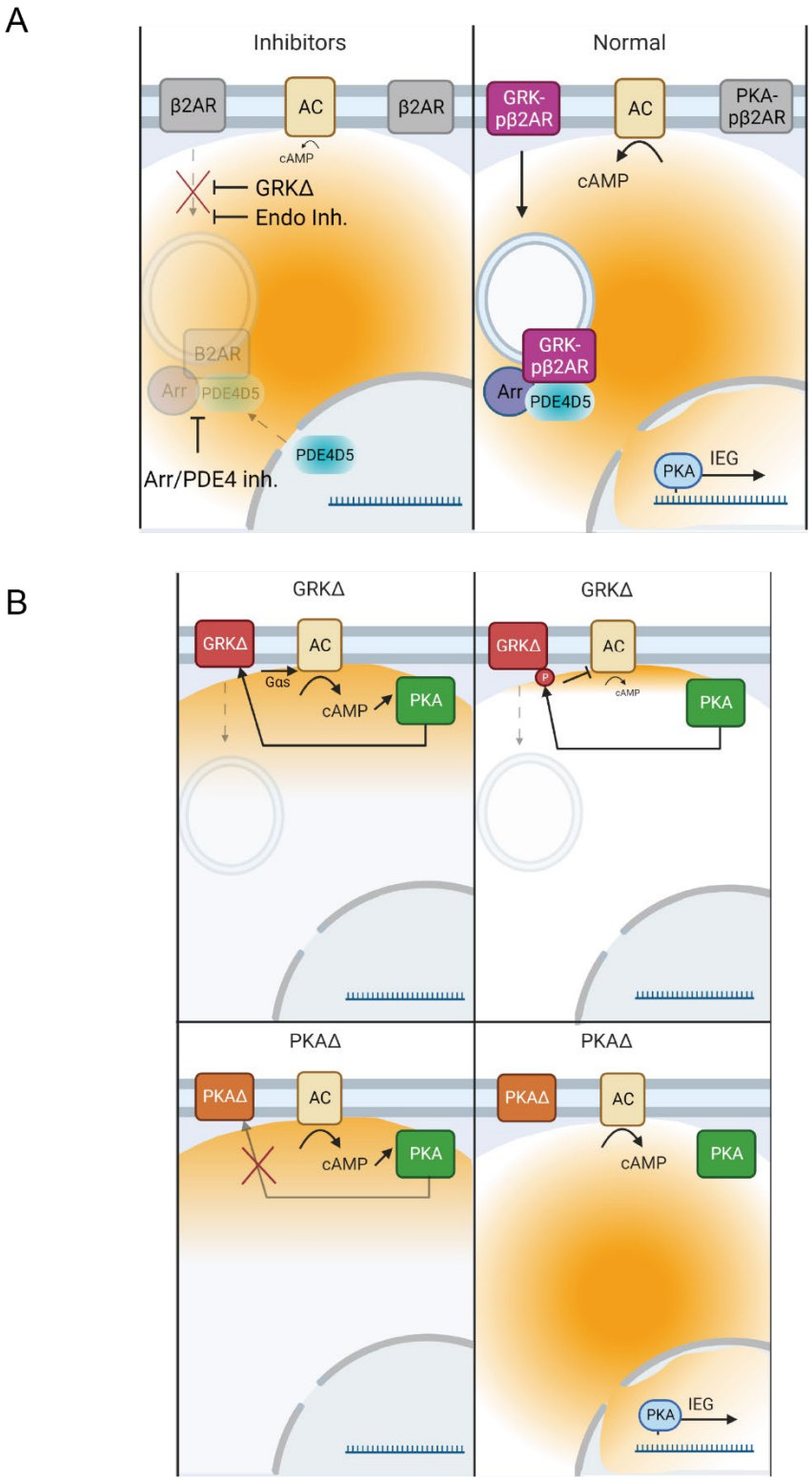
A
Inhibitors
Normal
β2AR
AC
β2AR
cAMP
GRKΔ
Endo Inh.
B2AR
Arr
PDE4D5
PDE4D5
Arr/PDE4 inh.
GRK-
pβ2AR
AC
PKA-
pβ2AR
cAMP
GRK-
pβ2AR
Arr
PDE4D5
PKA
IEG
B
GRKΔ
GRKΔ
AC
Gαs
cAMP
PKA
GRKΔ
AC
P
cAMP
PKA
PKAΔ
PKAΔ
AC
cAMP
PKA
PKAΔ
AC
cAMP
PKA
PKA
IEG

Figure 2.8. Summary of proposed mechanism and alternative hypothesis

(A) Summary Diagram - Stimulation of β_2AR promotes GRK and PKA-mediated phosphorylation of the receptor. GRK-pβ_2AR undergo endocytosis, which subsequently sequesters PDE4D5 from the nucleus to the endosome, facilitating cAMP signal to reach the nucleus and promote IEG gene expression. (B) Diagram of alternative interpretation of presented data.

Supplementary Figure 2.1

A

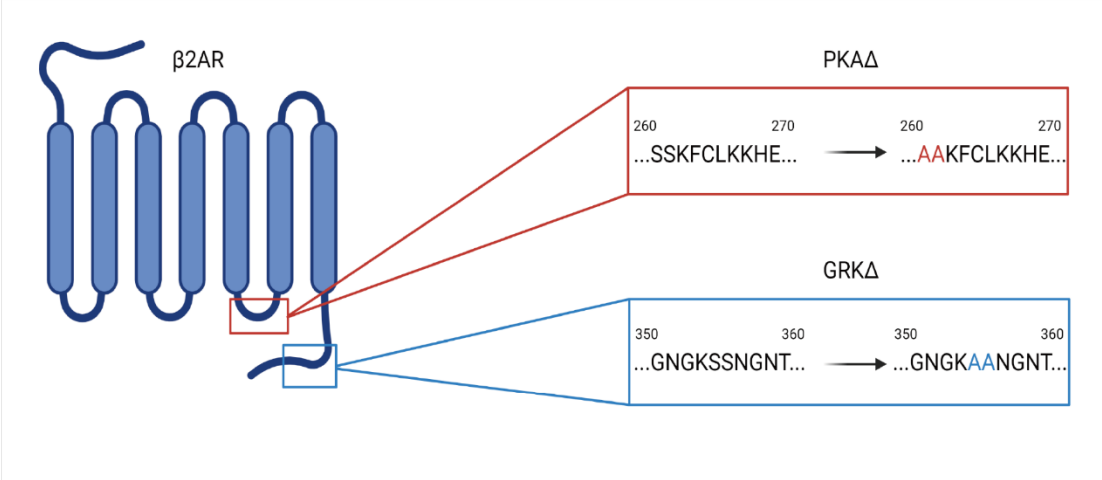

Supplemental Figure 2.1. Diagram of β2AR point mutations

(A) Diagram of serine to alanine point mutations on β2AR for the PKA phosphorylation site (S261/263A; PKAΔ) or the GRK phosphorylation site (S355/356A; GRKΔ).

Supplementary Figure 2.2

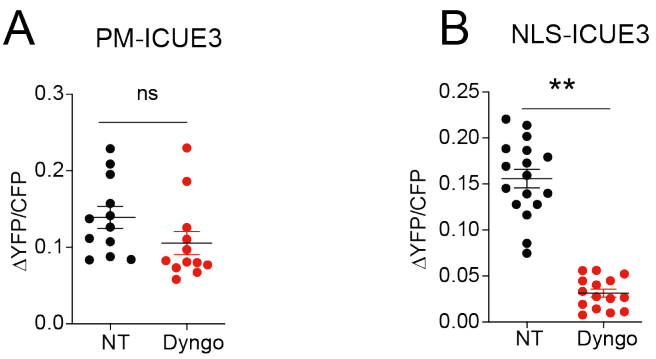

Supplemental Figure 2.2. Inhibition of endocytosis blocks β2AR indued nuclear cAMP signal in hippocampal neurons overexpressing β2AR.

(A and B) Primary hippocampal neurons isolated from DKO mice were transfected with cAMP biosensor PM-ICUE3 or NLS-ICUE3 together with WT β_2AR. Cells were pretreated with Dyngo4a (10 μM) 30 minutes prior to stimulation with 1 μM ISO. Changes in cAMP FRET ratio were measured. The maximum changes in ICUE3 FRET (YFP/CFP) ratio relative to baseline after ISO treatment are plotted. Data represent mean ± SEM of individual neurons from eight isolations. **p<0.01 vs no-pretreatment (NT) Student's t-test.

Supplementary Figure 2.3

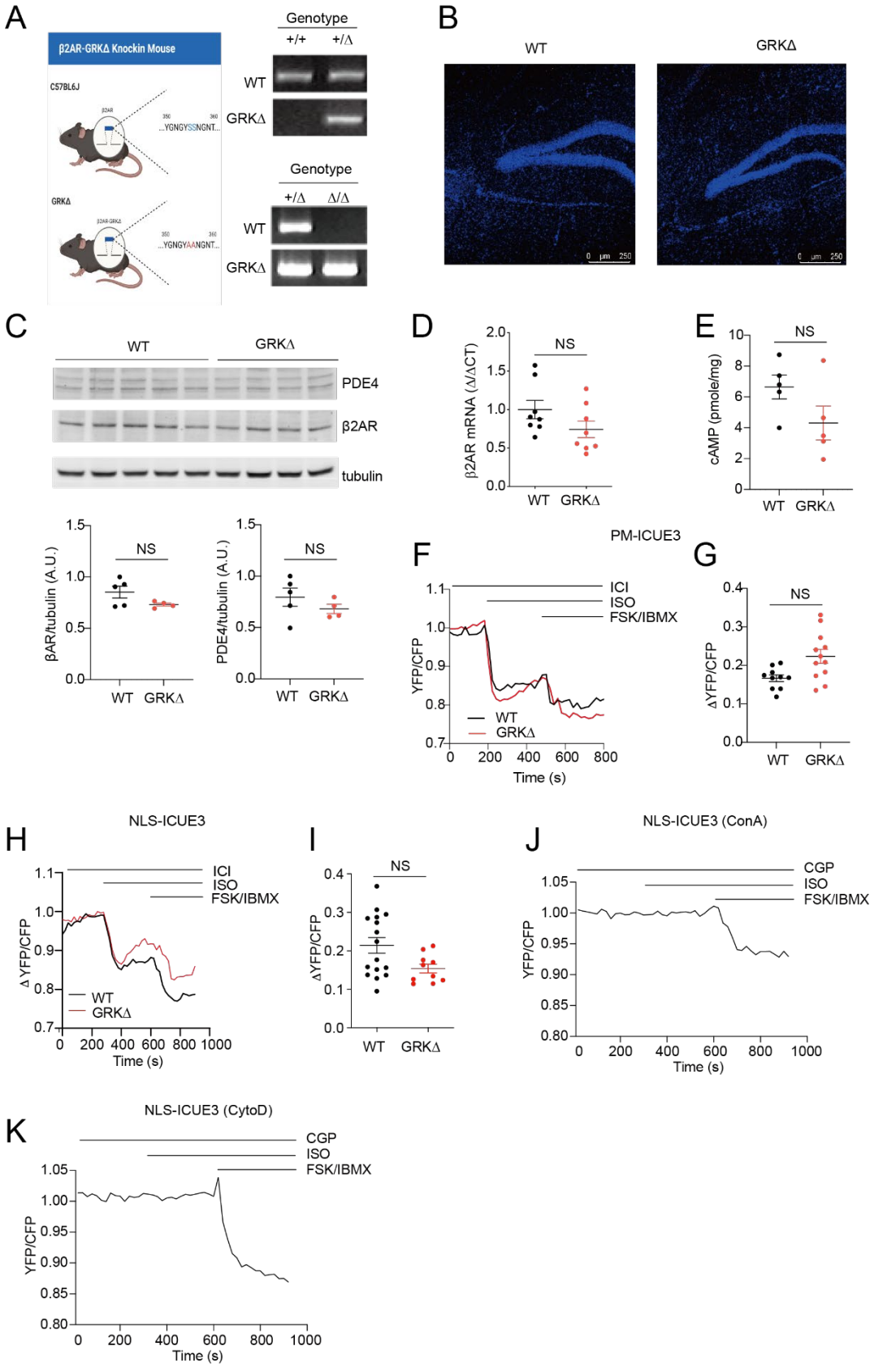

Supplemental Figure 2.3. Receptor expression, signaling, and gene expression in WT and GRKΔ hippocampi; inhibition of endocytosis blocks β2AR induced nuclear cAMP signal in hippocampal neurons

(A) Diagram of serine to alanine mutation in GRKΔ mice and genotyping for GRKΔ knockin mice. (B) DAPI image of hippcampi from WT and GRKΔ mice. (C) Western blot from adult WT and GRKΔ hippocampi measuring β_2AR, PDE4, and γ-tubulin. Quantification of β_2AR and PDE4 relative to γ-tubulin from western blot. (D) Quantification β_2AR mRNA expression in WT and GRKΔ hippocampi. (E) cAMP (pmole/mg) from adult WT and GRKΔ hippocampi. (F-I) Deletion of the GRK phosphorylation site of β_2AR does not affect β_1AR cAMP signaling in primary hippocampal neurons. Primary hippocampal neurons isolated from WT or GRKΔ mice were transfected with cAMP biosensor NLS-ICUE3 or PM-ICUE3. Neurons were pretreated with ICI-118551 (1 μM or 100 nM). The YFP/CFP ratio was recorded before and after stimulation with 100 nM ISO and followed by 10 μM forskolin (FSK) and 1 μM IBMX. (g and i) Maximal increases in NLS- and PM-ICUE3 YFP/CFP ratio relative to baseline after ISO treatment in the absence or presence of ICI (1 μM). (J-K) Representative traces of FRET experiments using endocytosis inhibitors ConA an CytoD. Traces quantified in Figure 2.3J.

Supplementary Figure 2.4

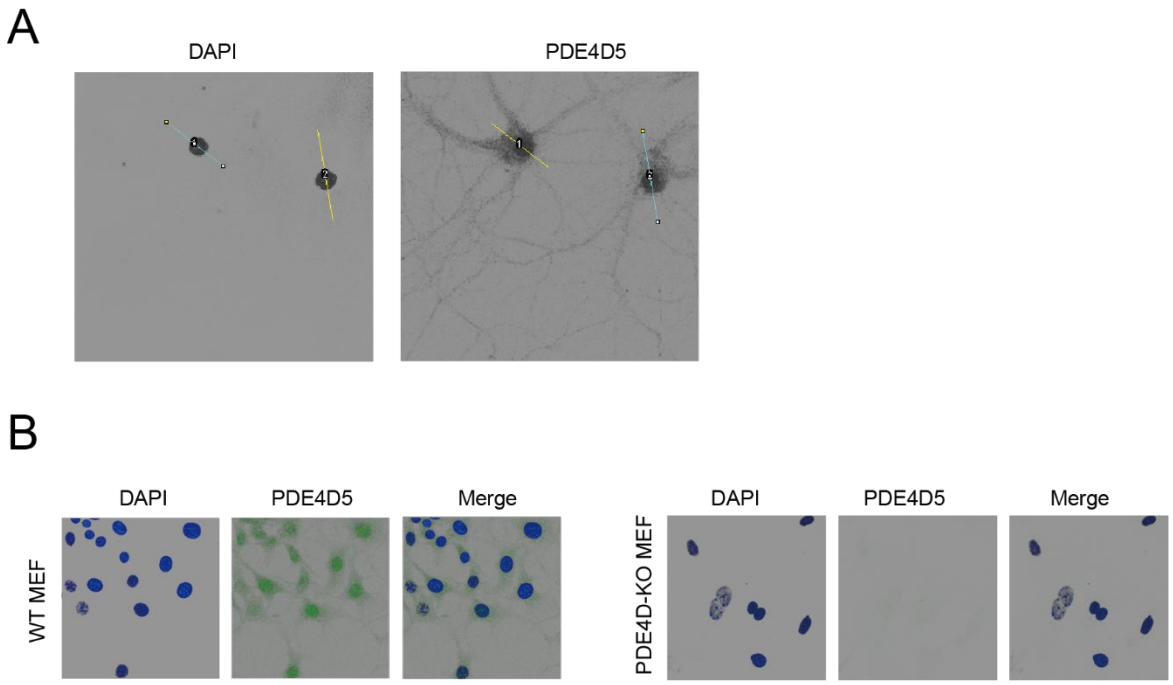

Supplemental Figure 2.4. PDE4D5 antibody specificity and % nuclear expression quantification.

(A) WT and PDE4D-KO MEF cells were stained for DAPI (Blue) and PDE4D5 (Green). (B) Example of analysis for % nuclear PDE expression across a defined line through the cell. The DAPI field is used to define the nucleus while the PDE4D5 field is used to define the cell. Relative intensity was determined by measuring area under the curves for each line trace and calculated as (1 / ((intensity of nuclear region/total intensity)).

Chapter 3: Role of beta-adrenergic receptors in learning and memory and stress response.

Introduction

Adrenergic signaling in the brain regulates wakefulness and arousal, attention, and is involved in learning and memory [54-58]. The LC is the source of the vast majority of NE and consequently adrenergic signaling in the CNS [55]. Adrenergic receptors are responsible for the action of NE in the brain. Beta-adrenergic receptors and their downstream signaling effectors are involved in multiple aspects of learning and memory in health and disease. Despite all these data showing adrenergic signaling involvement in CNS function, very little is known about the specific mechanisms by which adrenergic signaling effects brain function.

The molecular basis of hippocampal learning and memory consolidation is thought to lie in long term potentiation via increases in immediate early gene (IEG) expression [47, 48]. Activation of GPCRs promotes nuclear cAMP signaling to enhance IEG expression [46] and IEG expression is a key step in the stabilization of LTP and formation of memories [41, 42]. Notably, in cases of GPCRs with known biased ligands, internalization is not necessary for enhanced IEG expression. GPCRs β_1AR and β_2AR can mediate nuclear cAMP signal upon stimulation and are known to be crucial to hippocampal learning and memory [140, 254-257, 281, 282].

The hippocampus has long been known to be crucial memory for memory function and formation [283-286]. Beta-adrenergic signaling is also known to play role in hippocampal function and memory (reviewed in [287]. In the previous chapter we elaborated a novel mechanism by which β_2AR facilitates nuclear cAMP and gene expression. In this chapter we sought to determine if loss of nuclear cAMP and subsequent IEG expression *in vitro* also manifested itself *in vivo* through alteration of IEG expression leading to learning and memory deficits. To that end we compared learning and memory performance of WT and GRKΔ mice in the Morris water maze (MWM) paradigms. Additionally, we examined stress responses and general activity of these mice to more fully capture the behavioral effects the loss of GRK-pβ_2AR caused in mice. Our data identify a loss of GRK phosphorylation of β_2AR leads to a loss of learning induced IEG expression and deficits in memory retention. Further, our data suggest that the memory deficits observed are confined to memory consolidation with working memory remaining intact. Inhibition of PDE4

ameliorates said memory deficiency in GRKΔ mice *in vivo* supporting our proposed mechanism of β_2AR internalization-mediated cAMP signaling and its effects on gene expression *in vivo*. In Chapter 2 we also found that β_1AR nuclear cAMP signal remained in GRKΔ mice. Here we find that while learning indued IEG expression is deficient in GRKΔ mice, acute stress induced IEG expression. Knockout of β_1AR removed elevated plus maze anxiety response and ablated acute stress response in the forced swim test which suggests a differential role of β_1AR and β_2AR in memory and stress response. While preliminary in nature, these data suggest a differential role for β_1AR and β_2AR in memory and stress response.

Results

Loss of GRK phosphorylation site on β_2AR causes memory retention deficits in a Morris water maze paradigm.

We used GRKΔ mice to study the *in vivo* consequences of β_2AR phosphorylation site inactivation. These mice were assessed for spatial learning and memory using a Morris water maze paradigm (**Figure 3.1A-3.1J and Supplementary Figure 3.1A-3.1H**). WT and GRKΔ mice both learned the maze task and each group has similar path efficiency to the platform (**Supplementary Figure 3.1B**). Swim speed differed between mice groups with GRKΔ mice swimming more slowly than WT mice (**Supplementary Figure 3.1A**). Meanwhile, distance traveled to the escape platform (**Figure 3.1C**) was swim speed independent and corrected integrated path length (CIPL) is normalized to swim speed (**Figure 3.1D**). These metrics were similar between WT and GRKΔ mice, indicating that GRKΔ mice learn the maze task despite the differences in latency (time) to escape platform between groups (**Supplementary Figure 3.1C**). There were no differences during maze training in thigmotaxic behavior between mice groups (**Figure 3.1E**) indicating similar stress/anxiety response during training. In the probe trial, which occurred 24-hours after the fifth day of training (**Figure 3.1B**) and assesses retention (long-term memory) of the learned maze task, GRKΔ mice spent significantly less time in the quadrant where the escape platform previously resided (target quadrant) (**Figure 3.1F**). Additionally, GRKΔ mice spent more time in the start quadrant of the maze than WT mice and had a longer CIPL (**Figure 3.1H and Supplementary Figures 3.1D and 3.1E**). There was no difference in time in the thigmotaxic zone, swim speed, or path efficiency during the probe trial (**Supplementary Figure 3.1F – 3.1H**). Additionally, WT mice found the escape platform's location faster than GRKΔ mice

during the probe trial (**Figure 3.1G**). These data suggest that there was a deficit in memory retention of the escape platform's location in GRKΔ mice during the probe trial.

Further examination of binned heat maps of probe trial performance indicated that WT mice immediately moved to the target quadrant in the first 20 seconds in the maze, perseverated around the target area for the next 20 seconds, and eventually spread farther from the target quadrant in the final 20 seconds but remained in the general vicinity of the target (**Figure 1I**). Conversely, GRKΔ mice spent most of the first 20 seconds in the start quadrant, proceeded towards the target quadrant in the next 20 seconds, and some mice swam around the target area but spent relatively little time in the target area (total mean % time for WT = 38.70 ± 3.794 SEM vs. GRKΔ = 18.58 ± 2.875 SEM) with little exploratory perseveration compared to WT mice in the final 20 seconds. GRKΔ mice also showed a larger initial heading error than WT mice (**Figure 3.1J**). These data indicate GRKΔ mice have less retention of the learned maze task than WT mice.

We next examined the role of immediate early gene expression (IEGs) in behaving mice as IEGs expression may be impaired in GRKΔ mice lacking internalization following β_2AR stimulation (**Chapter 1 and** [49]). WT and GRKΔ mice were subjected to five days of MWM training (**Figure 3.2A and 3.2B and Supplementary Figures 3.2A-3.2E**). MWM training increased cFOS and FOSB expression in WT but not in GRKΔ mice (**Figure 3.1C and 3.1D**). RHOB and OLIG2 gene expression was not changed with MWM training (**Supplemental Figure 3.2F and 3.2G**) indicating these genes may not be involved in stabilization of long-term memory. Together, these data suggest loss of learning-induced β_2AR-mediated nuclear cAMP signaling and subsequent gene expression result in a deficit in long-term memory stabilization and consolidation. In comparison, acute stress induced by the FST paradigm (**Figure 3.1E and 3.1F**) resulted in increased cFOS and FOSB expression in both GRKΔ and WT mice (**Figure 3.1G and 3.1H**), suggesting acute stress-mediated transcriptional regulation of the IEGs is not affected by GRK phosphorylation of β_2AR. We also assessed general activity and anxiety responses of GRKΔ and WT mice in an elevated plus maze (EPM), an open field activity assay, and a forced swim test (FST) (**Figure 3.1A**). The EPM takes advantage of instinctual predation avoidance behaviors in mice (**Figure 3.2I-3.2K)**. GRKΔ mice spent significantly more time in the open arms of the EPM than WT mice (**Figure 3.2I**),

indicating GRKΔ mice have a differential anxiety response compared to WT. WT and GRKΔ mice show no differences in general activity in the open field test (**Figure 3.2L and 3.2M)**. There was no difference in FST acute anxiety response (**Figure 3.2F**). Together, these data indicate no differences between WT and GRKΔ mice in general activity and acute response to stress but a reduced anxiety response in GRKΔ mice relative to WT controls.

While GRKΔ mice showed memory retention deficits in the water maze, they were still able to learn the maze task. We therefore hypothesized that working memory was still intact in GRKΔ mice. To test this hypothesis, we used the working memory variant of the Morris water maze (WM-MWM), which has four learning trials each day with a fixed start and platform location. The platform location and start location change day to day (**Figure 3.3A**), thus the WM-MWM teaches the maze task to find the platform day to day, but the memory of the previous platform location does not help performance. Over the six days, GRKΔ and WT mice both had similar performance in the WM-MWM over the four learning trials despite having significantly slower swim speed (**Figure 3.3B-3.3G**). Therefore, these data suggest that GRKΔ mice have intact working memory but despite impaired long-term memory retention.

Inhibition of the PDE4 rescues behavioral performance in mice with mutant β_2ARs lacking the GRK phosphorylation site.

We next examined if inhibition of PDE4 rescues memory retention in the MWM in GRKΔ mice. GRKΔ mice were given PDE4 inhibitor roflumilast (3 mg/kg) or vehicle control via oral gavage 1-hour prior to or 3-hour post MWM testing (**Figure 3.4A**). All groups were able to learn the maze task (**Figure 3.4B – 3.4G**). However, in the probe trial, the roflumilast pretreatment group spent significantly more time in the target quadrant (**Figure 3.4H and 3.4I**). All Groups had similar probe trial escape latencies (**Figure 3.4J**). Examination of the binned heatmaps from the probe trial suggest that the roflumilast pretreatment group had an improved memory and rapidly approached the target quadrant in the first 20 seconds of maze testing, perseverate, and spent more time near the target quadrant when compared to GRKΔ-Vehicle mice (**Figure 3.4H)**. The roflumilast post treated mice followed a similar pattern to the Vehicle group during the probe, searching the entirety of the maze rather than perseverating around the maze previous location suggesting a lack of memory retention of the learned maze task. Initial heading error was similar between

groups (**Figure 3.4K**) while path efficiency, CIPL, swim speed, and thigmotaxis were similar across groups (**Supplementary Figures 3.4A-3.4D**). These data indicate a partial rescue of memory retention with roflumilast pretreatment.

β_1AR mice show a lack of stress response.

Data from Chapter 2 (**Figure 2.3B, 2.3D, 2.3E and 2.3G and Supplementary Figure 2.3F and 2.3G**) indicate that both PM and nuclear β_1AR-mediated cAMP signal remains in both WT and GRKΔ mice. Our data also suggest while learning induced IEG expression requires internalization of β_2AR, acute stress induced IEG expression does not (**Figure 3.2A-3.2H**). We therefore hypothesized that stressed induced nuclear cAMP signal was mediated by β_1AR. To test this hypothesis we took WT, β_1KO, and β_2KO mice and performed a series of behavioral tests (**Figure 3.5A**). In the open field test, β_1KO mice have significantly reduced mean speed and distance traveled than WT or β_2KO mice (**Figure 3.5B and 3.5C**). In the elevated plus maze, WT mice spend significantly more time in the closed arms than the open, consistent with normal mouse predation avoidance behavior while β_2KO mice have the inverse phenotype, spending more time in the open rather than closed arms suggesting differential anxiety response, which is consistent with observations of GRKΔ mice (**Figure 3.5D**). β_1KO mice, however, show roughly equal distribution between arms (**Figure 3.5D**). β_2KO mice traveled farther and moved faster on average than either WT or β_1KO mice on the EPM (**Figures 3.5E and 3.5F**). In the FST, β_2KO show a slight reduction in time immobile compared to WT mice. Strikingly, β_1KO mice show almost no immobile time in the FST (**Figure 3.5G**).

An internalized pool of β_1AR is partially responsible for β_1AR-mediated nuclear signaling and that signaling is partially dependent on catecholamine transporters and is affected by internalization.

Work from Dr. Paul Gasser [158] suggests an internalized pool of β_1AR may exist in on the nuclear envelope. A nuclear pool of β_1AR, which would require both catecholamine transporters and passing MAO-A sinks for NE to reach the receptors on the nuclear envelope may explain the differences in stress vs learning mediated IEG expression. We hypothesize that stressful conditions may induce more or more sustained NE release than learning conditions, allowing enough NE to reach this nuclear pool of β_1AR. To partially test this hypothesis, we began examining internal β_1AR-mediated nuclear cAMP signaling using FRET. We observed that β_1AR-mediated nuclear cAMP signal is partially attenuated by catecholamine

transporter inhibitors (**Figures 3.6A and 3.6B**). Additionally, blockade of surface beta-adrenergic receptors using membrane impermeant sotalol in addition to catecholamine transporters partially attenuated and altered the dynamics of β_1AR-mediated nuclear cAMP signal (**Figures 3.6D and 3.6E**). Finally, we observed that inhibition of internalization also partially attenuated β_1AR-mediated nuclear cAMP signal (**Figures 3.6F and 3.6G**)

Discussion

In Chapter 2 we provided data suggesting a mechanism by which endosomal GPCRs deliver cAMP to the nucleus promoting gene expression in physiology and disease [270]. Our data reveal that deletion of GRK phosphorylation sites on β_2AR prevents nuclear cAMP signaling and nuclear PKA-mediated IEGs expression. Further, our data suggest arrestin/PDE4D5 interactions are necessary for nuclear cAMP signal to reach the nucleus. In this Chapter we took GRKΔ and assessed the for a behavioral phenotype using a battery of behavioral assays meant to assay spatial learning and memory, general activity, and anxiety-related responses. We hypothesized that, given our proposed mechanism from Chapter 1, GRKΔ mice would have spatial learning and memory deficits caused by reduced IEG expression after learning. Further, our mechanism suggests inhibition of PDE4 should rescue said behavioral phenotype. Our data show GRKΔ mice have deficits in memory consolidation but not in working memory as well as deficits in learning induced IEG expression. Further, inhibition of PDE4 rescues nuclear long-term memory deficits in mice GRKΔ mice. Together this work indicates that endosomal GRK-phosphorylated β_2AR recruits a β-arrestin/PDE4D5 complex, which indirectly promotes cAMP signal propagation into the nucleus to promote IEGs expression which, in turn, promotes consolidation of short-term, working memory into long-term memory.

During learning, following learning-induced receptor stimulation, cAMP is generated and activates PKA which then phosphorylates cAMP response element binding protein (CREB) in the nucleus. IEGs have conserved, overrepresented transcription factor binding sites including CREB [288]. CREB binds to cAMP response element (CRE) after phosphorylation of CREB by PKA at serine-133 [30]. Activation of CREB leads to transcription of IEGs such as cFOS and FOSB. These IEGs then help stabilize long-term potentiation and are critical to the formation of long-term memory [47, 48]. In Chapter 2, we detected cAMP signal in the nucleus of hippocampal neurons which is correlated to downstream IEGs expression.

Moreover, a nuclear but not cytosolic PKI inhibits β_2AR-induced gene expression in hippocampal neurons. These data support the necessity of GPCR machinery, through β-arrestin/PDE interactions, to deliver cAMP to the nucleus to promote gene expression in hippocampal neuron. Here we show GRKΔ mice have memory retention deficits, and, following maze training, GRKΔ mice also have deficient IEG expression while WT mice show increased IEG expression providing evidence that GPCR machinery shown to be necessary for nuclear cAMP signal *in vitro* is indeed necessary for memory formation *in vivo*. Crucially, GRKΔ mice have intact working memory. This not only suggests how GRKΔ mice improve day to day in maze learning (through task learning rather than platform location memory) but is consistent with the notion that IEG expression is necessary to stabilize LTP/consolidate learning into long term memory.

A critical role for PDE4 in β_2AR regulated nuclear cAMP signaling is also supported by evidence showing that inhibition of various PDE isoforms benefits learning and memory in both rodents and humans in health and various disease states with PDE4D inhibition showing improved memory but no emetic side effects in Alzheimer's models [252, 289-292]. Additionally, the β-arrestin2/PDE4D complex is critical in the formation of fear memory [293] supporting a necessary role for β-arrestin/PDE4D interaction for memory consolidation. In agreement, pretreatment but not posttreatment with roflumilast partially rescued the memory deficit observed in GRKΔ mutant mice. These data suggest that IEG expression must at least partially coincide with learning in order to properly consolidate memory. Our data does not show a complete restoration of consolidation memory in GRKΔ mice. This was expected due to limitations with our drug treatment paradigm. It has been observed that hypothermia, correlating to nausea, in mice is a side effect in broad spectrum PDE4 inhibition [294]. Indeed, it is the presence of GI and other side effects of broad spectrum PDE4 inhibitors that has cause clinical trial failure and limited their clinical efficacy [248-251]. Additionally, after oral administration of PDE4 inhibitor roflumilast, some time is necessary for the drug to be absorbed, cross the blood-brain barrier, and inhibit PDE4 in relevant brain regions. To account for this time delay after administration and to limit any potential side effects in our mice from broad spectrum PDE4 on maze performance, the time of administration was chosen to be 1-hour prior to maze running. This likely lead to imprecise timing of gene expression and actual learning of the maze task resulting in less clear memory of the maze location. This could be reflected in the binned probe trial performance heat maps (**Figure 3.4H and 3.4K**) where the GRKΔ-pretreatment group shows less accurate initial heading than WT

mice did (**Figure 3.1H-3.1J**) and the fact that GRKΔ-pretreatment mice spend more time in and around the edges of the quadrant than over the previous platform location. Another interpretation of these data is that the time spent near the edge of the maze by all groups is a stress effect from the gavage procedure or vehicle/drug treatment. Indeed, thigmotaxis is higher in these mice than non-treatment controls during the probe trial (**Supplementary Figure 3.1G and Supplementary Figure 3.4A**). However, GRKΔ-pretreatment mice still spend more time in the target quadrant with less exploration of the non-target portions of the maze suggesting memory of the escape platform's previous location while the other groups appear to be exploring the entirety of the maze, suggesting they are searching for the platform.

In addition to PKA signaling, β_2AR can also signal through β-arrestin to stimulate the MAPK/ERK pathway which then signals to the nucleus [295]. Stimulation of β_2AR can also lead to the phosphorylation of L-type calcium channels (LTCC) and calcium to promote gene expression and LTP [127, 128] . How these pathways interact with our proposed mechanism and involved in memory and learning remains to be determined. Additionally, the mechanism of how the two β-arrestin isoforms (β-arrestin1 and β-arrestin2) and endosomal β2AR regulate PDE4D5 localization remains to be explored. The β-arrestin2/PDE4 complex has been shown to be critical in the formation of fear learning [293], the same study shows normal memory retention in the Morris water maze and normal elevated plus maze performance in β-arrestin2 KO mice. These data appear to conflict with the observations showing impaired memory consolidation and elevated plus maze performance in GRKΔ mice in the water maze. These observations highlight gaps in our knowledge regarding the exact role of individual β-arrestin proteins in neurons and the subcellular effects when the protein is deleted in animals. Further studies are necessary to dissect endosomal receptor, arrestin, and PDE networks and their role in fine tuning subcellular cAMP signaling in a cell and tissue specific manner both *in vitro* and *in vivo* [265].

In addition to classical agonist stimulated signaling pathways, some ligands for β_2AR can trigger signaling biased towards either G-protein or arrestin pathways through stabilizing distinct receptor conformations that favor G-protein or β-arrestin binding [296]. β-arrestin biased agonists such as carvedilol have been shown to mediate memory consolidation [137] and extinction [138]. Carvedilol has also shown benefits to memory and learning in models of Alzheimer's disease, senescence, oxidative

damage, and general cognitive impairment [297-299]. In agreement, we show mice lacking GRK phosphorylation of β_2AR show deficits in memory retention and a loss of learning induced IEGs expression. These data support the idea that β-arrestin mediated β_2AR signaling is necessary for memory consolidation.

An interesting and unexpected observation occurred during our assessment of GRKΔ mice. While GRKΔ mice have deficits in IEGs expression following maze learning, both wild type and mutant mice have strong IEGs expression following the forced swim test (FST), which tests acute stress response. In addition, GRKΔ mice show significantly reduced general anxiety response in the elevated plus maze showing the opposite normal phenotype, spending significantly more time in open arms that closed arms. These data suggest that IEGs expression mediated by stress utilizes a different pathway than IEGs expression for learning and memory. Indeed, we have observed that the β_1AR mediated nuclear cAMP signaling remains intact in GRKΔ neurons; consistent with the early finding that β_1AR is involved in behavioral stress responses [300]. Both β_1AR and β_3AR are involved in memory [287]. To test the hypothesis that β_1AR may be responsible for the observed stress effects, we took β_1- and β_2KO mice and subject them to several behavioral tests. Interestingly, β_2KO mice show a similar phenotype as GRKΔ mice, spending more time in the open arms than closed arms. They are also more active on the EPM than either WT or β_1KO mice, moving faster and traveling farther than either group suggesting a true inverse response of anxiety-like behaviors. β_1KO mice, however, spend roughly equal amounts of time in open and closed arms indicating no preference with either arm but rather a lack of anxiety-like response in the EPM. In the FST, β_1KO mice show almost complete loss of floating behavior. This suggests acute stress response is mediated by β_1AR. It has been shown β_1AR can signal from subcellular compartments such as Golgi and ER/SR providing evidence for location biased adrenergic signaling [157, 159-161]. Additionally, work from Dr. Paul Gasser suggests β_1AR can signal from the nuclear envelope in astrocytes with the aid of catecholamine transporters which transport NE into the cell [158]. We sought to determine if an internal pool of β_1AR exists in neurons using FRET based nuclear cAMP sensors and inhibitors of catecholamine transporters PMAT and OCT3 as well as cell surface beta-adrenergic antagonist sotalol. Out data indicate an internal pool of β_1AR does contribute to overall β_1AR mediated

nuclear cAMP signaling but that it is not the only contributor. Surface β_1AR also contributes to the observed signal.

Taken together, our data show a subpopulation of GRK phosphorylated β_2AR in mice is critical for nuclear cAMP signaling, IEG expression, and long-term memory consolidation in a MWM paradigm. Further, these data suggest a mechanism by which NE signaling in the brain may contribute to memory consolidation and partially explain the beneficially memory effects observed with PDE4 inhibitors. Additionally, these data support our proposition that β_1AR and β_2AR have differing roles in the CNS contributing to memory as well as stress response.

Study Limitations and alternative interpretations

When interpreting behavioral data from global knockin mice such as the GRKΔ mice used in this study it is important to consider alternative interpretations and caveats when examining the behavioral data. GRKΔ mice have constitutively active β_2AR making them susceptible to stress effects. These animals are extensively handled and acclimated to compensate for this, but the stress of the water maze could affect performance. Metrics of thigmotaxis indicate this is unlikely but slower than WT swim speed could be a result of these effects. Additionally, β_2ARs function in myriad systems including thermoregulation. Therefore, water temperature could play a role in GRKΔ performance as could affects from any number of systems. Future studies should be conducted in neuron specific knockin mice to remove these confounding factors.

As discussed in Chapter 2, an alternative explanation of our data is GRKΔ neurons are simply worse are producing cAMP at the plasma membrane due to a lack of receptor desensitization making the receptor susceptible to PKA phosphorylation leading to adenylyl cyclase desensitization. Behaviorally, in this scenario, GRKΔ mice would still show the same memory consolidation deficit and intact working memory. Roflumilast pretreatment but not post treatment would still partially rescue behavioral performance. However, here, rather than inhibit PDE4D5 as the primary effect, roflumilast would also reduce the number of plasma membrane receptors necessary to produce enough cAMP to propagate to the nucleus. Fitting with this interpretation, a preliminary study using PKAΔ 261/262 mice show intact learning and memory in the Morris water maze although with a notable lack of perseveration in the probe

trial (data not shown). Generating dual PKAΔ-GRKΔ mice would allow for testing this hypothesis with endogenous neurons using FRET and behaviorally as well.

Methods

Experimental model and subject details

Animals

Animals were housed in a UC Davis AAALAC certified vivarium on a 12-hour day/night cycle (7am to 7pm), grouped 3-5 mice per cage, and provided free access to food and water. E18 rat embryos were obtained from pregnant Sprague-Dawley rats (#001, Charles River Laboratories, Cambridge, MA). GRKΔ mice were developed by Cyagen (Santa Clara, CA) and backcrossed 9 times to obtain a clean C57Bl6/J background. These mice were used to produce P0-P1 pups or aged to 70-130 days for behavioral and biochemical studies. Wild type C57Bl6/J mice were obtained from Jackson Laboratories (Bar Harbor, ME; #000664) to produce P0-P1 postnatal WT pups and aged to 70-130 days for behavioral and biochemical studies. β_1-KO and β_2-KO animals were generated in our animal colony and aged 70-130 days before behavioral testing. Animals were grouped without blinding but were randomized during experiments. Groups were spread across multiple cages to minimize cage effects. Male and female animals were used in behavioral experiments. All animals were handled according to approved institutional animal care and use committee (IACUC) protocols (#21993, #20641, and #22371) of the University of California at Davis and in accordance with NIH guidelines for the use of animals.

Method Details

Cell culture

Primary Neuron Culture

Primary mouse hippocampal neurons were isolated and cultured from early postnatal (P0-P1) wild type C57Bl6/J (Jackson Laboratories) and E18 rat embryonic primary hippocampal neurons were isolated from embryos from female Sprague-Dawley rats [127]. Briefly, pups were decapitated, brains were removed and placed in ice cold HBSS, and hippocampi dissected out under a dissection scope.

Hippocampi were then dissociated by 0.25% trypsin treatment in HBSS at 37°C for 16 minutes. After digestion, hippocampi were moved to cold HBSS containing 25% FBS gently mixed, then moved HBSS containing 10% FBS and gently mixed, and finally into HBSS prewarmed in an incubator containing 5% CO2 at 37°C. Hippocampi were then triturated at room temperature using a Pipet-aid (Drummond) set to slow using a 10 mL serological pipet until no more pieces of tissue were visible. Solution was spun down for 4 minutes at 1100 RPM, HBSS aspirated, and pellet resuspended in Neurobasal medium supplemented with GlutaMax (Thermo Fisher Scientific, Waltham, MA), gentamicin (Promega), B-27 (Thermo Fisher Scientific, Waltham, MA) and 10% FBS and counted. Neurons were plated on poly-D-lysine-coated (Sigma-Aldrich, St. Louis MO: #P6407) #0 12 mm glass coverslips (Glaswarenfabrik Karl Hecht GmbH & Co. KG, Sondheim, Germany; REF 92100100030) for imaging and FRET at a density of 7500 cells/cm^2 and 10,000 cells/cm^2, respectively.

Neurons were transfected using the Ca^{2+}-phosphate method as previously describe [127]. Briefly, cultured neurons at either 3-5 days *in vitro* (DIV), 6–8 days DIV, or 10–12 DIV were switched to pre-warmed Eagle's minimum essential medium (EMEM, Thermo Scientific, MA) supplemented with GlutaMax 1 hour before transfection; conditioned media were saved. DNA precipitates were prepared by 2×HBS (pH 7.02 WT, and rat neurons) and 2 M $CaCl_2$. After incubation with DNA precipitates for 1 h, neurons were incubated in 10% CO_2 pre-equilibrium EMEM for 20 min, then replaced with conditioned medium. FRET biosensor PM-ICUE3, and NLS-ICUE3 have been previously described [279].

Förster Resonance Energy Transfer (FRET)

FRET measurements were performed as previously described [227]. Briefly, WT mouse or rat primary hippocampal neurons were transfected with NLS-ICUE3 via the calcium phosphate method. Cells were imaged on a Zeiss Axiovert 200M microscope with a 40×/1.3 numerical aperture oil-immersion lens and a cooled CCD camera using MetaFluor software. Dual emission ratio imaging was acquired with a 420DF20 excitation filter, a 450DRLP diachronic mirror, and two emission filters (475DF40 for cyan and 535DF25 for yellow). The acquisition was set with 0.2 s exposure in both channels and 20 s elapses. Images in both channels were subjected to background subtraction, and ratios of yellow-to-cyan were

calculated at different time points. For traces, ratios were normalized to baseline. Maximum FRET ratios were calculated as % change from baseline after treatment. Cells were treated as described in figures.

qRT-PCR

Total RNA was extracted from cells and tissue following treatment and behavioral protocols using Tri-Reagent (Sigma-Aldrich T9424, St. Louis, MO) via manufacturer's protocols. Briefly, cells tissue was homogenized in Tri-Reagent and phase separated using chloroform. The clear, aqueous layer was transferred to a fresh tube and precipitated with isopropyl alcohol. Following precipitation, the RNA pellet was washed twice using 80% ethanol, dried, mixed with RNAse/DNAse free water. Genomic DNA was removed using a DNAse kit (Sigma-Aldrich AMPD1) per manufacturer's protocol. RNA was then quantified using a CLARIOStarPlus microplate reader. Reverse transcription was carried out on extracted RNA using a high-capacity cDNA reverse transcription kit (Applied Biosystems #4368814 and a thermocycler (Veriti 96-well Thermal Cycler, Applied Biosystems). qRT-PCR was carried out on cDNA using PowerUp SYBR Green Master Mix (Applied Biosystems, #A25742) and appropriate primers using a QuantStudio3 Real Time PCR system (Applied Biosystems).

Brain Tissue Harvest

Following completion of maze training or handling, animals were anesthetized with isoflurane, brains removed, and hippocampi excised as previously described [280]. Briefly, tissue was snap frozen for biochemical analysis, fixed in 10% buffered formalin phosphate (SF100, Thermo Fisher Scientific, Waltham MA) at 4 C for histochemical staining, or placed in TRI reagent (T9424, Sigma-Aldrich, St. Louis, MO) for RNA extraction. After 3 days in formalin, brains were transferred to 30% sucrose and left a minimum of 3 days to dehydrate at 4C. Following dehydration, brains were mounted in Tissue Tek OCT medium (#4853, Sakura Finetek, Torrance, CA), frozen, and cryo-sectioned using a Leica CM1860 cryostat into 40 µM sections which were mounted onto tissue-specific glass slides (Thermo-Fisher #12-550-15, Waltham, MA) for staining.

Behavior

Mice were handled for 5 days prior to maze testing to acclimate mice to technicians and being moved prior to the start of behavioral tests (**Figures 3.1A, 3.4A, and , 3.5A**). For treatment groups, animals were vehicle gavaged during handling. This handling procedure and movement to the maze room without testing was conducted for handling control groups used in qRT-PCR. Before each day of behavioral testing, mice were moved to the testing room and allowed to acclimate for 1 hour. Sessions were recorded using an overhead camera and, where indicated, mice were tracked using AnyMaze Software version 4.99b. Heat maps were generated from raw X, Y coordinate output from AnyMaze and processed using RStudio (RStudio, Waltham, MA).

Morris water maze

The Morris water maze (MWM) was used to assess spatial learning in memory in rodents. Using distal cues surrounding the maze, animals learned to locate a submerged, invisible escape platform. Spatial learning was assessed across repeated trials over several days. Reference (long-term memory of the learned task) was assessed in a probe trial by removing the platform and allowing the rodent to freely swim while tracking software monitors their performance [301, 302]. The maze consisted of a water tank 110 cm in diameter and a clear escape platform approximately 10 cm in diameter. Cues (white on black background) were placed at the four cardinal points of the maze wall. Water was clouded using non-toxic tempera paint, kept at a level 2 cm above the submerged escape platform, and maintained at 25 ± 2 degrees centigrade. Mice were placed in the maze at a start point in front of one of the maze cues on the perimeter of the maze facing towards the maze wall. Animals were then allowed to swim until they found the platform or 60 seconds has elapsed. Animals that did not find the escape platform in the time allotted were guided to the platform where they remained for 10 seconds. If the animal left before 10 seconds had elapsed, they were returned to the platform and gently held there for 10 seconds. The acquisition phase of the maze consisted of four spatial learning trials that took place over 5 days using each of the four start points each day in a pseudorandom order. The probe trial, which assesses memory retention, occurred 24 hours after the last trial. The mice were again placed in the maze between the triangle and plus-sign maze cues in quadrant 3 (**Figure 3A**) with the platform removed. The animals swam freely for 60 seconds while being tracked by an overhead camera and tracking software. The thigmotaxis zone was defined in

the tracking software as a ring 7 cm in width around the edge of the maze perimeter. A mouse was excluded from analysis if they spent 90% of their time in the start quadrant during the probe trial indicating floating. Data points were also excluded if they were detected as an outlier using the ROUT method with Q set to 1% in Prism software (GraphPad Inc., San Diego, CA). Two WT and one GRKΔ mice were excluded using these methods.

Roflumilast administration

Three days prior to maze testing, mice were gavaged using vehicle only (200 µL) to acclimate all groups to the procedure. Mice were weighed the day before water maze testing with PDE4 inhibitor therapy was conducted to determine dosage of drug. Roflumilast (Ark Pharm, Inc.; AK110425) was administered at a dose of 3 mg/kg. Roflumilast was dissolved in DMSO and then added to vehicle to yield a concentration of 0.4 mg/mL roflumilast and 10 µL/mL. Gavage volumes based on animal weight and dosage were rounded to the nearest 50 µL and allowed for gavage volumes of 200-300 µL. Vehicle consisted of 0.5% carboxymethylcellulose (Sigma-Aldrich #419338) and 2% polysorbate 20 (Acros Organics # 23336-0010) dissolved in milliQ water. 10 µL of DMSO per mL of vehicle was also added to be consistent with roflumilast groups. Roflumilast and vehicle were made fresh just before administration of the Pretreatment and vehicle groups and were kept in the dark via aluminum foil wrap and kept on ice. One hour prior roflumilast or vehicle was administered to the Pretreatment and Vehicle groups and three hours after the end of maze testing, the post treatment group was administered roflumilast for the duration of maze learning (**Figure 3.4A**). Animals were not administered drug or vehicle prior to the probe trial.

Working Memory water maze

The working memory water maze (WM-MWM) was used to assess working memory in rodents [302]. The procedure used the same maze setup and platform as the standard MWM with the following changes as described previously [301, 302]. Each day the animals were placed in the maze at a single start position and a fixed escape platform location (**Figure 3.3A**). Animals performed four 60 second trials each day from this same start position. The following day they repeated the same training pattern for a new start position and platform location. This was done for 6 days. Mice were monitored via overhead

camera and tracking software. Mice were excluded if they failed to learn the platform location across 6 days of training. One WT and one GRKΔ mouse were excluded using this method. The first two runs on day of WT and GRKΔ mice were excluded due to platform misplacement. Data are presented as the average of the four daily trials for all six days of learning. Three days of training have platform locations close to start location and 3 have far platform locations far from start locations (**Figure 3.3A**) to eliminate search pattern and start location-platform location variability effects. Simple linear regression was used to determine learning.

Forced Swim Test

The forced swim test (FST) is one of the most commonly used behavioral assays for assessing depressive-like behavior in rodents with high interlaboratory reliability [303]. It is also an acute stress test [304]. It and other acute stress tests are known to induce IEGs expression [305]. After acclimation, mice were placed into a clear cylindrical tank 200 mm in diameter and 300 mm tall with water to a depth of 225 mm held at room temperature (25 ± 2 C) with an opaque barrier surrounding 3 sides and were allowed to swim for a total of 6 minutes. The procedure was recorded via overhead camera and scored for active vs. passive behaviors by a blinded technician.

Elevated Plus Maze

The elevated plus maze (EPM) is one of the most widely used assays for the assessment of anxiety-like behavior in mice taking advantage of the natural tendency of mice to explore novel environments and their aversion for open and elevated spaces [306]. The EPM consists of open and closed arms arranged in a cross with two open arms and two walled in, closed arms. The maze is 1050 mm tall. Each arm is 1180 mm long and 110 mm wide. The closed arms have walls 180 mm high. The center intersection of the maze measures 110 mm by 110 mm. Prior to testing, the maze was cleaned with 70% ethanol so that all mice experience the same scent environment. Mice were then placed in the center space facing away from the technician. The mice were then allowed to freely explore the maze for 5 minutes. Each trial run was recorded and parameters such as distance traveled, number of arm entries, time spent in each arm and percent entry into open arm were tabulated using AnyMaze software. After the end of each trial, the mice were put back in their home cage and the maze apparatus was cleaned

with 70% ethanol, removing any waste and scent cues. Mice were excluded if they jumped off the maze apparatus.

Open Field

The open field activity assay is used to assess general motility and activity. It consists of an open top box with plastic sides measuring approximately 355 mm x 355 mm and 455 mm tall. AnyMaze tracking software and an overhead camera track the animals' movements within the chamber. The mouse was placed in the center of the field facing away from the technician and allowed to freely explore the field for 10 minutes. Upon completion of the testing trial, the animal was returned to its home cage and the maze is cleaned with 70% ethanol, removing any waste and scent cues.

Diagram development.

Diagrams were created with BioRender.com

Data Analysis

Data were analyzed using GraphPad Prism9 software (GraphPad Inc., San Diego, CA) and expressed as mean ± S.E.M. as indicated in figure legends. Differences between two groups were assessed by appropriate two-tailed unpaired Student's *t*-test. Differences among three or more groups were assessed by one-way ANOVA with Tukey's post hoc test. $P < 0.05$ was considered statistically significant.

Figure 3.1

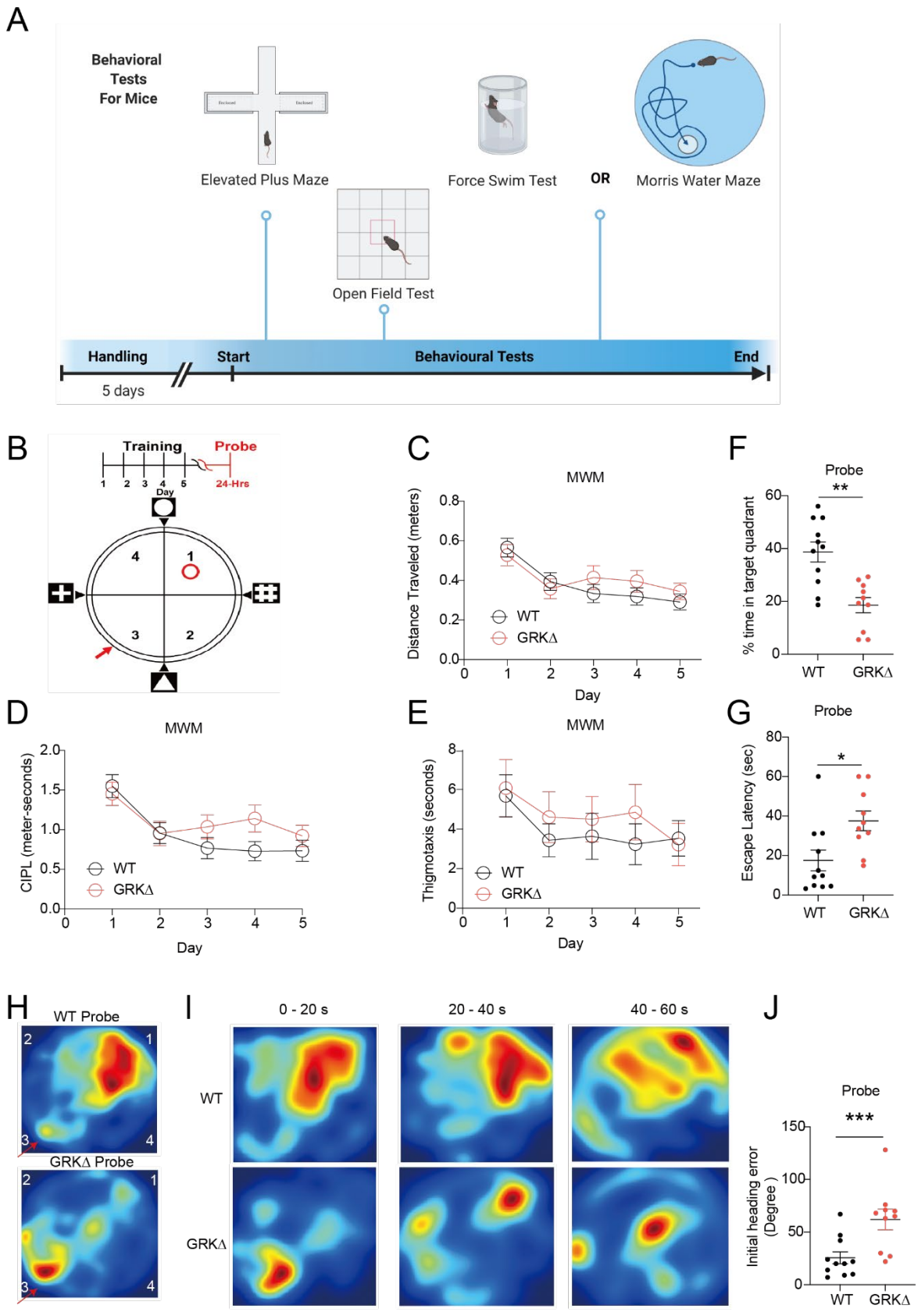
A
Behavioral Tests For Mice
Elevated Plus Maze
Force Swim Test
OR
Morris Water Maze
Open Field Test
Handling
5 days
Start
Behavioural Tests
End
B
Training
Probe
24-Hrs
Day
C
MWM
Distance Traveled (meters)
WT
GRKΔ
Day
F
Probe
% time in target quadrant
WT
GRKΔ
D
MWM
CIPL (meter-seconds)
E
MWM
Thigmotaxis (seconds)
G
Probe
Escape Latency (sec)
H
WT Probe
GRKΔ Probe
I
0 - 20 s
20 - 40 s
40 - 60 s
WT
GRKΔ
J
Probe
Initial heading error (Degree)

Figure 3.1. Transgenic mice lacking GRK phosphorylation site on β_2AR show memory deficiency in a Morris water maze paradigm.

(A) Diagram of behavioral testing paradigms for WT and GRKΔ. Mice are handled then run through the elevated plus maze then open field test then are either run in the Morris water maze or the forced swim test. (B) Diagram of Morris water maze (MWM) testing paradigm. Red arrow indicates probe start point, black arrows next to extramaze cues indicate pseudorandomized training start points. (C) Distance swam to the escape platform during maze training. (D) Corrected integrated path length (CIPL), an index of the efficiecy of the path taken by the animal to get from starting position to the escape platform normalized for swim speed, to the escape platform. A value of 0 indicates a straight line from start to finish and indicates optimized performance. (E) Time thigmotaxis during maze testing. (F) Percent time in target quadrant, quadrant 1, during probe trial. (G) Escape latency (time to first platform entry during probe trial. Data represent mean ± SEM of individual mice. *$p<0.05$ and **$p<0.01$ via student's t-test. (H) Heat map of MWM probe trial for WT (N = 11) and β_2AR GRKΔ (N = 10) mice. Red arrow indicates probe start point. Platform was previously in quadrant 1 as indicated in (B) diagram. (I) Heat maps of WT and GRKΔ mice during the probe trial broken into 20 second bins for the duration of the 60 second probe trial. (J) initial heading error for WT and GRKΔ mice during the probe trial. $p<0.001$ vs WT via student's t-test. See also Supplementary Figure S3.1

Figure 3.2

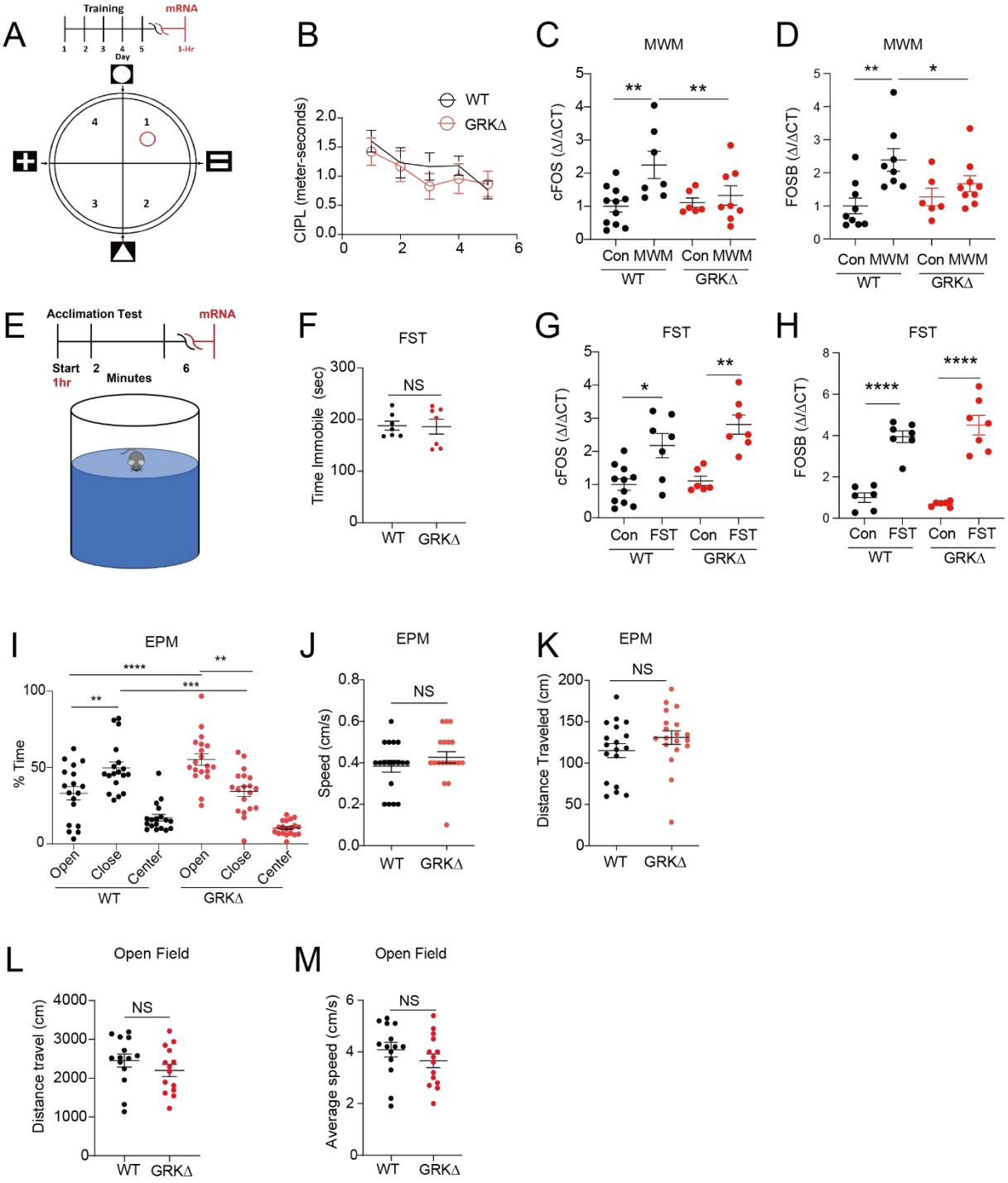
A
Training
mRNA
1 2 3 4 5
Day
1-Hr
4 1 3 2
B
WT
GRKΔ
CIPL (meter-seconds)
C
MWM
cFOS (Δ/ΔCT)
Con MWM Con MWM
WT GRKΔ
D
MWM
FOSB (Δ/ΔCT)
Con MWM Con MWM
WT GRKΔ
E
Acclimation Test
mRNA
Start 2 6
1hr
Minutes
F
FST
Time Immobile (sec)
NS
WT GRKΔ
G
FST
cFOS (Δ/ΔCT)
Con FST Con FST
WT GRKΔ
H
FST
FOSB (Δ/ΔCT)
Con FST Con FST
WT GRKΔ
I
EPM
% Time
Open Close Center Open Close Center
WT GRKΔ
J
EPM
Speed (cm/s)
NS
WT GRKΔ
K
EPM
Distance Traveled (cm)
NS
WT GRKΔ
L
Open Field
Distance travel (cm)
NS
WT GRKΔ
M
Open Field
Average speed (cm/s)
NS
WT GRKΔ

Figure 3.2. Transgenic mice lacking GRK phosphorylation site on β_2AR show deficiency in learning but not stress induced immediate early genes expression in hippocampi along with differential anxiety-like responses in the elevated plus maze.

(A) Diagram of MWM paradigm. WT and GRKΔ mice were trained for 5 days and then hippocampi extracted 1-hour after the end of maze learning on day 5 and processed for RNA. (B) Corrected integrated path length (CIPL), an index of the efficiecy of the path taken by the animal to get from starting position to the escape platform normalized for swim speed, to the escape platform for learning mice examined for gene expression. A value of 0 indicates a straight line from start to finish and indicates optimized performance. (C and D) Transcriptional changes of cFOS and FOSB relative to WT-control were assessed by qRT-PCR. Control qRT-PCR groups reflect animals that were handled and moved to the maze room in the same manner as tested animals but were not exposed to any behavioral paradigms. Data represent mean ± SEM of individual mice. *p<0.05, **p<0.01 vs control via 1-way ANOVA followed by Tukey's test. (E) Diagram of forced swim test (FST) procedure and RNA isolation from hippocampi 1-hour post FST exposure. (F) Time immobile in the Forced Swim Test (G and H) Transcriptional changes relative to WT-control were assessed by qRT-PCR. Control qRT-PCR groups reflect animals that were handled and moved to the maze room in the same manner as tested animals but were not exposed to any behavioral paradigms. Data represent mean ± SEM of individual mice. *p<0.05, **p<0.01, ****p<0.0001 vs control via 1-way ANOVA followed by Tukey's test. WT-con N=11, WT-MWM N=7, WT-FST N=7, GRKΔ-Con N=6, GRKΔ-MWM N=9, GRKΔ-FST N=7. (I) Percent time in open arms, closed arms, and center of elevated plus maze. (J) Mean speed during elevated plus maze for WT and GRKΔ mice. (K) Total distance traveled during elevated plus maze for WT and GRKΔ mice. (L and M) Distance traveled and average speed in an open field teast. Data represent mean ± SEM of individual mice. **p<0.01, ***p<0.001 vs WT-open; ### p<0.01 vs GRKΔ open via 1-way ANOVA followed by Tukey's test. See also Supplementary Figure S3.2.

Figure 3.3

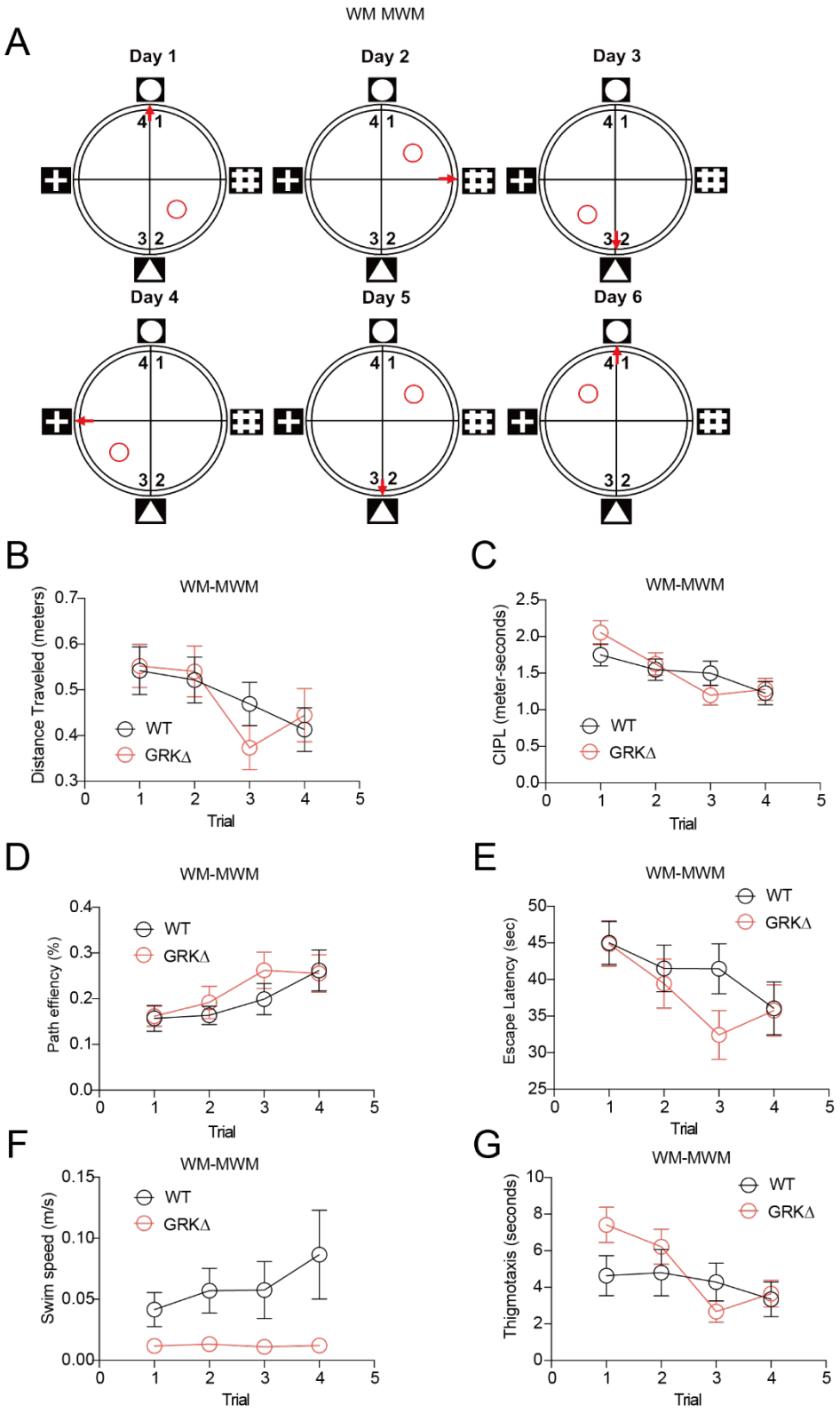
WM MWM
A
Day 1
Day 2
Day 3
Day 4
Day 5
Day 6
4 1
3 2
B
WM-MWM
Distance Traveled (meters)
Trial
WT
GRKΔ
C
WM-MWM
CIPL (meter-seconds)
Trial
WT
GRKΔ
D
WM-MWM
Path effiency (%)
Trial
WT
GRKΔ
E
WM-MWM
Escape Latency (sec)
Trial
WT
GRKΔ
F
WM-MWM
Swim speed (m/s)
Trial
WT
GRKΔ
G
WM-MWM
Thigmotaxis (seconds)
Trial
WT
GRKΔ

Figure 3.3. GRKΔ mice have intact working memory.
Behavioral performance in the working memory variant of the Morris water maze (WM-MWM). Diagram of the start positions (red arrows) and platform positions (red circles) for each day's four learning trials for the WM-MWM. (B-G) Performance metrics between WT and GRKΔ mice in the working memory Morris water maze across 4 daily trials. Data are presented as mean ± SEM. Learning curves in B-E are significantly non-linear via linear regression analysis $p<0.05$. N=5 for WT and GRKΔ mice in WM-MWM.

Figure 3.4

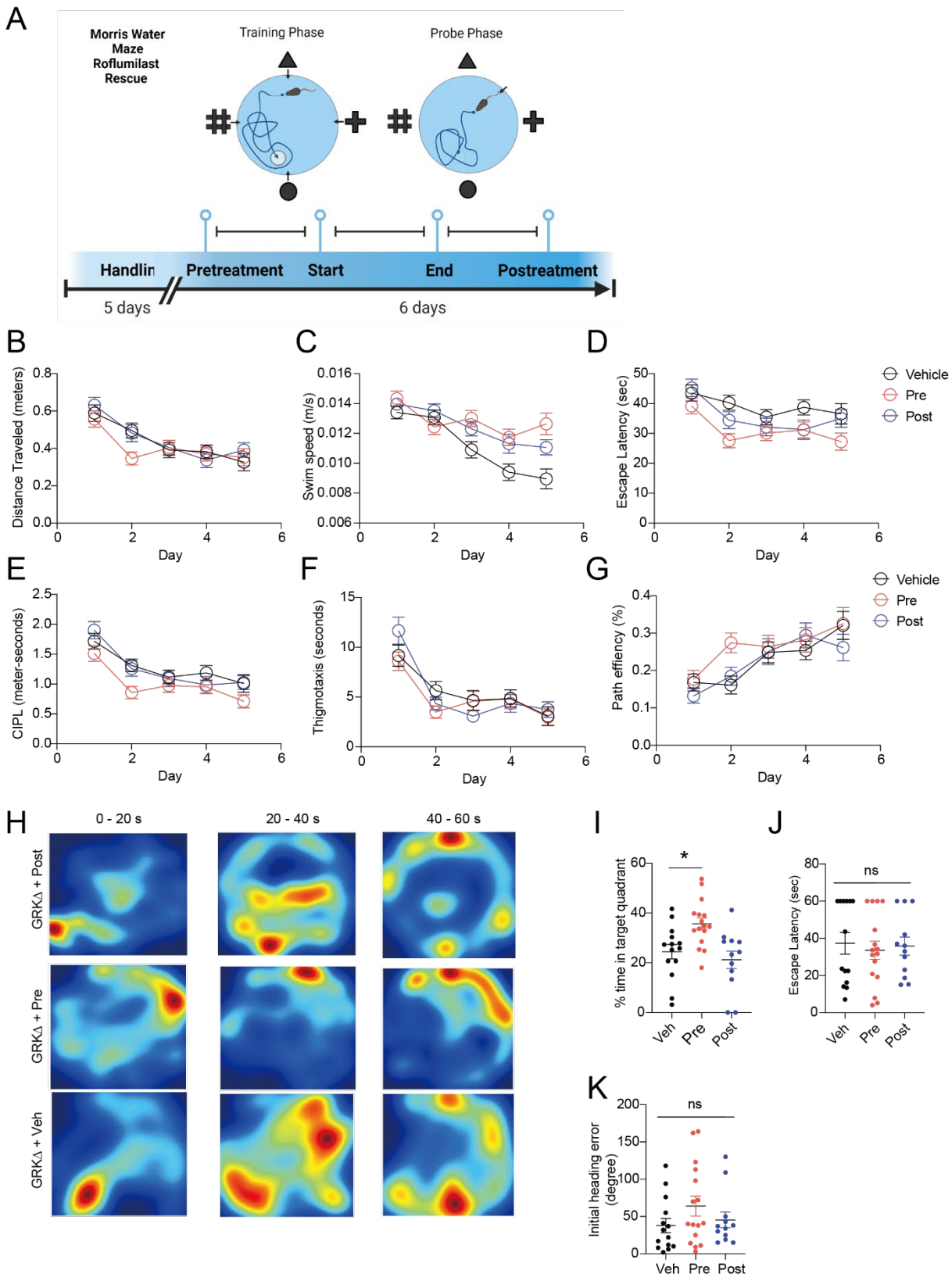
A
Morris Water Maze Roflumilast Rescue
Training Phase
Probe Phase
Handlin
Pretreatment
Start
End
Postreatment
5 days
6 days
B
Distance Traveled (meters)
Day
C
Swim speed (m/s)
Day
D
Escape Latency (sec)
Day
Vehicle
Pre
Post
E
CIPL (meter-seconds)
Day
F
Thigmotaxis (seconds)
Day
G
Path effiency (%)
Day
Vehicle
Pre
Post
H
0 - 20 s
20 - 40 s
40 - 60 s
GRKΔ + Post
GRKΔ + Pre
GRKΔ + Veh
I
% time in target quadrant
*
Veh
Pre
Post
J
Escape Latency (sec)
ns
Veh
Pre
Post
K
Initial heading error (degree)
ns
Veh
Pre
Post

Figure 3.4. Inhibiting PDE4 partially recovers memory retention in the Morris water maze in transgenic mice lacking GRK phosphorylation site on β_2AR.

(A) Diagram of roflumilast treatment paradigm for rescue experiment. Mice were sham gavaged during handling to minimize stress from the procedure during testing. (B-G) Metrics of learning in the Morris water maze in GRKΔ mice treated with vehicle (N = 14) or PDE4 inhibitor roflumilast (3 mg/kg). Mice were treated with roflumilast 1-hour prior to the start of maze testing (pre, N = 16) or 3-hours following the completion of maze testing (post, N = 12). (H) Heat maps are broken into 20 second bins during the probe trial. (I) Percentage of time in target quadrant following maze learning during the probe trial. *$p<0.05$ via 1-way ANOVA followed by Tukey's test. (J) Escape latency for probe trial. (K) Initial heading error during the probe trial. Data represent mean ± SEM of individual mice. See also Supplementary Figure S3.3.

Figure 3.5

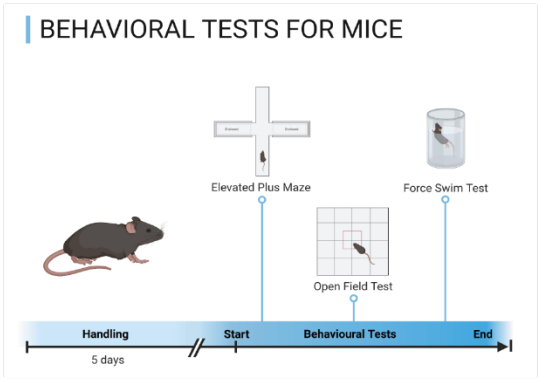
A
BEHAVIORAL TESTS FOR MICE
Elevated Plus Maze
Force Swim Test
Open Field Test
Handling
5 days
Start
Behavioural Tests
End

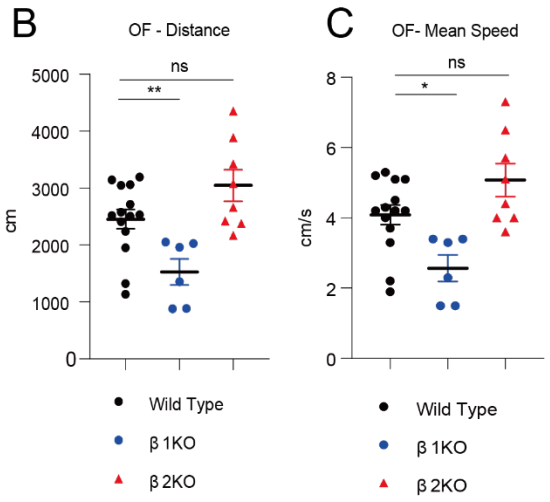
B
OF - Distance
cm
ns
**
Wild Type
β 1KO
β 2KO
C
OF- Mean Speed
cm/s
ns
*
Wild Type
β 1KO
β 2KO

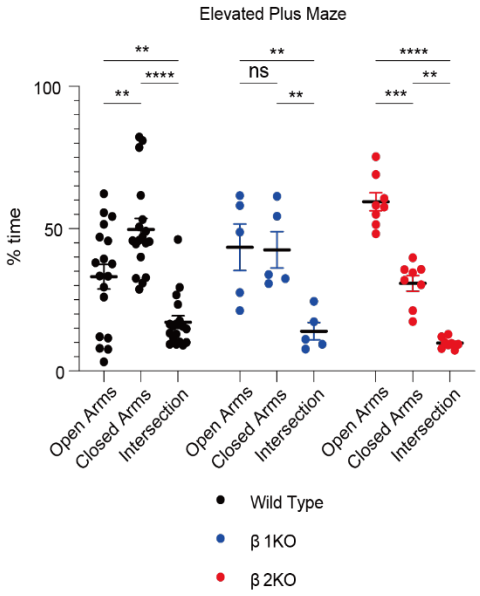
D
Elevated Plus Maze
% time
Open Arms
Closed Arms
Intersection
Wild Type
β 1KO
β 2KO

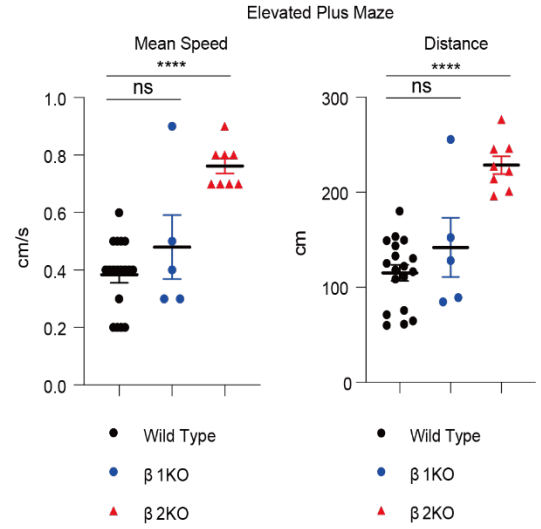
E
Elevated Plus Maze
Mean Speed
cm/s
ns
Wild Type
β 1KO
β 2KO
F
Distance
cm
ns
Wild Type
β 1KO
β 2KO

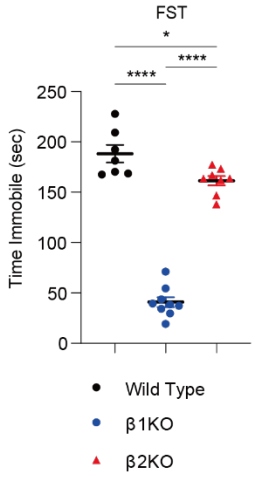
G
FST
Time Immobile (sec)
Wild Type
β1KO
β2KO

Figure 3.5. Knockout of β1AR eliminates stress mediated responses in mice.

(A) Diagram of behavioral paradigms performed on WT, β1KO, and β2KO mice. (B and C) Distance traveled and mean speed in an open field test. *p<0.05, **p<0.01 vs WT using a 1-way ANOVA followed by Tukey's test. (D) Percent time in open arms, closed arms, and center of elevated plus maze. (E) Mean speed during elevated plus maze for WT, β1KO, and β2KO mice. (F) Total distance traveled during elevated plus maze for WT, β1KO, and β2KO mice. (G) Time immobile in a FST for WT, β1KO, and β2KO mice. Data represent mean ± SEM of individual mice. **p<0.01, ***p<0.001, ****p<0.0001 vs open arms via 1-way ANOVA followed by Tukey's test. ****p<0.0001 vs WT (mean speed and distance traveled). *p<0.05 vs WT, ****p<0.0001 vs β1KO (FST).

Figure 3.6

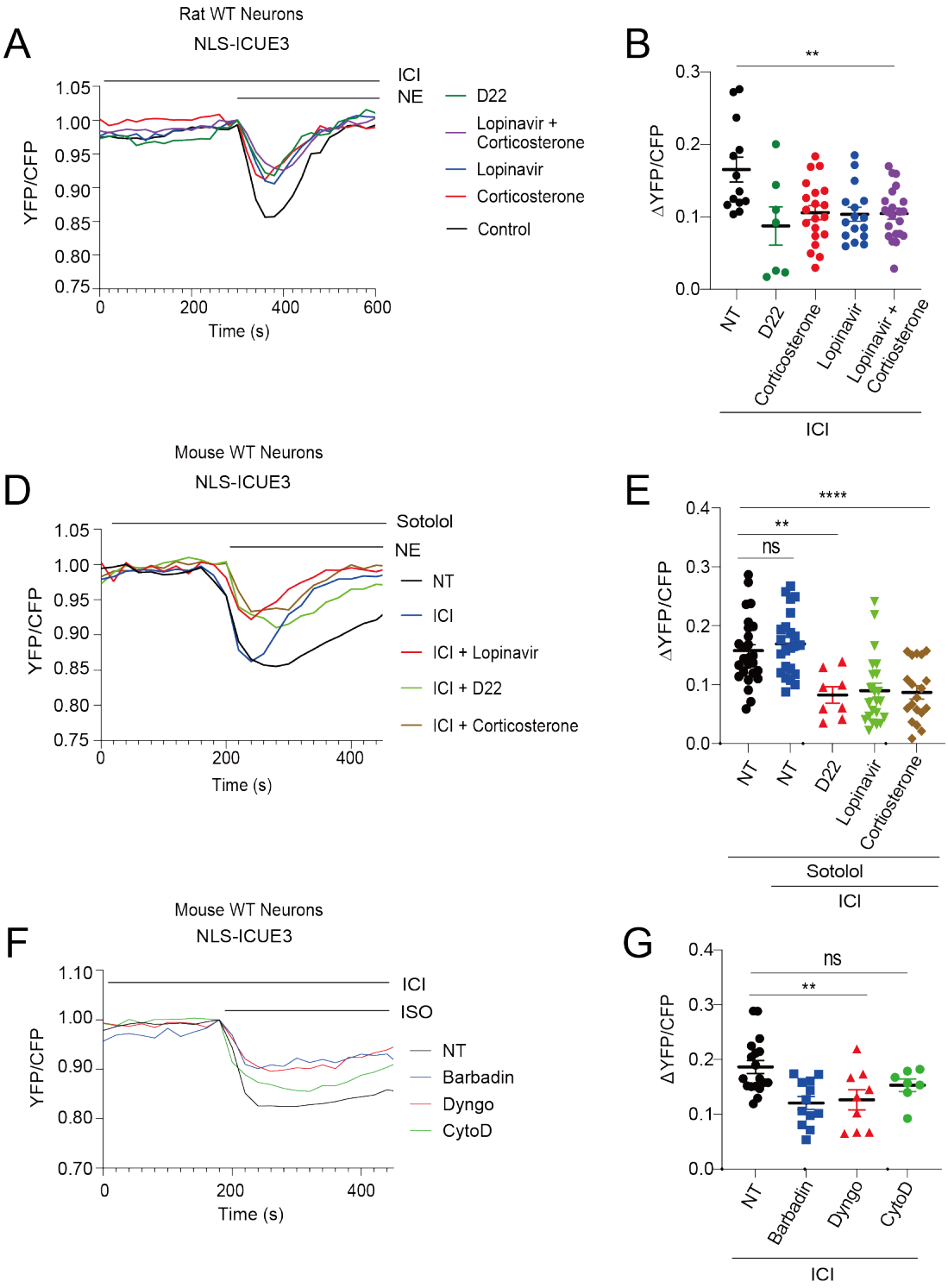
A
Rat WT Neurons
NLS-ICUE3
YFP/CFP
Time (s)
ICI
NE
D22
Lopinavir + Corticosterone
Lopinavir
Corticosterone
Control
B
ΔYFP/CFP
**
NT
D22
Corticosterone
Lopinavir
Lopinavir + Cortiosterone
ICI
D
Mouse WT Neurons
NLS-ICUE3
YFP/CFP
Time (s)
Sotolol
NE
NT
ICI
ICI + Lopinavir
ICI + D22
ICI + Corticosterone
E
ΔYFP/CFP
****
**
ns
NT
NT
D22
Lopinavir
Cortiosterone
Sotolol
ICI
F
Mouse WT Neurons
NLS-ICUE3
YFP/CFP
Time (s)
ICI
ISO
NT
Barbadin
Dyngo
CytoD
G
ΔYFP/CFP
ns
**
NT
Barbadin
Dyngo
CytoD
ICI

Figure 3.6. Blockade of catecholamine transporters reduces β1AR mediated nuclear cAMP signaling in primary hippocampal neurons.

(A and B) Primary hippocampal neurons isolated from e18 rat embryos were transfected with cAMP biosensor NLS-ICUE3 (B) Neurons were pretreated with β2AR antagonist 100 nM ICI-118,551 (ICI, 5 minutes) with or without catecholamine transporter (OCT3 and PMAT) inhibitor Decynium-22 (D22, 1 μM, 10 mins), OCT3 inhibitor corticosterone (10 μM, 10 mins), PMAT inhibitor lopinavir (10 μM, 10 mins), or corticosterone+lopinavir (10 μm/10 μM, 10 mins) before stimulation with 100 nM norepinephrine (NE) as indicated. The changes in YFP/CFP FRET ratio were recorded. Dot plots show the maximum FRET response (YFP/CFP) ratio relative to baseline in WT neurons after NE treatment. Data represent mean ± SEM. (D and E) Primary hippocampal neurons isolated from P0 or P1 WT mouse pups were transfected with cAMP biosensor NLS-ICUE3. Neurons were pretreated with membrane impermeant β2AR antagonist sotolol (25 μM, 10 mins) and with or without 100 nM ICI (5 minutes), D22 (1 μM, 10 mins), corticosterone (10 μM, 10 mins), lopinavir (10 μM, 10 mins), or corticosterone+lopinavir (10 μm/10 μM, 10 mins) before stimulation with 100 nM norepinephrine (NE) as indicated. The changes in YFP/CFP FRET ratio were recorded. Dot plots show the maximum FRET response (YFP/CFP) ratio relative to baseline in WT neurons after NE treatment. Data represent mean ± SEM. (F and G) Primary hippocampal neurons isolated from P0 or P1 WT mouse pups were transfected with cAMP biosensor NLS-ICUE3. Neurons were pretreated with 100 nM ICI (5 minutes) and with or without endocytosis inhibitors Barbadin (30 μM, 30 mins), Dyngo4a (1 μM, 30 mins), or cytochalasin D (CytoD 10 μM, 30 mins) before stimulation with 100 nM ISO as indicated. The changes in YFP/CFP FRET ratio were recorded. Dot plots show the maximum FRET response (YFP/CFP) ratio relative to baseline in WT neurons after ISO treatment. Data represent mean ± SEM.

Supplementary Figure 3.1

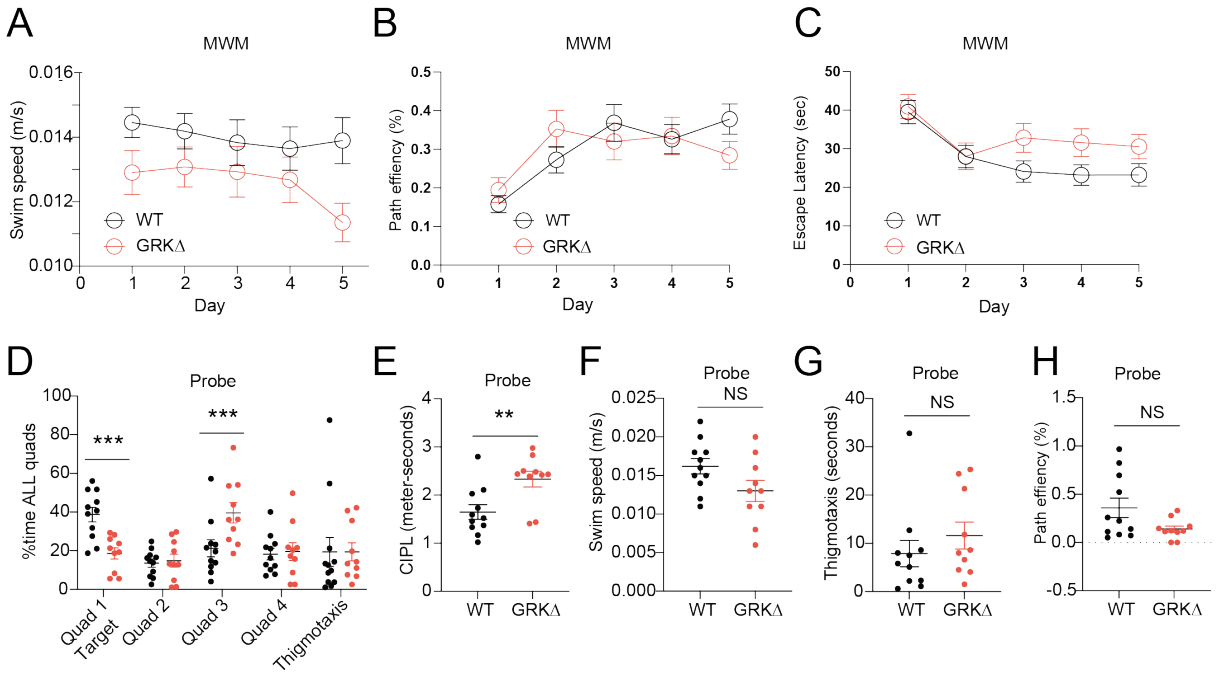

Supplemental Figure 3.1. Behavioral metrics of MWM maze performance.

(A) Average swim speed during maze testing. (B) Path efficiency of WT and GRKΔ mice in the Morris water maze. (C) Latency to escape platform in MWM training and probe trials. (D) Percent time in individual quadrants for WT and GRKΔ mice during probe trial. ***p<0.001 vs WT via 1-way ANOVA followed by Tukey's test. (E) CIPL for WT and GRKΔ mice during the probe trial. **p<0.01 vs WT via student's t-test (F) average swim speed for WT and GRKΔ mice during the probe trial (G) Time thigmotaxis in the MWM during probe trial. (H) path efficiency for WT and GRKΔ mice during the probe trial. Data represent mean ± SEM of individual mice.

Supplementary Figure 3.2

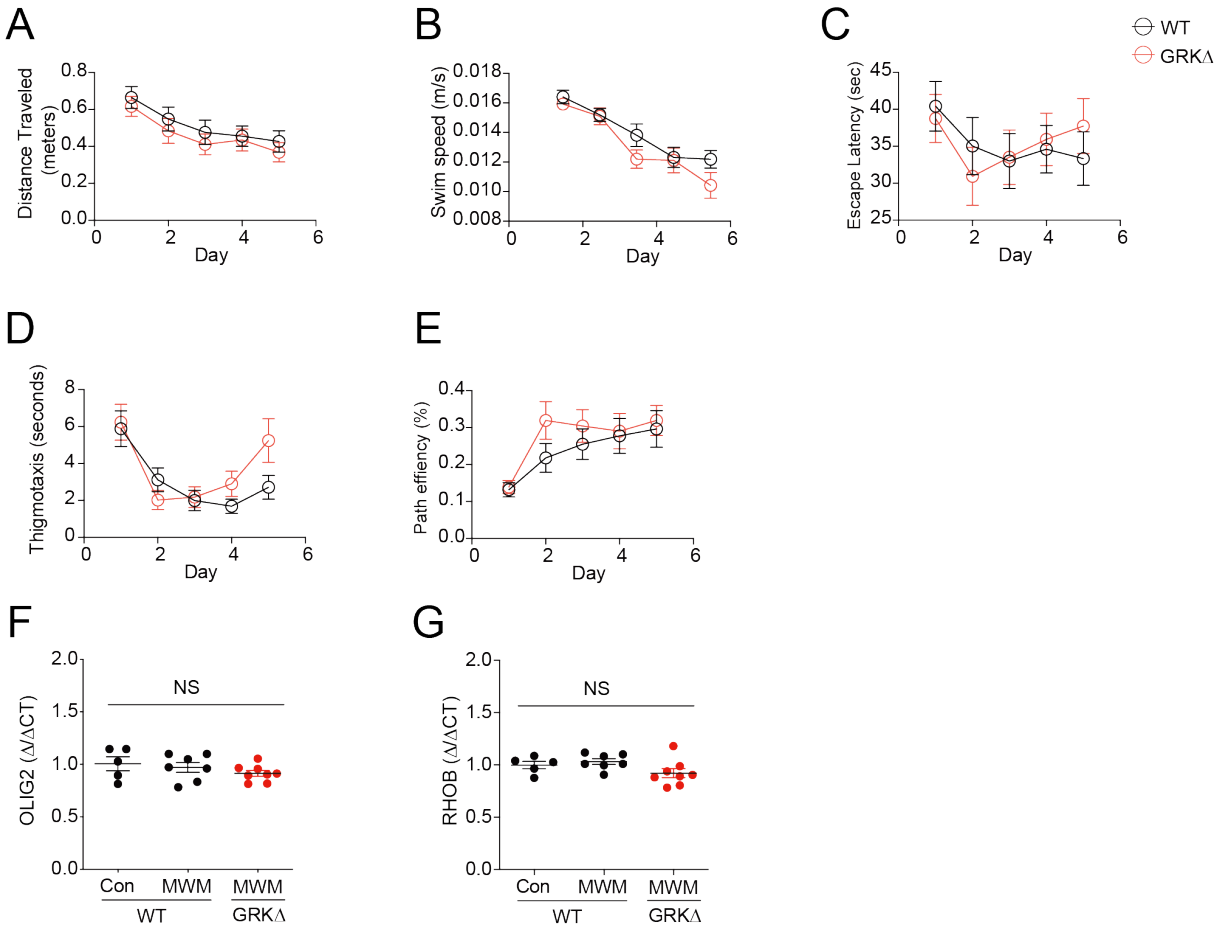

Supplemental Figure 3.2. Behavioral metrics of MWM maze performance for learning induced mRNA expression; IEG expression in WT and GRKΔ hippocampi.

(A-E) Morris water maze performance metrics for mice used in gene expression experiments in Figure 2. (F and G) Relative gene expression of OLIG2 and RHOB from WT and GRKΔ hippocampi with and without MWM training as assessed via qRT-PCR 1-hour after maze learning ended. Data represent mean ± SEM of individual mice.

Supplementary Figure 3.3

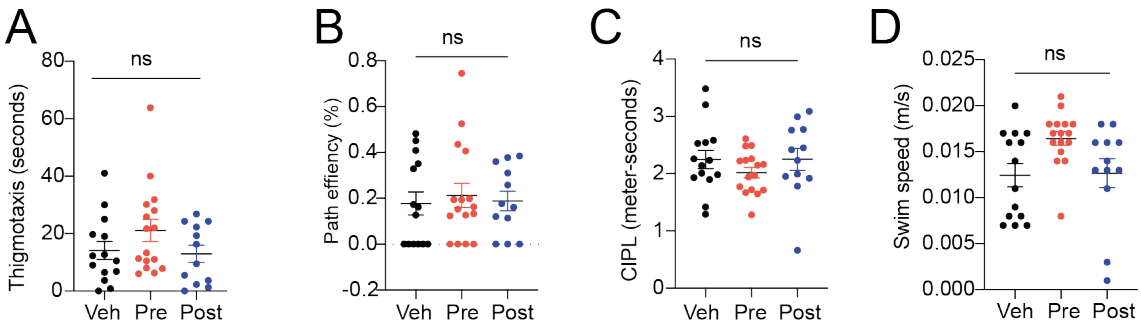

Supplementary Figure 3.3. MWM performance metrics for GRKΔ mice treated with vehicle or pretreated with roflumilast (3 mg/kg) 1-hour prior to maze testing or post-treated with roflumilast (3 mg/kg) 3-hours after maze training.

(A-D) Metrics of performance in the probe trial of the MWM for GRKΔ mice treated with vehicle, pre, or post roflumilast. Data represent mean ± SEM of individual mice.

Chapter 4: Future perspectives on beta-adrenergic signaling in the CNS: What is next?

Introduction

Adrenergic signaling in the brain regulates wakefulness and arousal, attention, and is involved in learning and memory [54-58]. The LC is the source of the vast majority of NE and consequently adrenergic signaling in the CNS [55]. It is known that beta-adrenergic signaling is involved in Alzheimer's disease (AD), Parkinson's disease (PD) exercise-induced cognitive benefits in I health and in diseases such AD and PD, depression, stress response, environmental enrichment benefits, Huntington's disease, ALS, MS, and generally in neuroinflammatory responses [307-311]. Some of these associations have been known for several decades [311]. Despite all these data showing adrenergic signaling involvement in the CNS, very little is known about the specific mechanisms by which adrenergic signaling participates in CNS function.

The work presented in this thesis project aimed to provide a small mechanistic contribution to how adrenergic signaling functions in CNS processes involved in hippocampal based learning and memory. To that end this work highlights a novel mechanism by which β_2ARs regulate nuclear cAMP signaling and IEG expression through the recruitment of arrestin/PDE4D5 to the cytosol. Further, it demonstrates that this mechanism is relevant to *in vivo* models of learning and memory. Over the course of this thesis project as more data was gathered supporting the proposed mechanism, interesting questions began to emerge regarding other roles of beta-adrenergic receptors in other aspects of CNS function. β_1AR mediated nuclear signaling remained in GRKΔ hippocampal neurons. And while learning induced IEG expression is deficit in GRKΔ mice, acute stress induced IEG expression remains intact. Knockout of β_1AR also ablates acute stress induced freezing in the forced swim test and removes anxiety response in the elevated plus maze. These data provide early evidence of a differential roles of beta-adrenergic receptors in CNS function.

This chapter will discuss what comes next for this line of research and CNS adrenergic signaling as a whole in health and disease.

βARs in neurodegenerative disorders and neuroinflammation

Beta-adrenergic receptors are involved in numerous disease states, implicated in both disease progression and possible therapeutic strategies. G-coupled protein receptors (GPCRs), consisting of seven transmembrane domains, are the largest and most diverse group of membrane receptors in eukaryotic cells and are responsible for mediating many of the physiological responses to hormones, neurotransmitters, and environmental inputs [109-111]. As such, GPCRs and their signaling cascades are highly druggable targets with 108 GPCRs accounting for ~34% of FDA approved drugs [112, 113]. Adrenergic receptors are highly drugged targets with numerous beta-blockers being used in hypertension and kidney, cardiovascular, and pulmonary disorders [312-317]. Additionally, beta blockers and beta agonists have been used to or been implicated in the treatment of AD, PD, and severe PTSD among others [45, 318-321]. The robust literature suggests that targeting adrenergic signaling and its downstream signaling effectors have potential for the treatment of many disorders. However, the lack of mechanistic information regarding the role adrenergic receptors play in these disorders and the difficulty in targeting specific receptors in specific brain regions has hindered progress. Studies of mechanistic insight such as this thesis work and general studies about the disorders discussed below, while no by no means exhaustive, provide insight into the future of therapeutics involving adrenergic signaling.

Parkinson's Disease

Recently, through an unbiased screening targeting endogenous gene expression with a library of 1126 compounds, including drugs approved by the US FDA and diverse with natural products, vitamins, health supplements, and alkaloids, our lab and collaborators have found that four compounds significantly reduced SNCA (alpha synuclein) mRNA and expression in human SK-N-MC neuroblastoma cells [45]. Alpha synuclein is the primary hyperphosphorylated protein found in Lewy bodies in Parkinson's disease. Unexpectedly, three of these four compounds were agonists for β_2AR in the central nervous system (CNS): metaproterenol, clenbuterol, and salbutamol. Subsequently, we have validated the critical role of β_2AR signaling in reducing SNCA gene expression both *in vitro* and *in vivo*, and in PD development in mouse models [45]. Deletion of the β_2AR gene abolishes the inhibitory effect of β_2AR agonists on SNCA gene expression, and treatment with β_2AR antagonists leads to increased SNCA gene expression [45]. Furthermore, we show that correlation of clinical usage of β_2AR agonists and reduced PD incidence in the

Norwegian population. Finally, administration of clenbuterol was protective against dopaminergic neuron death in the MPTP model of PD. Together, these data indicate that β_2AR is a critical regulator of theα-synuclein gene driving risk of PD [45]. Additionally, Stimulation of β_2AR is known to induce Akt signaling, a classic pro-survival pathway in the heart, immune cells, and neurons [43, 322, 323]. Dysfunction of Akt signaling is implicated in PD pathogenesis as well as other neurodegenerative disorders [324-326]. Phosphorylation of GSK3β, a downstream substrate of Akt, has been suggested as a mechanism for α-synuclein aggregation and neuronal toxicity in rotenone-induced PD model animals [327, 328]. Meanwhile, brain derived neurotrophic factor (BDNF) is a neurotrophin that regulates development and survival of neurons. Low levels of BDNF are found in early stages of PD and BDNF levels negatively correlate with motor impairment in later stages [329]. β_2AR stimulation increases BDNF synthesis [330] which may be an indirect mechanism by which β_2AR stimulation promotes neuron survival. Given these regulatory mechanisms involve gene transcription and Akt activation, both of which involve receptor internalization, it is reasonable to surmise that studies utilizing GRKΔ mice could provide mechanistic insight into these observations and suggest new drug targets/treatments for the treatment of PD.

Alzheimer's Disease

The polymorphisms of β_2AR and α_2AR contribute to sporadic late-onset AD [331-333]. Drugs targeting β_2AR, α_1AR, and α_2AR modify disease progress in AD animal models with overexpression of human familial APP and/or PSEN genes [334-337]; Moreover, drugs targeting α_1AR is effective on AD patients with agitation and aggression [337] whereas drugs targeting α_2AR reduce AD incidence in humans. [338] The impacts of beta-blockers on human AD remains inconclusive. [339-341] These observations are likely complicated by the fact that most beta-blockers selectively target β_1AR and have direct effects on cognition. Cardiovascular effects could also contribute to the overall impacts of the drugs on AD. Additionally, those on beta blocker therapies for cardiovascular disorders may not survive long enough to develop later stages of AD complicating interpretations of results. Work from our lab has shown amyloid beta, whose presence in the brain in the form of oligomers and plaques is a defining disease characteristic, can bind to β_2AR and induce signaling by itself or enhance ligand induced signaling [342]. Amyloid precursor processing involves internalization of γ-secretase, and it is therefore

possible that internalization of β_2AR could be induced by amyloid beta driving APP processing in a feedforward mechanism. Additionally, amyloid beta binding to β_2AR has been shown to activate PKA dependent AMPA receptor reactivity [343]. Activation of β_2AR and subsequent PKA mediated activation of LTCC is also known [122]. The PKA-pβ_2AR subpopulation may, therefore, play a role in excitotoxity in AD as well as aberrant LTP.

Exercise and Environmental Enrichment

Exercise and increased stimulatory activity is known the improve many chronic disorders. β_2AR signaling is stimulated during exercise and is cardioprotective [173, 344]. Additionally, exercise is associated with improved motor function in PD patients as well as a slowing of motor function decline [345, 346]. Exercise also improves mental health in PD patients, helping to alleviate PD associated depression while also exerting positive effects on global cognitive function in PD patients, and is an effective contributor to PD treatment regimens [346, 347]. Exercise has been shown to increase norepinephrine levels in the pons-medulla, spinal cord, hippocampus, and medial amygdala as well. Exercise also increased endogenous norepinephrine activity [348] Exercise also increases levels of BDNF [349]. BDNF is thought to mediate exercise enhanced cognition and synaptic plasticity [350]. Low levels of BDNF are found in early stages of PD and BDNF levels correlate with motor impairment in later stages. These increases in BDNF levels in later stages of PD are thought to be compensatory [329]. β_2AR stimulation in astrocytes increases BDNF synthesis and noradrenergic blockade inhibits exercise induced BDNF mRNA increases [330, 351]. Additionally, environmental enrichment has been shown to improve cognitive symptoms in models of AD by reducing neuroinflammation [188]. Other prospective studies have shown the benefit of exercise of cognitive enrichment in AD patients is beneficial. However other metanalysis studies have not found benefits (Reviewed in [352]). Exercise also negatively correlated to depression incidence (Reviewed in [353]). Taken together, these data suggest that exercise produces beneficial effects in AD, PD, depression, or other neuroinflammatory disorders and β_2AR signaling may play a role in these exercise-mediated benefits. However, due to a lack of mechanistic understanding of how adrenergic signaling confers exercise or enrichment mediated benefits, how to utilize exercise and cognitive enrichment in CNS disorders remains unclear.

Neuroinflammation

Neuroinflammation is associated with many neurodegenerative disorders. Beta-adrenergic receptors are known to be involved in inflammatory responses in the periphery and the brain and activate microglia [165, 354-356]. Stimulation of β2AR signaling has been shown to reduce neuroinflammatory response following ischemic stroke [357] but also has been shown to increase stroke size [357]. However, beta-adrenergic stimulation has been found to be pro inflammatory in a model of AD [358]. Further, stress induced microglial activation requires beta-adrenergic signaling [359] and beta-adrenergic receptors contribute to environmental enrichment induced reduction in neuroinflammation [188]. From these data it is clear that beta-adrenergic signaling plays an important role in neuroinflammatory responses. However, it is also clear that beta-adrenergic signaling can be harmful or beneficial depending on the nature of the insult leading to inflammation. As such more research is warranted to better understand beta-adrenergic signaling in neuroinflammation.

Future directions examining subcellular β_2AR-mediated sequestration of PDE4D5

The work presented in this dissertation work highlight a novel mechanism by which internalization of β_2AR facilitates nuclear cAMP signal, gene expression, and memory consolidation via arrestin-mediated PDE4D5 sequestration out of the nucleus to the cytosol. Despite the novelty and data supporting these assertions, the proposed mechanism still leaves many questions to be pursued. The source of cAMP reaching the endosome remains in dispute. There are multiple known PDEs that are anchored to the PM or are cytosolic in nature which may block cAMP generated at the PM by the PKA-pβ_2AR or other PM sources of cAMP from reaching the nucleus without degradation. However, it is possible cAMP generated at the PM can propagate to the nucleus either by rearrangement of PDE microdomains caused by internalization of β_2AR or due to generation of enough cAMP at the PM to overcome PDE blockades as proposed in the limitations and alternative interpretations sections in Chapters 2 and 3. We have also put forth an alternative possible mechanism for endosomal generated cAMP signals reaching the nucleus through activation of AC9 [273] on non-beta receptor carrying endosomes by Gs signaling from endosomes carrying β_2AR. Essentially, there exit subpopulations of endosomes, some endosomes that facilitate sequestration of PDE4D5 and other endosomes that

produce cAMP. This, however, is not the lone possible source of nuclear cAMP observed in our studies. Further studies are needed to address these concerns.

In addition to determining the source of our observed nuclear cAMP, how beta arrestin mediates transport of PDE4D5 out of the nucleus remains to elucidated. It is known that arrestin and PDE4D are associated with β_2AR [230, 268]. GPCRs are divided into two classes with respect to arrestin binding [360-362]. Class A receptors form transient complexes with arrestins, dissociating rapidly while Class B GPCRs have high affinity binding for both β-arrestin1 and β-arrestin2 and form stable arrestin-receptor complexes. β_2AR is the classic example of a Class A receptor while examples of Class B receptors are vasopressin 2 receptors and angiotensin II type 1 receptors [363]. β-arrestin2 is known to preferentially operate on or near the PM in receptor internalization whereas β-arrestin1 has a stronger nuclear distribution. β-arrestin2 has both nuclear export sequence and a nuclear location sequence [274, 275]. β-arrestin1, however, only has an NLS motif [275] and is known to translocate to the nucleus and facilitate gene expression [364]. These data suggest a possible mechanism whereby β-arrestin2 forms a transient complex with β_2AR, transports to the receptor to the endosome, detaches from the receptor and β-arrestin1 then transports PDE4D5 out of the nucleus to the receptor. However, this proposed mechanism begs the question as to how β-arrestin1 is leaving the nucleus as it lacks an NES motif. β-arrestin1 and 2 are known to form complexes with each other [365] and, as β-arrestin2 has both NLS and NES motifs, β-arrestin2 could facilitate the movement of a PDE4D5/β-arrestin1 complex out of the nucleus. It is also possible for numerous other mechanisms as β-arrestins have a large interactome [366]. There also remains the possibility that other Gs coupled Type A GPCRs can function in a similar manner as our proposed β_2AR-mediated mechanism. Detailed studies will be necessary to further define this mechanism and determine the generalizability of this mechanism.

Our data show that β_1AR is necessary for acute stress and anxiety responses. However, our preliminary data does not fully support the hypothesis that nuclear envelope-located β_1AR is responsible for β_1AR-mediated nuclear cAMP signal. Indeed, we only see partial loss of nuclear cAMP signal when we block catecholamine transporters. It is possible that other transporters may play a role in our observations. Blocking all available transporters of NE may fully ablate β_1AR mediated nuclear cAMP but

that remains to be determined. There is also data indicating β_1AR is involved in memory as well as stress and that blockade of β_1AR may contribute to rather than alleviate stress phenotypes as observed here [282, 287, 367, 368]. Further studies examining fear learning, also known to have a strong adrenergic signaling component, are also merited. It is likely that all three beta-adrenergic receptors play a role in both learning and memory, both spatial and fear, and the interaction of stress and memory.

As highlighted in this chapter, adrenergic signaling in the brain remains understudied but also has great potential for understanding fundamental brain functions as well as the pathogenesis of myriad disease states. These data presented here offer a small contribution to our mechanistic understanding of beta-adrenergic signaling in memory and stress response. Future studies can and will build on these insights to provide greater understanding of the brain in health and disease.

References

1. Sara, S.J., *The locus coeruleus and noradrenergic modulation of cognition.* Nature reviews. Neuroscience, 2009. **10**(3): p. 211-23.
2. Berridge, C.W. and B.D. Waterhouse, *The locus coeruleus-noradrenergic system: modulation of behavioral state and state-dependent cognitive processes.* Brain research. Brain research reviews, 2003. **42**(1): p. 33-84.
3. Devilbiss, D.M. and B.D. Waterhouse, *Phasic and tonic patterns of locus coeruleus output differentially modulate sensory network function in the awake rat.* J Neurophysiol, 2011. **105**(1): p. 69-87.
4. De Martino, B., B.A. Strange, and R.J. Dolan, *Noradrenergic neuromodulation of human attention for emotional and neutral stimuli.* Psychopharmacology (Berl), 2008. **197**(1): p. 127-36.
5. Maity, S., et al., *Norepinephrine triggers metaplasticity of LTP by increasing translation of specific mRNAs.* Learn Mem, 2015. **22**(10): p. 499-508.
6. Hu, H., et al., *Emotion enhances learning via norepinephrine regulation of AMPA-receptor trafficking.* Cell, 2007. **131**(1): p. 160-73.
7. McGaugh, J.L., *Making lasting memories: remembering the significant.* Proc Natl Acad Sci U S A, 2013. **110 Suppl 2**: p. 10402-7.
8. Murchison, C.F., et al., *A distinct role for norepinephrine in memory retrieval.* Cell, 2004. **117**(1): p. 131-43.
9. Takeuchi, T., A.J. Duszkiewicz, and R.G. Morris, *The synaptic plasticity and memory hypothesis: encoding, storage and persistence.* Philos Trans R Soc Lond B Biol Sci, 2014. **369**(1633): p. 20130288.
10. Lomo, T. *Frequency potentiation of excitatory synaptic activity in dentate area of hippocampal formation*. in *Acta Physiologica Scandinavica*. 1966. Blackwell Science Ltd PO BOX 88, OSNEY MEAD, OXFORD OX2 0NE, OXON, ENGLAND.
11. Lines, J., et al., *Synapse-Specific Regulation Revealed at Single Synapses Is Concealed When Recording Multiple Synapses.* Front Cell Neurosci, 2017. **11**: p. 367.
12. Nakazawa, K., et al., *Hippocampal CA3 NMDA receptors are crucial for memory acquisition of one-time experience.* Neuron, 2003. **38**(2): p. 305-15.
13. Forner, S., et al., *Systematic Phenotyping and Characterization of the 5xFAD mouse model of Alzheimer's Disease.* bioRxiv, 2021: p. 2021.02.17.431716.
14. Martin, S.J., P.D. Grimwood, and R.G. Morris, *Synaptic plasticity and memory: an evaluation of the hypothesis.* Annu Rev Neurosci, 2000. **23**: p. 649-711.
15. Abraham, W.C., O.D. Jones, and D.L. Glanzman, *Is plasticity of synapses the mechanism of long-term memory storage?* NPJ Sci Learn, 2019. **4**: p. 9.
16. Nicoll, R.A., *A Brief History of Long-Term Potentiation.* Neuron, 2017. **93**(2): p. 281-290.
17. Puzzo, D., et al., *Chapter 1 - Molecular Mechanisms of Learning and Memory**The authors declare no competing financial interests*, in *Genes, Environment and Alzheimer's Disease*, O. Lazarov and G. Tesco, Editors. 2016, Academic Press: San Diego. p. 1-27.
18. Bliss, T.V. and T. Lomo, *Long-lasting potentiation of synaptic transmission in the dentate area of the anaesthetized rabbit following stimulation of the perforant path.* J Physiol, 1973. **232**(2): p. 331-56.
19. Collingridge, G.L., S. Kehl, and H.t. McLennan, *Excitatory amino acids in synaptic transmission in the Schaffer collateral-commissural pathway of the rat hippocampus.* The Journal of physiology, 1983. **334**(1): p. 33-46.
20. Mayer, M.L., G.L. Westbrook, and P.B. Guthrie, *Voltage-dependent block by Mg2+ of NMDA responses in spinal cord neurones.* Nature, 1984. **309**(5965): p. 261-263.
21. Dolphin, A., M. Errington, and T. Bliss, *Long-term potentiation of the perforant path in vivo is associated with increased glutamate release.* Nature, 1982. **297**(5866): p. 496-497.
22. Lisman, J.E. and M.A. Goldring, *Feasibility of long-term storage of graded information by the Ca2+/calmodulin-dependent protein kinase molecules of the postsynaptic density.* Proceedings of the National Academy of Sciences, 1988. **85**(14): p. 5320-5324.
23. Miller, S.G. and M.B. Kennedy, *Regulation of brain Type II Ca2+ calmodulin-dependent protein kinase by autophosphorylation: A Ca2+-triggered molecular switch.* Cell, 1986. **44**(6): p. 861-870.

24. MacDermott, A.B., et al., *NMDA-receptor activation increases cytoplasmic calcium concentration in cultured spinal cord neurones.* Nature, 1986. **321**(6069): p. 519-522.
25. Ascher, P. and L. Nowak, *The role of divalent cations in the N-methyl-D-aspartate responses of mouse central neurones in culture.* The Journal of physiology, 1988. **399**(1): p. 247-266.
26. Lynch, G., et al., *Intracellular injections of EGTA block induction of hippocampal long-term potentiation.* Nature, 1983. **305**(5936): p. 719-721.
27. Lu, Y., K. Christian, and B. Lu, *BDNF: a key regulator for protein synthesis-dependent LTP and long-term memory?* Neurobiol Learn Mem, 2008. **89**(3): p. 312-23.
28. Frey, U., Y.Y. Huang, and E.R. Kandel, *Effects of cAMP simulate a late stage of LTP in hippocampal CA1 neurons.* Science, 1993. **260**(5114): p. 1661-4.
29. Zhong, H., et al., *Subcellular dynamics of type II PKA in neurons.* Neuron, 2009. **62**(3): p. 363-74.
30. Delghandi, M.P., M. Johannessen, and U. Moens, *The cAMP signalling pathway activates CREB through PKA, p38 and MSK1 in NIH 3T3 cells.* Cell Signal, 2005. **17**(11): p. 1343-51.
31. Finkbeiner, S., et al., *CREB: A Major Mediator of Neuronal Neurotrophin Responses.* Neuron, 1997. **19**(5): p. 1031-1047.
32. Bahrami, S. and F. Drablos, *Gene regulation in the immediate-early response process.* Adv Biol Regul, 2016. **62**: p. 37-49.
33. Morgan, J.I. and T. Curran, *Stimulus-transcription coupling in the nervous system: involvement of the inducible proto-oncogenes fos and jun.* Annual review of neuroscience, 1991. **14**(1): p. 421-451.
34. Gomard, T., et al., *Fos family protein degradation by the proteasome.* Biochem Soc Trans, 2008. **36**(Pt 5): p. 858-63.
35. Greenberg, M.E. and E.B. Ziff, *Stimulation of 3T3 cells induces transcription of the c-fos proto-oncogene.* Nature, 1984. **311**(5985): p. 433-438.
36. Cullinan, W.E., et al., *Pattern and time course of immediate early gene expression in rat brain following acute stress.* Neuroscience, 1995. **64**(2): p. 477-505.
37. Miyata, S., et al., *Time course of Fos and Fras expression in the hypothalamic supraoptic neurons during chronic osmotic stimulation.* Brain Res Mol Brain Res, 2001. **90**(1): p. 39-47.
38. Baille-Le Crom, V., et al., *Time course and regional expression of C-FOS and HSP70 in hippocampus and piriform cortex following soman-induced seizures.* J Neurosci Res, 1996. **45**(5): p. 513-24.
39. Zhong, J., et al., *c-Fos expression in the paternal mouse brain induced by communicative interaction with maternal mates.* Mol Brain, 2014. **7**: p. 66.
40. Barros, V.N., et al., *The pattern of c-Fos expression and its refractory period in the brain of rats and monkeys.* Front Cell Neurosci, 2015. **9**: p. 72.
41. Miyashita, T., et al., *Long-Term Memory Engram Cells Are Established by c-Fos/CREB Transcriptional Cycling.* Cell Rep, 2018. **25**(10): p. 2716-2728 e3.
42. Minatohara, K., M. Akiyoshi, and H. Okuno, *Role of Immediate-Early Genes in Synaptic Plasticity and Neuronal Ensembles Underlying the Memory Trace.* Front Mol Neurosci, 2015. **8**: p. 78.
43. O'Dell, T.J., et al., *beta-Adrenergic receptor signaling and modulation of long-term potentiation in the mammalian hippocampus.* Learn Mem, 2015. **22**(9): p. 461-71.
44. Kellenberger, S., et al., *Formoterol and isoproterenol induce c-fos gene expression in osteoblast-like cells by activating beta2-adrenergic receptors.* Bone, 1998. **22**(5): p. 471-8.
45. Mittal, S., et al., *beta2-Adrenoreceptor is a regulator of the alpha-synuclein gene driving risk of Parkinson's disease.* Science, 2017. **357**(6354): p. 891-898.
46. Ciccarelli, M., et al., *Chapter 11 - Adrenergic Receptors*, in *Endocrinology of the Heart in Health and Disease*, J.C. Schisler, C.H. Lang, and M.S. Willis, Editors. 2017, Academic Press. p. 285-315.
47. Kandel, E.R., *The molecular biology of memory: cAMP, PKA, CRE, CREB-1, CREB-2, and CPEB.* Mol Brain, 2012. **5**: p. 14.
48. Yin, J.C. and T. Tully, *CREB and the formation of long-term memory.* Curr Opin Neurobiol, 1996. **6**(2): p. 264-8.
49. Tsvetanova, N.G. and M. von Zastrow, *Spatial encoding of cyclic AMP signaling specificity by GPCR endocytosis.* Nat Chem Biol, 2014. **10**(12): p. 1061-5.
50. Gold, P.E., *Protein synthesis inhibition and memory: formation vs amnesia.* Neurobiology of learning and memory, 2008. **89**(3): p. 201-11.

51. Harley, C.W., *Norepinephrine and the dentate gyrus.* Progress in brain research, 2007. **163**: p. 299-318.
52. McIntyre, C.K., et al., *Role of the basolateral amygdala in memory consolidation.* Annals of the New York Academy of Sciences, 2003. **985**: p. 273-93.
53. McGaugh, J.L., *The amygdala modulates the consolidation of memories of emotionally arousing experiences.* Annual review of neuroscience, 2004. **27**: p. 1-28.
54. Muzzio, I.A., C. Kentros, and E. Kandel, *What is remembered? Role of attention on the encoding and retrieval of hippocampal representations.* J Physiol, 2009. **587**(Pt 12): p. 2837-54.
55. Sara, S.J., *Locus Coeruleus in time with the making of memories.* Curr Opin Neurobiol, 2015. **35**: p. 87-94.
56. O'Donnell, J., et al., *Norepinephrine: a neuromodulator that boosts the function of multiple cell types to optimize CNS performance.* Neurochem Res, 2012. **37**(11): p. 2496-512.
57. Breton-Provencher, V., G.T. Drummond, and M. Sur, *Locus Coeruleus Norepinephrine in Learned Behavior: Anatomical Modularity and Spatiotemporal Integration in Targets.* Front Neural Circuits, 2021. **15**: p. 638007.
58. Berridge, C.W., B.E. Schmeichel, and R.A. Espana, *Noradrenergic modulation of wakefulness/arousal.* Sleep Med Rev, 2012. **16**(2): p. 187-97.
59. Fuxe, K., et al., *From the Golgi-Cajal mapping to the transmitter-based characterization of the neuronal networks leading to two modes of brain communication: wiring and volume transmission.* Brain Res Rev, 2007. **55**(1): p. 17-54.
60. Fuxe, K., et al., *The discovery of central monoamine neurons gave volume transmission to the wired brain.* Prog Neurobiol, 2010. **90**(2): p. 82-100.
61. Olson, L. and K. Fuxe, *Further mapping out of central noradrenaline neuron systems: projections of the "subcoeruleus" area.* Brain Res, 1972. **43**(1): p. 289-95.
62. Le Foll, B., *Chapter 55 - Neuropharmacology of Nicotine*, in *Biological Research on Addiction*, P.M. Miller, Editor. 2013, Academic Press: San Diego. p. 561-571.
63. Byrum, C.E. and P.G. Guyenet, *Afferent and efferent connections of the A5 noradrenergic cell group in the rat.* J Comp Neurol, 1987. **261**(4): p. 529-42.
64. Coote, J.H., *Noradrenergic projections to the spinal cord and their role in cardiovascular control.* J Auton Nerv Syst, 1985. **14**(3): p. 255-62.
65. Guyenet, P.G., *Central noradrenergic neurons: the autonomic connection.* Prog Brain Res, 1991. **88**: p. 365-80.
66. Sharma, Y., et al., *Comparative anatomy of the locus coeruleus in humans and nonhuman primates.* J Comp Neurol, 2010. **518**(7): p. 963-71.
67. Swanson, L.W. and B.K. Hartman, *The central adrenergic system. An immunofluorescence study of the location of cell bodies and their efferent connections in the rat utilizing dopamine-beta-hydroxylase as a marker.* J Comp Neurol, 1975. **163**(4): p. 467-505.
68. Segal, M. and S. Landis, *Afferents to the hippocampus of the rat studied with the method of retrograde transport of horseradish peroxidase.* Brain Res, 1974. **78**(1): p. 1-15.
69. Waterhouse, B.D., et al., *The distribution of neocortical projection neurons in the locus coeruleus.* J Comp Neurol, 1983. **217**(4): p. 418-31.
70. Berridge, C.W. and B.D. Waterhouse, *The locus coeruleus-noradrenergic system: modulation of behavioral state and state-dependent cognitive processes.* Brain Res Brain Res Rev, 2003. **42**(1): p. 33-84.
71. Chandler, D.J., W.J. Gao, and B.D. Waterhouse, *Heterogeneous organization of the locus coeruleus projections to prefrontal and motor cortices.* Proc Natl Acad Sci U S A, 2014. **111**(18): p. 6816-21.
72. Chandler, D.J., C.S. Lamperski, and B.D. Waterhouse, *Identification and distribution of projections from monoaminergic and cholinergic nuclei to functionally differentiated subregions of prefrontal cortex.* Brain Res, 2013. **1522**: p. 38-58.
73. Berridge, C.W. and S.L. Foote, *Effects of locus coeruleus activation on electroencephalographic activity in neocortex and hippocampus.* J Neurosci, 1991. **11**(10): p. 3135-45.
74. Nieuwenhuys, R., *Chemoarchitecture of the brain, 77 Springer Verlag*. 1985, Stuttgart.
75. Aston-Jones, G., *Brain structures and receptors involved in alertness.* Sleep Med, 2005. **6 Suppl 1**: p. S3-7.

76. Aston-Jones, G. and F.E. Bloom, *Activity of norepinephrine-containing locus coeruleus neurons in behaving rats anticipates fluctuations in the sleep-waking cycle.* J Neurosci, 1981. **1**(8): p. 876-86.
77. Rajkowski, J., P. Kubiak, and G. Aston-Jones, *Locus coeruleus activity in monkey: phasic and tonic changes are associated with altered vigilance.* Brain Res Bull, 1994. **35**(5-6): p. 607-16.
78. Berridge, C.W., et al., *Effects of locus coeruleus inactivation on electroencephalographic activity in neocortex and hippocampus.* Neuroscience, 1993. **55**(2): p. 381-93.
79. Kiernan, J.A. and M.L. Barr, *Barr's the human nervous system: an anatomical viewpoint*. 2009: Lippincott Williams & Wilkins.
80. Khakpour-Taleghani, B., et al., *The locus coeruleus involves in consolidation and memory retrieval, but not in acquisition of inhibitory avoidance learning task.* Behav Brain Res, 2008. **189**(2): p. 257-62.
81. Devauges, V. and S.J. Sara, *Memory retrieval enhancement by locus coeruleus stimulation: evidence for mediation by beta-receptors.* Behav Brain Res, 1991. **43**(1): p. 93-7.
82. Wagatsuma, A., et al., *Locus coeruleus input to hippocampal CA3 drives single-trial learning of a novel context.* Proc Natl Acad Sci U S A, 2018. **115**(2): p. E310-E316.
83. Hansen, N., *The Longevity of Hippocampus-Dependent Memory Is Orchestrated by the Locus Coeruleus-Noradrenergic System.* Neural Plast, 2017. **2017**: p. 2727602.
84. Loughlin, S.E., S.L. Foote, and F.E. Bloom, *Efferent projections of nucleus locus coeruleus: topographic organization of cells of origin demonstrated by three-dimensional reconstruction.* Neuroscience, 1986. **18**(2): p. 291-306.
85. Grzanna, R. and M.E. Molliver, *The locus coeruleus in the rat: an immunohistochemical delineation.* Neuroscience, 1980. **5**(1): p. 21-40.
86. Vegh, A.M.D., et al., *Part and Parcel of the Cardiac Autonomic Nerve System: Unravelling Its Cellular Building Blocks during Development.* J Cardiovasc Dev Dis, 2016. **3**(3).
87. Wurtman, R.J. and L.A. Pohorecky, *Adrenocortical control of epinephrine synthesis in health and disease.* Adv Metab Disord, 1971. **5**: p. 53-76.
88. Isobe, K., K. Takekoshi, and Y. Kawakami, *Phenylethanolamine N-Methyltransferase*, in *Encyclopedia of Endocrine Diseases*, L. Martini, Editor. 2004, Elsevier: New York. p. 591-593.
89. Sved, A.F. and J.P. Card, *Brain Adrenergic Neurons*, in *Encyclopedia of Neuroscience*, L.R. Squire, Editor. 2009, Academic Press: Oxford. p. 295-302.
90. Bohn, M.C., M. Goldstein, and I.B. Black, *Expression and development of phenylethanolamine N-methyltransferase (PNMT) in rat brain stem: studies with glucocorticoids.* Dev Biol, 1986. **114**(1): p. 180-93.
91. Wang, Y., et al., *Optogenetic Control of Heart Rhythm by Selective Stimulation of Cardiomyocytes Derived from Pnmt(+) Cells in Murine Heart.* Sci Rep, 2017. **7**: p. 40687.
92. Kitahama, K., et al., *Adrenergic neurons in human brain demonstrated by immunohistochemistry with antibodies to phenylethanolamine-N-methyltransferase (PNMT): discovery of a new group in the nucleus tractus solitarius.* Neurosci Lett, 1985. **53**(3): p. 303-8.
93. Zhou, J., *Norepinephrine transporter inhibitors and their therapeutic potential.* Drugs Future, 2004. **29**(12): p. 1235-1244.
94. Torres, G.E., R.R. Gainetdinov, and M.G. Caron, *Plasma membrane monoamine transporters: structure, regulation and function.* Nat Rev Neurosci, 2003. **4**(1): p. 13-25.
95. Gaweska, H. and P.F. Fitzpatrick, *Structures and Mechanism of the Monoamine Oxidase Family.* Biomol Concepts, 2011. **2**(5): p. 365-377.
96. Domino, E.F., *Monoamine oxidase substrates and substrate affinity.* Schizophr Bull, 1980. **6**(2): p. 292-7.
97. Cesura, A.M., *Monoamine Oxidase B*, in *xPharm: The Comprehensive Pharmacology Reference*, S.J. Enna and D.B. Bylund, Editors. 2007, Elsevier: New York. p. 1-10.
98. Chen, K. and J.C. Shih, *Monoamine Oxidase A and B: Structure, Function, and Behavior*, in *Advances in Pharmacology*, D.S. Goldstein, G. Eisenhofer, and R. McCarty, Editors. 1997, Academic Press. p. 292-296.
99. Chen, K. and J.C. Shih, *Monoamine oxidase A and B: structure, function, and behavior.* Adv Pharmacol, 1998. **42**: p. 292-6.

100. Schapira, A.H.V., *Chapter 18 - Neuroprotection in Parkinson's Disease*, in *Blue Books of Neurology*, A.H.V. Schapira, A.E.T. Lang, and S. Fahn, Editors. 2010, Butterworth-Heinemann. p. 301-320.
101. Cho, H.U., et al., *Redefining differential roles of MAO-A in dopamine degradation and MAO-B in tonic GABA synthesis.* Exp Mol Med, 2021. **53**(7): p. 1148-1158.
102. Meyer, J.H., et al., *Elevated monoamine oxidase a levels in the brain: an explanation for the monoamine imbalance of major depression.* Arch Gen Psychiatry, 2006. **63**(11): p. 1209-16.
103. Fowler, J.S., et al., *Brain monoamine oxidase A inhibition in cigarette smokers.* Proc Natl Acad Sci U S A, 1996. **93**(24): p. 14065-9.
104. Glassman, A.H., et al., *Smoking cessation and the course of major depression: a follow-up study.* Lancet, 2001. **357**(9272): p. 1929-32.
105. Newman, T.K., et al., *Monoamine oxidase A gene promoter variation and rearing experience influences aggressive behavior in rhesus monkeys.* Biol Psychiatry, 2005. **57**(2): p. 167-72.
106. McDermott, R., et al., *Monoamine oxidase A gene (MAOA) predicts behavioral aggression following provocation.* Proc Natl Acad Sci U S A, 2009. **106**(7): p. 2118-23.
107. Mentis, A.A., et al., *From warrior genes to translational solutions: novel insights into monoamine oxidases (MAOs) and aggression.* Transl Psychiatry, 2021. **11**(1): p. 130.
108. Wang, Y., et al., *Monoamine Oxidases Desensitize Intracellular beta1AR Signaling in Heart Failure.* Circ Res, 2021. **129**(10): p. 965-967.
109. O'Connor, C. and J. Adams, *Essentials of Cell Biology*, C. O'Connor, Editor. 2010, Nature Publishing Group Education Cambridge, MA.
110. Kroeze, W.K., D.J. Sheffler, and B.L. Roth, *G-protein-coupled receptors at a glance.* J Cell Sci, 2003. **116**(Pt 24): p. 4867-9.
111. Rosenbaum, D.M., S.G. Rasmussen, and B.K. Kobilka, *The structure and function of G-protein-coupled receptors.* Nature, 2009. **459**(7245): p. 356-63.
112. Hauser, A.S., et al., *Pharmacogenomics of GPCR Drug Targets.* Cell, 2018. **172**(1-2): p. 41-54.e19.
113. Fang, Y., T. Kenakin, and C. Liu, *Editorial: Orphan GPCRs As Emerging Drug Targets.* Front Pharmacol, 2015. **6**: p. 295.
114. Leung, C.C.Y. and Y.H. Wong, *Role of G Protein-Coupled Receptors in the Regulation of Structural Plasticity and Cognitive Function.* Molecules, 2017. **22**(7).
115. Schena, G. and M.J. Caplan, *Everything You Always Wanted to Know about beta3-AR * (* But Were Afraid to Ask).* Cells, 2019. **8**(4).
116. Ahmadirad, N., et al., *The Role of Adrenergic Receptors on Neural Excitability and Synaptic Plasticity: A Narrative Review.* Journal of Rafsanjan University of Medical Sciences, 2020. **18**(10): p. 1049-1064.
117. Philipp, M., M. Brede, and L. Hein, *Physiological significance of alpha(2)-adrenergic receptor subtype diversity: one receptor is not enough.* Am J Physiol Regul Integr Comp Physiol, 2002. **283**(2): p. R287-95.
118. Perez, D.M., *alpha1-Adrenergic Receptors in Neurotransmission, Synaptic Plasticity, and Cognition.* Front Pharmacol, 2020. **11**: p. 581098.
119. Perez, D.M., *Current Developments on the Role of alpha1-Adrenergic Receptors in Cognition, Cardioprotection, and Metabolism.* Front Cell Dev Biol, 2021. **9**: p. 652152.
120. Rasmussen, S.G., et al., *Crystal structure of the human beta2 adrenergic G-protein-coupled receptor.* Nature, 2007. **450**(7168): p. 383-7.
121. Sprang, S., *GEFs: master regulators of G-protein activation.* Trends in Biochemical Sciences, 2001. **26**(4): p. 266-267.
122. Yan, X., et al., *Adenylyl cyclase/cAMP-PKA-mediated phosphorylation of basal L-type Ca(2+) channels in mouse embryonic ventricular myocytes.* Cell Calcium, 2011. **50**(5): p. 433-43.
123. Davare, M.A., et al., *A beta2 adrenergic receptor signaling complex assembled with the Ca2+ channel Cav1.2.* Science, 2001. **293**(5527): p. 98-101.
124. Balijepalli, R.C., et al., *Localization of cardiac L-type Ca(2+) channels to a caveolar macromolecular signaling complex is required for beta(2)-adrenergic regulation.* Proc Natl Acad Sci U S A, 2006. **103**(19): p. 7500-5.
125. Patriarchi, T., et al., *Phosphorylation of Cav1.2 on S1928 uncouples the L-type Ca2+ channel from the beta2 adrenergic receptor.* EMBO J, 2016. **35**(12): p. 1330-45.

126. Qian, H., et al., *beta2-Adrenergic receptor supports prolonged theta tetanus-induced LTP.* Journal of neurophysiology, 2012. **107**(10): p. 2703-12.
127. Shen, A., et al., *Functionally distinct and selectively phosphorylated GPCR subpopulations co-exist in a single cell.* Nat Commun, 2018. **9**(1): p. 1050.
128. Qian, H., et al., *Phosphorylation of Ser1928 mediates the enhanced activity of the L-type Ca2+ channel Cav1.2 by the beta2-adrenergic receptor in neurons.* Sci Signal, 2017. **10**(463).
129. Krasel, C., et al., *Beta-arrestin binding to the beta2-adrenergic receptor requires both receptor phosphorylation and receptor activation.* J Biol Chem, 2005. **280**(10): p. 9528-35.
130. Kern, R.C., D.S. Kang, and J.L. Benovic, *Arrestin2/clathrin interaction is regulated by key N- and C-terminal regions in arrestin2.* Biochemistry, 2009. **48**(30): p. 7190-200.
131. Laporte, S.A., et al., *The interaction of beta-arrestin with the AP-2 adaptor is required for the clustering of beta 2-adrenergic receptor into clathrin-coated pits.* J Biol Chem, 2000. **275**(30): p. 23120-6.
132. Irannejad, R., et al., *Conformational biosensors reveal GPCR signalling from endosomes.* Nature, 2013. **495**(7442): p. 534-8.
133. Feinstein, T.N., et al., *Noncanonical Control of Vasopressin Receptor Type 2 Signaling by Retromer and Arrestin*.* Journal of Biological Chemistry, 2013. **288**(39): p. 27849-27860.
134. Van Dyke, R.W., *Heterotrimeric G protein subunits are located on rat liver endosomes.* BMC Physiol, 2004. **4**: p. 1.
135. Sposini, S. and A.C. Hanyaloglu, *Spatial encryption of G protein-coupled receptor signaling in endosomes; Mechanisms and applications.* Biochem Pharmacol, 2017. **143**: p. 1-9.
136. Godbole, A., et al., *Internalized TSH receptors en route to the TGN induce local Gs-protein signaling and gene transcription.* Nat Commun, 2017. **8**(1): p. 443.
137. Liu, X., et al., *beta-Arrestin-biased signaling mediates memory reconsolidation.* Proc Natl Acad Sci U S A, 2015. **112**(14): p. 4483-8.
138. Huang, B., et al., *beta-Arrestin-biased beta-adrenergic signaling promotes extinction learning of cocaine reward memory.* Sci Signal, 2018. **11**(512).
139. Li, Y., et al., *Regulation of amygdalar PKA by beta-arrestin-2/phosphodiesterase-4 complex is critical for fear conditioning.* Proc Natl Acad Sci U S A, 2009. **106**(51): p. 21918-23.
140. Gao, V., et al., *Astrocytic beta2-adrenergic receptors mediate hippocampal long-term memory consolidation.* Proc Natl Acad Sci U S A, 2016. **113**(30): p. 8526-31.
141. Wu, Y., L. Zeng, and S. Zhao, *Ligands of Adrenergic Receptors: A Structural Point of View.* Biomolecules, 2021. **11**(7).
142. Nooh, M.M., et al., *SAP97 controls the trafficking and resensitization of the beta-1-adrenergic receptor through its PDZ2 and I3 domains.* PLoS One, 2013. **8**(5): p. e63379.
143. Steinberg, S.F., *Beta1-Adrenergic Receptor Regulation Revisited.* Circ Res, 2018. **123**(11): p. 1199-1201.
144. Gardner, L.A., A.P. Naren, and S.W. Bahouth, *Assembly of an SAP97-AKAP79-cAMP-dependent protein kinase scaffold at the type 1 PSD-95/DLG/ZO1 motif of the human beta(1)-adrenergic receptor generates a receptosome involved in receptor recycling and networking.* J Biol Chem, 2007. **282**(7): p. 5085-5099.
145. Suzuki, T., et al., *Distinct regulation of beta 1- and beta 2-adrenergic receptors in Chinese hamster fibroblasts.* Mol Pharmacol, 1992. **41**(3): p. 542-8.
146. Shiina, T., et al., *Interaction with beta-arrestin determines the difference in internalization behavor between beta1- and beta2-adrenergic receptors.* J Biol Chem, 2000. **275**(37): p. 29082-90.
147. Liang, W., et al., *Differences in endosomal targeting of human (beta)1- and (beta)2-adrenergic receptors following clathrin-mediated endocytosis.* J Cell Sci, 2004. **117**(Pt 5): p. 723-34.
148. Boucrot, E., et al., *Endophilin marks and controls a clathrin-independent endocytic pathway.* Nature, 2015. **517**(7535): p. 460-5.
149. Daaka, Y., et al., *Essential role for G protein-coupled receptor endocytosis in the activation of mitogen-activated protein kinase.* J Biol Chem, 1998. **273**(2): p. 685-8.
150. Tohgo, A., et al., *The stability of the G protein-coupled receptor-beta-arrestin interaction determines the mechanism and functional consequence of ERK activation.* J Biol Chem, 2003. **278**(8): p. 6258-67.
151. Ahn, S., et al., *Differential kinetic and spatial patterns of beta-arrestin and G protein-mediated ERK activation by the angiotensin II receptor.* J Biol Chem, 2004. **279**(34): p. 35518-25.

152. Wei, H., et al., *Stable interaction between beta-arrestin 2 and angiotensin type 1A receptor is required for beta-arrestin 2-mediated activation of extracellular signal-regulated kinases 1 and 2.* J Biol Chem, 2004. **279**(46): p. 48255-61.
153. Eichel, K., D. Jullie, and M. von Zastrow, *beta-Arrestin drives MAP kinase signalling from clathrin-coated structures after GPCR dissociation.* Nat Cell Biol, 2016. **18**(3): p. 303-10.
154. Xu, J., et al., *beta 1-adrenergic receptor association with the synaptic scaffolding protein membrane-associated guanylate kinase inverted-2 (MAGI-2). Differential regulation of receptor internalization by MAGI-2 and PSD-95.* J Biol Chem, 2001. **276**(44): p. 41310-7.
155. Xu, B., et al., *GRK5 Controls SAP97-Dependent Cardiotoxic beta1 Adrenergic Receptor-CaMKII Signaling in Heart Failure.* Circ Res, 2020. **127**(6): p. 796-810.
156. Xiang, Y., E. Devic, and B. Kobilka, *The PDZ binding motif of the beta 1 adrenergic receptor modulates receptor trafficking and signaling in cardiac myocytes.* J Biol Chem, 2002. **277**(37): p. 33783-90.
157. Irannejad, R., et al., *Functional selectivity of GPCR-directed drug action through location bias.* Nat Chem Biol, 2017. **13**(7): p. 799-806.
158. Benton, K.C., et al., *Norepinephrine activates β1-adrenergic receptors localized to the inner nuclear membrane in cortical astrocytes.* bioRxiv, 2021.
159. Boivin, B., et al., *Functional beta-adrenergic receptor signalling on nuclear membranes in adult rat and mouse ventricular cardiomyocytes.* Cardiovasc Res, 2006. **71**(1): p. 69-78.
160. Wang, Y., et al., *Intracellular beta1-Adrenergic Receptors and Organic Cation Transporter 3 Mediate Phospholamban Phosphorylation to Enhance Cardiac Contractility.* Circ Res, 2021. **128**(2): p. 246-261.
161. Nash, C.A., et al., *Golgi localized beta1-adrenergic receptors stimulate Golgi PI4P hydrolysis by PLCepsilon to regulate cardiac hypertrophy.* Elife, 2019. **8**.
162. Ciccarelli, M., et al., *Adrenergic receptors and metabolism: role in development of cardiovascular disease.* Front Physiol, 2013. **4**: p. 265.
163. Collins, S. and R.S. Surwit, *The beta-adrenergic receptors and the control of adipose tissue metabolism and thermogenesis.* Recent Prog Horm Res, 2001. **56**: p. 309-28.
164. Johnson, M., *The beta-adrenoceptor.* Am J Respir Crit Care Med, 1998. **158**(5 Pt 3): p. S146-53.
165. Agac, D., et al., *The beta2-adrenergic receptor controls inflammation by driving rapid IL-10 secretion.* Brain Behav Immun, 2018. **74**: p. 176-185.
166. Woo, A.Y. and R.P. Xiao, *beta-Adrenergic receptor subtype signaling in heart: from bench to bedside.* Acta Pharmacol Sin, 2012. **33**(3): p. 335-41.
167. Myagmar, B.E., et al., *Adrenergic Receptors in Individual Ventricular Myocytes: The Beta-1 and Alpha-1B Are in All Cells, the Alpha-1A Is in a Subpopulation, and the Beta-2 and Beta-3 Are Mostly Absent.* Circ Res, 2017. **120**(7): p. 1103-1115.
168. Pollard, C.M., et al., *Deletion of Osteopontin Enhances beta(2)-Adrenergic Receptor-Dependent Anti-Fibrotic Signaling in Cardiomyocytes.* Int J Mol Sci, 2019. **20**(6).
169. Zhu, C., et al., *Cardiomyocyte β2-Adrenergic Receptor Plays A Protective Role in Cardiac Fibrosis.* The FASEB Journal, 2020. **34**(S1): p. 1-1.
170. Hata, J.A., et al., *Lymphocyte levels of GRK2 (betaARK1) mirror changes in the LVAD-supported failing human heart: lower GRK2 associated with improved beta-adrenergic signaling after mechanical unloading.* J Card Fail, 2006. **12**(5): p. 360-8.
171. Akhter, S.A., et al., *Reversal of impaired myocardial beta-adrenergic receptor signaling by continuous-flow left ventricular assist device support.* J Heart Lung Transplant, 2010. **29**(6): p. 603-9.
172. Rengo, G., et al., *Reduction of lymphocyte G protein-coupled receptor kinase-2 (GRK2) after exercise training predicts survival in patients with heart failure.* Eur J Prev Cardiol, 2014. **21**(1): p. 4-11.
173. Leosco, D., et al., *Effects of exercise training on cardiovascular adrenergic system.* Front Physiol, 2013. **4**: p. 348.
174. Battiprolu, P.K., et al., *Metabolic stress-induced activation of FoxO1 triggers diabetic cardiomyopathy in mice.* J Clin Invest, 2012. **122**(3): p. 1109-18.
175. Fu, Q., et al., *Insulin induces IRS2-dependent and GRK2-mediated beta2AR internalization to attenuate betaAR signaling in cardiomyocytes.* Cell Signal, 2015. **27**(3): p. 707-15.

176. Fu, Q., Q. Wang, and Y.K. Xiang, *Insulin and beta Adrenergic Receptor Signaling: Crosstalk in Heart.* Trends Endocrinol Metab, 2017. **28**(6): p. 416-427.
177. Shen, A., et al., *beta-blockers augment L-type Ca(2+) channel activity by targeting spatially restricted beta2AR signaling in neurons.* Elife, 2019. **8**.
178. Daaka, Y., L.M. Luttrell, and R.J. Lefkowitz, *Switching of the coupling of the beta2-adrenergic receptor to different G proteins by protein kinase A.* Nature, 1997. **390**(6655): p. 88-91.
179. Xiao, R.P., et al., *Coupling of beta2-adrenoceptor to Gi proteins and its physiological relevance in murine cardiac myocytes.* Circ Res, 1999. **84**(1): p. 43-52.
180. Kilts, J.D., et al., *Beta(2)-adrenergic and several other G protein-coupled receptors in human atrial membranes activate both G(s) and G(i).* Circ Res, 2000. **87**(8): p. 705-9.
181. Xiang, Y., et al., *Caveolar localization dictates physiologic signaling of beta 2-adrenoceptors in neonatal cardiac myocytes.* J Biol Chem, 2002. **277**(37): p. 34280-6.
182. Chen-Izu, Y., et al., *G(i)-dependent localization of beta(2)-adrenergic receptor signaling to L-type Ca(2+) channels.* Biophys J, 2000. **79**(5): p. 2547-56.
183. Vasquez, C. and D.L. Lewis, *The beta2-adrenergic receptor specifically sequesters Gs but signals through both Gs and Gi/o in rat sympathetic neurons.* Neuroscience, 2003. **118**(3): p. 603-10.
184. Barnes, P.J., *Distribution of Receptor Targets in the Lung.* Proceedings of the American Thoracic Society, 2004. **1**(4): p. 345-351.
185. Billington, C.K., R.B. Penn, and I.P. Hall, *beta2 Agonists.* Handb Exp Pharmacol, 2017. **237**: p. 23-40.
186. Morgan, S.J., et al., *beta-Agonist-mediated relaxation of airway smooth muscle is protein kinase A-dependent.* J Biol Chem, 2014. **289**(33): p. 23065-23074.
187. Walker, J.K., et al., *Beta-arrestin-2 regulates the development of allergic asthma.* J Clin Invest, 2003. **112**(4): p. 566-74.
188. Xu, H., et al., *Enriched environment enhances beta-adrenergic signaling to prevent microglia inflammation by amyloid-beta.* EMBO Mol Med, 2018. **10**(9).
189. Grisanti, L.A., et al., *Pro-inflammatory responses in human monocytes are beta1-adrenergic receptor subtype dependent.* Mol Immunol, 2010. **47**(6): p. 1244-54.
190. Ortega, E., I. Galvez, and L. Martin-Cordero, *Adrenergic Regulation of Macrophage-Mediated Innate/Inflammatory Responses in Obesity and Exercise in this Condition: Role of beta2 Adrenergic Receptors.* Endocr Metab Immune Disord Drug Targets, 2019. **19**(8): p. 1089-1099.
191. Shen, A., et al., *Functionally distinct and selectively phosphorylated GPCR subpopulations co-exist in a single cell.* Nat Commun, 2018. **(in press)**.
192. Davare, M.A., et al., *A beta2 adrenergic receptor signaling complex assembled with the Ca2+ channel Cav1.2.* Science, 2001. **293**(5527): p. 98-101.
193. Tsvetanova, N.G., et al., *G Protein-Coupled Receptor Endocytosis Confers Uniformity in Responses to Chemically Distinct Ligands.* Mol Pharmacol, 2017. **91**(2): p. 145-156.
194. Schmidt, M., F.J. Dekker, and H. Maarsingh, *Exchange protein directly activated by cAMP (epac): a multidomain cAMP mediator in the regulation of diverse biological functions.* Pharmacol Rev, 2013. **65**(2): p. 670-709.
195. Kaupp, U.B. and R. Seifert, *Cyclic nucleotide-gated ion channels.* Physiol Rev, 2002. **82**(3): p. 769-824.
196. Schindler, R.F. and T. Brand, *The Popeye domain containing protein family--A novel class of cAMP effectors with important functions in multiple tissues.* Prog Biophys Mol Biol, 2016. **120**(1-3): p. 28-36.
197. Conti, M. and J. Beavo, *Biochemistry and physiology of cyclic nucleotide phosphodiesterases: essential components in cyclic nucleotide signaling.* Annu Rev Biochem, 2007. **76**: p. 481-511.
198. Barouch, L.A., et al., *Nitric oxide regulates the heart by spatial confinement of nitric oxide synthase isoforms.* Nature, 2002. **416**(6878): p. 337-9.
199. Calderone, A., et al., *Nitric oxide, atrial natriuretic peptide, and cyclic GMP inhibit the growth-promoting effects of norepinephrine in cardiac myocytes and fibroblasts.* J Clin Invest, 1998. **101**(4): p. 812-8.
200. Hare, J.M. and W.S. Colucci, *Role of nitric oxide in the regulation of myocardial function.* Prog Cardiovasc Dis, 1995. **38**(2): p. 155-66.

201. Hare, J.M., et al., *Increased sensitivity to nitric oxide synthase inhibition in patients with heart failure: potentiation of beta-adrenergic inotropic responsiveness.* Circulation, 1998. **97**(2): p. 161-6.
202. Brixius, K., et al., *Mechanisms of beta 3-adrenoceptor-induced eNOS activation in right atrial and left ventricular human myocardium.* Br J Pharmacol, 2004. **143**(8): p. 1014-22.
203. Li, J., et al., *beta2- but not beta1-adrenoceptor activation modulates intracellular oxygen availability.* J Physiol, 2010. **588**(Pt 16): p. 2987-98.
204. Zhang, Z., et al., *Nebivolol protects against myocardial infarction injury via stimulation of beta 3-adrenergic receptors and nitric oxide signaling.* PLoS One, 2014. **9**(5): p. e98179.
205. Patel, N.S., et al., *Identification of new PDE9A isoforms and how their expression and subcellular compartmentalization in the brain change across the life span.* Neurobiol Aging, 2018. **65**: p. 217-234.
206. Maurice, D.H., et al., *Advances in targeting cyclic nucleotide phosphodiesterases.* Nat Rev Drug Discov, 2014. **13**(4): p. 290-314.
207. Huston, E., et al., *Helix-1 of the cAMP-specific phosphodiesterase PDE4A1 regulates its phospholipase-D-dependent redistribution in response to release of Ca2+.* J Cell Sci, 2006. **119**(Pt 18): p. 3799-810.
208. Houslay, M.D. and G.S. Baillie, *Beta-arrestin-recruited phosphodiesterase-4 desensitizes the AKAP79/PKA-mediated switching of beta2-adrenoceptor signalling to activation of ERK.* Biochem Soc Trans, 2005. **33**(Pt 6): p. 1333-6.
209. Perera, R.K., et al., *Microdomain switch of cGMP-regulated phosphodiesterases leads to ANP-induced augmentation of beta-adrenoceptor-stimulated contractility in early cardiac hypertrophy.* Circ Res, 2015. **116**(8): p. 1304-11.
210. Penmatsa, H., et al., *Compartmentalized cyclic adenosine 3',5'-monophosphate at the plasma membrane clusters PDE3A and cystic fibrosis transmembrane conductance regulator into microdomains.* Mol Biol Cell, 2010. **21**(6): p. 1097-110.
211. Ahmad, F., et al., *Differential regulation of adipocyte PDE3B in distinct membrane compartments by insulin and the beta3-adrenergic receptor agonist CL316243: effects of caveolin-1 knockdown on formation/maintenance of macromolecular signalling complexes.* Biochem J, 2009. **424**(3): p. 399-410.
212. Al-Tawashi, A. and C. Gehring, *Phosphodiesterase activity is regulated by CC2D1A that is implicated in non-syndromic intellectual disability.* Cell Commun Signal, 2013. **11**(1): p. 47.
213. Neves, S.R., P.T. Ram, and R. Iyengar, *G protein pathways.* Science, 2002. **296**(5573): p. 1636-9.
214. Chen, J., et al., *Neuronal expression of soluble adenylyl cyclase in the mammalian brain.* Brain Res, 2013. **1518**: p. 1-8.
215. Kobialka, M. and W.A. Gorczyca, *Particulate guanylyl cyclases: multiple mechanisms of activation.* Acta Biochim Pol, 2000. **47**(3): p. 517-28.
216. Francis, S.H., M.A. Blount, and J.D. Corbin, *Mammalian cyclic nucleotide phosphodiesterases: molecular mechanisms and physiological functions.* Physiol Rev, 2011. **91**(2): p. 651-90.
217. Brand, T., *The Popeye Domain Containing Genes and Their Function as cAMP Effector Proteins in Striated Muscle.* J Cardiovasc Dev Dis, 2018. **5**(1).
218. Schneider, E.H. and R. Seifert, *Inactivation of Non-canonical Cyclic Nucleotides: Hydrolysis and Transport.* Handb Exp Pharmacol, 2017. **238**: p. 169-205.
219. Herbst, S., et al., *Transmembrane redox control and proteolysis of PdeC, a novel type of c-di-GMP phosphodiesterase.* EMBO J, 2018. **37**(8).
220. Baillie, G.S., G.S. Tejeda, and M.P. Kelly, *Therapeutic targeting of 3',5'-cyclic nucleotide phosphodiesterases: inhibition and beyond.* Nat Rev Drug Discov, 2019. **18**(10): p. 770-796.
221. Clister, T., et al., *AKAP95 Organizes a Nuclear Microdomain to Control Local cAMP for Regulating Nuclear PKA.* Cell Chem Biol, 2019. **26**(6): p. 885-891 e4.
222. Xie, Z., et al., *Cellular and subcellular localization of PDE10A, a striatum-enriched phosphodiesterase.* Neuroscience, 2006. **139**(2): p. 597-607.
223. Kelly, M.P., et al., *Select 3',5'-cyclic nucleotide phosphodiesterases exhibit altered expression in the aged rodent brain.* Cell Signal, 2014. **26**(2): p. 383-97.
224. Richter, W., et al., *Signaling from beta1- and beta2-adrenergic receptors is defined by differential interactions with PDE4.* EMBO J, 2008. **27**(2): p. 384-93.

225. Blackman, B.E., et al., *PDE4D and PDE4B function in distinct subcellular compartments in mouse embryonic fibroblasts.* J Biol Chem, 2011. **286**(14): p. 12590-601.
226. Leroy, J., et al., *Spatiotemporal dynamics of beta-adrenergic cAMP signals and L-type Ca2+ channel regulation in adult rat ventricular myocytes: role of phosphodiesterases.* Circ Res, 2008. **102**(9): p. 1091-100.
227. De Arcangelis, V., et al., *Differential association of phosphodiesterase 4D isoforms with beta2-adrenoceptor in cardiac myocytes.* J Biol Chem, 2009. **284**(49): p. 33824-32.
228. Perry, S.J., et al., *Targeting of cyclic AMP degradation to beta 2-adrenergic receptors by beta-arrestins.* Science, 2002. **298**(5594): p. 834-6.
229. Li, X., et al., *Phosphodiesterase-4 influences the PKA phosphorylation status and membrane translocation of G-protein receptor kinase 2 (GRK2) in HEK-293beta2 cells and cardiac myocytes.* Biochem J, 2006. **394**(Pt 2): p. 427-35.
230. Shi, Q., et al., *Heterologous desensitization of cardiac beta-adrenergic signal via hormone-induced betaAR/arrestin/PDE4 complexes.* Cardiovasc Res, 2017. **113**(6): p. 656-670.
231. Vaughan, D.J., et al., *Role of the G protein-coupled receptor kinase site serine cluster in beta2-adrenergic receptor internalization, desensitization, and beta-arrestin translocation.* J Biol Chem, 2006. **281**(11): p. 7684-92.
232. Salazar, N.C., et al., *GRK2 blockade with betaARKct is essential for cardiac beta2-adrenergic receptor signaling towards increased contractility.* Cell Commun Signal, 2013. **11**: p. 64.
233. Baillie, G., S.J. MacKenzie, and M.D. Houslay, *Phorbol 12-myristate 13-acetate triggers the protein kinase A-mediated phosphorylation and activation of the PDE4D5 cAMP phosphodiesterase in human aortic smooth muscle cells through a route involving extracellular signal regulated kinase (ERK).* Mol Pharmacol, 2001. **60**(5): p. 1100-11.
234. Liu, S., et al., *Phosphodiesterases coordinate cAMP propagation induced by two stimulatory G protein-coupled receptors in hearts.* Proc Natl Acad Sci U S A, 2012. **109**(17): p. 6578-83.
235. Zhang, J.Z., et al., *Phase Separation of a PKA Regulatory Subunit Controls cAMP Compartmentation and Oncogenic Signaling.* Cell, 2020. **182**(6): p. 1531-1544 e15.
236. Yarla, N.S., et al., *Targeting the paracrine hormone-dependent guanylate cyclase/cGMP/phosphodiesterases signaling pathway for colorectal cancer prevention.* Semin Cancer Biol, 2019. **56**: p. 168-174.
237. Francis, S.H. and J.D. Corbin, *Phosphodiesterase-5 inhibition: the molecular biology of erectile function and dysfunction.* Urol Clin North Am, 2005. **32**(4): p. 419-29, vi.
238. Schwartz, B.G. and R.A. Kloner, *Drug interactions with phosphodiesterase-5 inhibitors used for the treatment of erectile dysfunction or pulmonary hypertension.* Circulation, 2010. **122**(1): p. 88-95.
239. Lee, D.I., et al., *Phosphodiesterase 9A controls nitric-oxide-independent cGMP and hypertrophic heart disease.* Nature, 2015. **519**(7544): p. 472-6.
240. Zoccarato, A., et al., *Cardiac Hypertrophy Is Inhibited by a Local Pool of cAMP Regulated by Phosphodiesterase 2.* Circ Res, 2015. **117**(8): p. 707-19.
241. Nthenge-Ngumbau, D.N. and K.P. Mohanakumar, *Can Cyclic Nucleotide Phosphodiesterase Inhibitors Be Drugs for Parkinson's Disease?* Mol Neurobiol, 2018. **55**(1): p. 822-834.
242. Tibbo, A.J., G.S. Tejeda, and G.S. Baillie, *Understanding PDE4's function in Alzheimer's disease; a target for novel therapeutic approaches.* Biochem Soc Trans, 2019. **47**(5): p. 1557-1565.
243. Pathak, G., et al., *PDE11A negatively regulates lithium responsivity.* Mol Psychiatry, 2017. **22**(12): p. 1714-1724.
244. Salpietro, V., et al., *A homozygous loss-of-function mutation in PDE2A associated to early-onset hereditary chorea.* Mov Disord, 2018. **33**(3): p. 482-488.
245. Boscutti, G., A.R. E, and C. Plisson, *PET Radioligands for imaging of the PDE10A in human: current status.* Neurosci Lett, 2019. **691**: p. 11-17.
246. Zhang, H.T., et al., *Antidepressant-like profile and reduced sensitivity to rolipram in mice deficient in the PDE4D phosphodiesterase enzyme.* Neuropsychopharmacology, 2002. **27**(4): p. 587-95.
247. Russell, D.S., et al., *Change in PDE10 across early Huntington disease assessed by [18F]MNI-659 and PET imaging.* Neurology, 2016. **86**(8): p. 748-54.
248. Kumar, N., et al., *Phosphodiesterase 4-targeted treatments for autoimmune diseases.* BMC Med, 2013. **11**: p. 96.

249. Dyke, H.J. and J.G. Montana, *Update on the therapeutic potential of PDE4 inhibitors.* Expert Opin Investig Drugs, 2002. **11**(1): p. 1-13.
250. Dietsch, G.N., et al., *Characterization of the inflammatory response to a highly selective PDE4 inhibitor in the rat and the identification of biomarkers that correlate with toxicity.* Toxicol Pathol, 2006. **34**(1): p. 39-51.
251. Sutherland, E.W. and T. Rall, *The properties of an adenine ribonucleotide produced with cellular particles, ATP, Mg++, and epinephrine or glucagon.* Journal of the American Chemical Society, 1957. **79**(13): p. 3608-3608.
252. Ricciarelli, R., et al., *Memory-enhancing effects of GEBR-32a, a new PDE4D inhibitor holding promise for the treatment of Alzheimer's disease.* Sci Rep, 2017. **7**: p. 46320.
253. Lefkowitz, R.J., *A brief history of G-protein coupled receptors (Nobel Lecture).* Angew Chem Int Ed Engl, 2013. **52**(25): p. 6366-78.
254. Levin, E.D., et al., *Nicotinic alpha7- or beta2-containing receptor knockout: effects on radial-arm maze learning and long-term nicotine consumption in mice.* Behav Brain Res, 2009. **196**(2): p. 207-13.
255. Branca, C., et al., *Administration of a selective beta2 adrenergic receptor antagonist exacerbates neuropathology and cognitive deficits in a mouse model of Alzheimer's disease.* Neurobiol Aging, 2014. **35**(12): p. 2726-2735.
256. Ramos, B.P., et al., *Beta2 adrenergic agonist, clenbuterol, enhances working memory performance in aging animals.* Neurobiol Aging, 2008. **29**(7): p. 1060-9.
257. Cipres-Flores, F.J., et al., *Beta-blockers and salbutamol limited emotional memory disturbance and damage induced by orchiectomy in the rat hippocampus.* Life Sci, 2019. **224**: p. 128-137.
258. Iyer, V., et al., *Differential phosphorylation and dephosphorylation of beta2-adrenoceptor sites Ser262 and Ser355,356.* Br J Pharmacol, 2006. **147**(3): p. 249-59.
259. Lyga, S., et al., *Persistent cAMP Signaling by Internalized LH Receptors in Ovarian Follicles.* Endocrinology, 2016. **157**(4): p. 1613-21.
260. Calebiro, D., et al., *Persistent cAMP-signals triggered by internalized G-protein-coupled receptors.* PLoS Biol, 2009. **7**(8): p. e1000172.
261. Xiang, Y.K., *Compartmentalization of beta-adrenergic signals in cardiomyocytes.* Circ Res, 2011. **109**(2): p. 231-44.
262. Conti, M., D. Mika, and W. Richter, *Cyclic AMP compartments and signaling specificity: role of cyclic nucleotide phosphodiesterases.* J Gen Physiol, 2014. **143**(1): p. 29-38.
263. Xiang, Y., et al., *Phosphodiesterase 4D is required for beta2 adrenoceptor subtype-specific signaling in cardiac myocytes.* Proc Natl Acad Sci U S A, 2005. **102**(3): p. 909-14.
264. Fischmeister, R., et al., *Compartmentation of cyclic nucleotide signaling in the heart: the role of cyclic nucleotide phosphodiesterases.* Circ Res, 2006. **99**(8): p. 816-28.
265. Zaccolo, M., A. Zerio, and M.J. Lobo, *Subcellular Organization of the cAMP Signaling Pathway.* Pharmacol Rev, 2021. **73**(1): p. 278-309.
266. Rasmussen, S.G., et al., *Structure of a nanobody-stabilized active state of the beta(2) adrenoceptor.* Nature, 2011. **469**(7329): p. 175-80.
267. Beautrait, A., et al., *A new inhibitor of the beta-arrestin/AP2 endocytic complex reveals interplay between GPCR internalization and signalling.* Nat Commun, 2017. **8**: p. 15054.
268. Baillie, G.S., et al., *beta-Arrestin-mediated PDE4 cAMP phosphodiesterase recruitment regulates beta-adrenoceptor switching from Gs to Gi.* Proc Natl Acad Sci U S A, 2003. **100**(3): p. 940-5.
269. Baillie, G.S., et al., *Mapping binding sites for the PDE4D5 cAMP-specific phosphodiesterase to the N- and C-domains of beta-arrestin using spot-immobilized peptide arrays.* Biochem J, 2007. **404**(1): p. 71-80.
270. Lobingier, B.T. and M. von Zastrow, *When trafficking and signaling mix: How subcellular location shapes G protein-coupled receptor activation of heterotrimeric G proteins.* Traffic, 2019. **20**(2): p. 130-136.
271. Miningou Zobon, N.T., J. Jedrzejewska-Szmek, and K.T. Blackwell, *Temporal pattern and synergy influence activity of ERK signaling pathways during L-LTP induction.* Elife, 2021. **10**.
272. Mika, D., W. Richter, and M. Conti, *A CaMKII/PDE4D negative feedback regulates cAMP signaling.* Proc Natl Acad Sci U S A, 2015. **112**(7): p. 2023-8.
273. Lazar, A.M., et al., *G protein-regulated endocytic trafficking of adenylyl cyclase type 9.* Elife, 2020. **9**.

274. Wang, P., et al., *Subcellular localization of beta-arrestins is determined by their intact N domain and the nuclear export signal at the C terminus.* J Biol Chem, 2003. **278**(13): p. 11648-53.
275. Hoeppner, C.Z., N. Cheng, and R.D. Ye, *Identification of a nuclear localization sequence in beta-arrestin-1 and its functional implications.* J Biol Chem, 2012. **287**(12): p. 8932-43.
276. McDonald, P.H., et al., *Beta-arrestin 2: a receptor-regulated MAPK scaffold for the activation of JNK3.* Science, 2000. **290**(5496): p. 1574-7.
277. Scott, M.G., et al., *Differential nucleocytoplasmic shuttling of beta-arrestins. Characterization of a leucine-rich nuclear export signal in beta-arrestin2.* J Biol Chem, 2002. **277**(40): p. 37693-701.
278. Zhang, Y., et al., *Single-particle cryo-EM structural studies of the beta2AR-Gs complex bound with a full agonist formoterol.* Cell Discov, 2020. **6**: p. 45.
279. Syed, A.U., et al., *Adenylyl cyclase 5-generated cAMP controls cerebral vascular reactivity during diabetic hyperglycemia.* J Clin Invest, 2019. **129**(8): p. 3140-3152.
280. Gerfen, C.R., *Basic neuroanatomical methods.* Curr Protoc Neurosci, 2003. **Chapter 1**: p. Unit 1 1.
281. Jurgens, C.W., et al., *Beta1 adrenergic receptor-mediated enhancement of hippocampal CA3 network activity.* J Pharmacol Exp Ther, 2005. **314**(2): p. 552-60.
282. Coutellier, L., P.M. Ardestani, and M. Shamloo, *beta1-adrenergic receptor activation enhances memory in Alzheimer's disease model.* Ann Clin Transl Neurol, 2014. **1**(5): p. 348-360.
283. Broadbent, N.J., L.R. Squire, and R.E. Clark, *Spatial memory, recognition memory, and the hippocampus.* Proc Natl Acad Sci U S A, 2004. **101**(40): p. 14515-20.
284. Pilly, P.K. and S. Grossberg, *How do spatial learning and memory occur in the brain? Coordinated learning of entorhinal grid cells and hippocampal place cells.* J Cogn Neurosci, 2012. **24**(5): p. 1031-54.
285. Naber, P.A., M.P. Witter, and F.H. Lopes Silva, *Networks of the hippocampal memory system of the rat. The pivotal role of the subiculum.* Ann N Y Acad Sci, 2000. **911**: p. 392-403.
286. Eichenbaum, H., et al., *Functional organization of the hippocampal memory system.* Proc Natl Acad Sci U S A, 1996. **93**(24): p. 13500-7.
287. Hagena, H., N. Hansen, and D. Manahan-Vaughan, *beta-Adrenergic Control of Hippocampal Function: Subserving the Choreography of Synaptic Information Storage and Memory.* Cereb Cortex, 2016. **26**(4): p. 1349-64.
288. Tullai, J.W., et al., *Immediate-early and delayed primary response genes are distinct in function and genomic architecture.* J Biol Chem, 2007. **282**(33): p. 23981-95.
289. Gilleen, J., et al., *An experimental medicine study of the phosphodiesterase-4 inhibitor, roflumilast, on working memory-related brain activity and episodic memory in schizophrenia patients.* Psychopharmacology (Berl), 2021. **238**(5): p. 1279-1289.
290. Blokland, A., et al., *Acute treatment with the PDE4 inhibitor roflumilast improves verbal word memory in healthy old individuals: a double-blind placebo-controlled study.* Neurobiol Aging, 2019. **77**: p. 37-43.
291. Vanmierlo, T., et al., *The PDE4 inhibitor roflumilast improves memory in rodents at non-emetic doses.* Behav Brain Res, 2016. **303**: p. 26-33.
292. Wang, H., et al., *The Phosphodiesterase-4 Inhibitor Roflumilast, a Potential Treatment for the Comorbidity of Memory Loss and Depression in Alzheimer's Disease: A Preclinical Study in APP/PS1 Transgenic Mice.* Int J Neuropsychopharmacol, 2020. **23**(10): p. 700-711.
293. Li, Y., et al., *Regulation of amygdalar PKA by beta-arrestin-2/phosphodiesterase-4 complex is critical for fear conditioning.* Proceedings of the National Academy of Sciences of the United States of America, 2009. **106**(51): p. 21918-23.
294. Boyd, A., et al., *Assessment of PDE4 Inhibitor-Induced Hypothermia as a Correlate of Nausea in Mice.* Biology (Basel), 2021. **10**(12).
295. Lefkowitz, R.J. and S.K. Shenoy, *Transduction of receptor signals by beta-arrestins.* Science, 2005. **308**(5721): p. 512-7.
296. Lamichhane, R., et al., *Biased Signaling of the G-Protein-Coupled Receptor beta2AR Is Governed by Conformational Exchange Kinetics.* Structure, 2020. **28**(3): p. 371-377 e3.
297. Arrieta-Cruz, I., et al., *Carvedilol reestablishes long-term potentiation in a mouse model of Alzheimer's disease.* J Alzheimers Dis, 2010. **21**(2): p. 649-54.

298. Kumar, A., S. Dogra, and A. Prakash, *Effect of carvedilol on behavioral, mitochondrial dysfunction, and oxidative damage against D-galactose induced senescence in mice.* Naunyn Schmiedebergs Arch Pharmacol, 2009. **380**(5): p. 431-41.
299. Prakash, A.K. and A. Kumar, *Effect of chronic treatment of carvedilol on oxidative stress in an intracerebroventricular streptozotocin induced model of dementia in rats.* J Pharm Pharmacol, 2009. **61**(12): p. 1665-72.
300. Gorman, A.L. and A.J. Dunn, *Beta-adrenergic receptors are involved in stress-related behavioral changes.* Pharmacol Biochem Behav, 1993. **45**(1): p. 1-7.
301. Vorhees, C.V. and M.T. Williams, *Morris water maze: procedures for assessing spatial and related forms of learning and memory.* Nat Protoc, 2006. **1**(2): p. 848-58.
302. Vorhees, C.V. and M.T. Williams, *Assessing spatial learning and memory in rodents.* ILAR J, 2014. **55**(2): p. 310-32.
303. Can, A., et al., *The mouse forced swim test.* J Vis Exp, 2012(59): p. e3638.
304. Commons, K.G., et al., *The Rodent Forced Swim Test Measures Stress-Coping Strategy, Not Depression-like Behavior.* ACS Chem Neurosci, 2017. **8**(5): p. 955-960.
305. Choi, S.H., et al., *Changes in c-Fos Expression in the Forced Swimming Test: Common and Distinct Modulation in Rat Brain by Desipramine and Citalopram.* Korean J Physiol Pharmacol, 2013. **17**(4): p. 321-9.
306. Komada, M., K. Takao, and T. Miyakawa, *Elevated plus maze for mice.* J Vis Exp, 2008(22).
307. Critchley, B.J., M. Isalan, and M. Mielcarek, *Neuro-Cardio Mechanisms in Huntington's Disease and Other Neurodegenerative Disorders.* Front Physiol, 2018. **9**: p. 559.
308. De Keyser, J., E. Zeinstra, and N. Wilczak, *Astrocytic beta2-adrenergic receptors and multiple sclerosis.* Neurobiol Dis, 2004. **15**(2): p. 331-9.
309. Bartus, R.T., et al., *beta2-Adrenoceptor agonists as novel, safe and potentially effective therapies for Amyotrophic lateral sclerosis (ALS).* Neurobiol Dis, 2016. **85**: p. 11-24.
310. Waeber, C., et al., *Beta-adrenergic receptor subtypes in the basal ganglia of patients with Huntington's chorea and Parkinson's disease.* Synapse, 1991. **8**(4): p. 270-80.
311. Enna, S.J., et al., *Huntington's chorea. Changes in neurotransmitter receptors in the brain.* N Engl J Med, 1976. **294**(24): p. 1305-9.
312. Morales, D.R., et al., *Respiratory effect of beta-blockers in people with asthma and cardiovascular disease: population-based nested case control study.* BMC Med, 2017. **15**(1): p. 18.
313. Ong, H.T., *Beta blockers in hypertension and cardiovascular disease.* BMJ, 2007. **334**(7600): p. 946-9.
314. Tomiyama, H. and A. Yamashina, *Beta-Blockers in the Management of Hypertension and/or Chronic Kidney Disease.* Int J Hypertens, 2014. **2014**: p. 919256.
315. Bakris, G.L., P. Hart, and E. Ritz, *Beta blockers in the management of chronic kidney disease.* Kidney Int, 2006. **70**(11): p. 1905-13.
316. Argulian, E., S. Bangalore, and F.H. Messerli, *Misconceptions and Facts About Beta-Blockers.* Am J Med, 2019. **132**(7): p. 816-819.
317. Whelton, P.K., et al., *2017 ACC/AHA/AAPA/ABC/ACPM/AGS/APhA/ASH/ASPC/NMA/PCNA Guideline for the Prevention, Detection, Evaluation, and Management of High Blood Pressure in Adults: A Report of the American College of Cardiology/American Heart Association Task Force on Clinical Practice Guidelines.* Hypertension, 2018. **71**(6): p. e13-e115.
318. Goodman, A.M., et al., *Heightened Hippocampal beta-Adrenergic Receptor Function Drives Synaptic Potentiation and Supports Learning and Memory in the TgF344-AD Rat Model during Prodromal Alzheimer's Disease.* J Neurosci, 2021. **41**(26): p. 5747-5761.
319. Chen, Y., et al., *alpha(2A) adrenergic receptor promotes amyloidogenesis through disrupting APP-SorLA interaction.* Proc Natl Acad Sci U S A, 2014. **111**(48): p. 17296-301.
320. Tournissac, M., et al., *Repurposing beta-3 adrenergic receptor agonists for Alzheimer's disease: beneficial effects in a mouse model.* Alzheimers Res Ther, 2021. **13**(1): p. 103.
321. Roullet, P., et al., *Traumatic memory reactivation with or without propranolol for PTSD and comorbid MD symptoms: a randomised clinical trial.* Neuropsychopharmacology, 2021. **46**(9): p. 1643-1649.
322. Ruiz-Medina, B.E., et al., *Isoproterenol-induced beta-2 adrenergic receptor activation negatively regulates interleukin-2 signaling.* Biochem J, 2018. **475**(18): p. 2907-2923.

323. Zhang, W., et al., *beta-Adrenergic receptor-PI3K signaling crosstalk in mouse heart: elucidation of immediate downstream signaling cascades.* PLoS One, 2011. **6**(10): p. e26581.
324. Timmons, S., et al., *Akt signal transduction dysfunction in Parkinson's disease.* Neurosci Lett, 2009. **467**(1): p. 30-5.
325. Greene, L.A., O. Levy, and C. Malagelada, *Akt as a Victim, Villain and Potential Hero in Parkinson's Disease Pathophysiology and Treatment.* Cellular and Molecular Neurobiology, 2011. **31**(7): p. 969-978.
326. Rai, S.N., et al., *The Role of PI3K/Akt and ERK in Neurodegenerative Disorders.* Neurotox Res, 2019. **35**(3): p. 775-795.
327. Yuan, Y.H., et al., *The molecular mechanism of rotenone-induced alpha-synuclein aggregation: emphasizing the role of the calcium/GSK3beta pathway.* Toxicol Lett, 2015. **233**(2): p. 163-71.
328. Hongo, H., et al., *Glycogen synthase kinase-3beta activation mediates rotenone-induced cytotoxicity with the involvement of microtubule destabilization.* Biochem Biophys Res Commun, 2012. **426**(1): p. 94-9.
329. Scalzo, P., et al., *Serum levels of brain-derived neurotrophic factor correlate with motor impairment in Parkinson's disease.* J Neurol, 2010. **257**(4): p. 540-5.
330. Juric, D.M., D. Loncar, and M. Carman-Krzan, *Noradrenergic stimulation of BDNF synthesis in astrocytes: mediation via alpha1- and beta1/beta2-adrenergic receptors.* Neurochem Int, 2008. **52**(1-2): p. 297-306.
331. Yu, J.T., et al., *Polymorphisms at the beta2-adrenergic receptor gene influence Alzheimer's disease susceptibility.* Brain Res, 2008. **1210**: p. 216-22.
332. Rosenberg, P.B., et al., *Effects of cardiovascular medications on rate of functional decline in Alzheimer disease.* Am J Geriatr Psychiatry, 2008. **16**(11): p. 883-92.
333. Koutroumani, M., et al., *The deletion variant of alpha2b-adrenergic receptor is associated with decreased risk in Alzheimer's disease and mild cognitive impairment.* J Neurol Sci, 2013. **328**(1-2): p. 19-23.
334. Wu, Q., et al., *Blocking beta 2-adrenergic receptor inhibits dendrite ramification in a mouse model of Alzheimer's disease.* Neural Regen Res, 2017. **12**(9): p. 1499-1506.
335. Katsouri, L., et al., *Prazosin, an alpha(1)-adrenoceptor antagonist, prevents memory deterioration in the APP23 transgenic mouse model of Alzheimer's disease.* Neurobiol Aging, 2013. **34**(4): p. 1105-15.
336. Patriarchi, T., O.R. Buonarati, and J.W. Hell, *Postsynaptic localization and regulation of AMPA receptors and Cav1.2 by beta2 adrenergic receptor/PKA and Ca(2+)/CaMKII signaling.* EMBO J, 2018. **37**(20).
337. Wang, L.Y., et al., *Prazosin for the treatment of behavioral symptoms in patients with Alzheimer disease with agitation and aggression.* Am J Geriatr Psychiatry, 2009. **17**(9): p. 744-51.
338. Zhang, F., et al., *beta-amyloid redirects norepinephrine signaling to activate the pathogenic GSK3beta/tau cascade.* Sci Transl Med, 2020. **12**(526).
339. Holm, H., et al., *Beta-blocker therapy and risk of vascular dementia: A population-based prospective study.* Vascul Pharmacol, 2020. **125-126**: p. 106649.
340. Safarudin, F., et al., *The Association of Beta-Blocker Use to Cognitive Impairment among Adults with Hypertension or Cardiovascular Diseases in the United States.* Chronic Pain Manag, 2020. **4**.
341. Thunell, J., et al., *Drug therapies for chronic conditions and risk of Alzheimer's disease and related dementias: A scoping review.* Alzheimers Dement, 2021. **17**(1): p. 41-48.
342. Wang, D., et al., *Amyloid beta peptide-(1-42) induces internalization and degradation of beta2 adrenergic receptors in prefrontal cortical neurons.* J Biol Chem, 2011. **286**(36): p. 31852-63.
343. Wang, D., et al., *Binding of amyloid beta peptide to beta2 adrenergic receptor induces PKA-dependent AMPA receptor hyperactivity.* FASEB J, 2010. **24**(9): p. 3511-21.
344. Patterson, A.J., et al., *Protecting the myocardium: a role for the beta2 adrenergic receptor in the heart.* Crit Care Med, 2004. **32**(4): p. 1041-8.
345. Lauze, M., J.F. Daneault, and C. Duval, *The Effects of Physical Activity in Parkinson's Disease: A Review.* J Parkinsons Dis, 2016. **6**(4): p. 685-698.
346. Wu, P.L., M. Lee, and T.T. Huang, *Effectiveness of physical activity on patients with depression and Parkinson's disease: A systematic review.* PLoS One, 2017. **12**(7): p. e0181515.

347. Oliveira de Carvalho, A., et al., *Physical Exercise For Parkinson's Disease: Clinical And Experimental Evidence.* Clin Pract Epidemiol Ment Health, 2018. **14**: p. 89-98.
348. Lin, T.W. and Y.M. Kuo, *Exercise benefits brain function: the monoamine connection.* Brain Sci, 2013. **3**(1): p. 39-53.
349. Neeper, S.A., et al., *Exercise and brain neurotrophins.* Nature, 1995. **373**(6510): p. 109.
350. Vaynman, S., Z. Ying, and F. Gomez-Pinilla, *Hippocampal BDNF mediates the efficacy of exercise on synaptic plasticity and cognition.* Eur J Neurosci, 2004. **20**(10): p. 2580-90.
351. Ivy, A.S., et al., *Noradrenergic and serotonergic blockade inhibits BDNF mRNA activation following exercise and antidepressant.* Pharmacol Biochem Behav, 2003. **75**(1): p. 81-8.
352. Meng, Q., M.S. Lin, and I.S. Tzeng, *Relationship Between Exercise and Alzheimer's Disease: A Narrative Literature Review.* Front Neurosci, 2020. **14**: p. 131.
353. Zhao, J.L., et al., *Exercise, brain plasticity, and depression.* CNS Neurosci Ther, 2020. **26**(9): p. 885-895.
354. Qian, L., et al., *beta2 Adrenergic receptor activation induces microglial NADPH oxidase activation and dopaminergic neurotoxicity through an ERK-dependent/protein kinase A-independent pathway.* Glia, 2009. **57**(15): p. 1600-9.
355. Sharma, D. and J.D. Farrar, *Adrenergic regulation of immune cell function and inflammation.* Semin Immunopathol, 2020. **42**(6): p. 709-717.
356. Xiao, H., et al., *IL-18 cleavage triggers cardiac inflammation and fibrosis upon beta-adrenergic insult.* Eur Heart J, 2018. **39**(1): p. 60-69.
357. Lechtenberg, K.J., et al., *Augmented beta2-adrenergic signaling dampens the neuroinflammatory response following ischemic stroke and increases stroke size.* J Neuroinflammation, 2019. **16**(1): p. 112.
358. Evans, A.K., et al., *Beta-adrenergic receptor antagonism is proinflammatory and exacerbates neuroinflammation in a mouse model of Alzheimer's Disease.* Neurobiol Dis, 2020. **146**: p. 105089.
359. Sugama, S., et al., *Stress-induced microglial activation occurs through beta-adrenergic receptor: noradrenaline as a key neurotransmitter in microglial activation.* J Neuroinflammation, 2019. **16**(1): p. 266.
360. Oakley, R.H., et al., *Differential affinities of visual arrestin, beta arrestin1, and beta arrestin2 for G protein-coupled receptors delineate two major classes of receptors.* J Biol Chem, 2000. **275**(22): p. 17201-10.
361. Oakley, R.H., et al., *Association of beta-arrestin with G protein-coupled receptors during clathrin-mediated endocytosis dictates the profile of receptor resensitization.* J Biol Chem, 1999. **274**(45): p. 32248-57.
362. Luttrell, L.M. and R.J. Lefkowitz, *The role of beta-arrestins in the termination and transduction of G-protein-coupled receptor signals.* J Cell Sci, 2002. **115**(Pt 3): p. 455-65.
363. Bottke, T., et al., *Exploring GPCR-arrestin interfaces with genetically encoded crosslinkers.* EMBO Rep, 2020. **21**(11): p. e50437.
364. Kang, J., et al., *A nuclear function of beta-arrestin1 in GPCR signaling: regulation of histone acetylation and gene transcription.* Cell, 2005. **123**(5): p. 833-47.
365. Chen, Q., et al., *Self-association of arrestin family members.* Handb Exp Pharmacol, 2014. **219**: p. 205-23.
366. Xiao, K., et al., *Functional specialization of beta-arrestin interactions revealed by proteomic analysis.* Proc Natl Acad Sci U S A, 2007. **104**(29): p. 12011-6.
367. Pandey, S.C., et al., *Beta-adrenergic receptor subtypes in stress-induced behavioral depression.* Pharmacol Biochem Behav, 1995. **51**(2-3): p. 339-44.
368. Stone, E.A., et al., *Beta adrenoceptor blockade mimics effects of stress on motor activity in mice.* Neuropsychopharmacology, 1995. **12**(1): p. 65-71.